Heparinoid Hydrogels for Cardiovascular Tissue Regeneration

by

Aliza Janse van Rensburg

JNSALI005

Presented for the Degree of Master of Science:

MSc (Med) in Biomedical Engineering

HUB5002W

Faculty of Health Sciences

Department of Human Biology

Division of Biomedical Engineering

in association with the

Cardiovascular Research Unit

Chris Barnard Division of Cardiothoracic Surgery

UNIVERSITY OF CAPE TOWN

Supervisor: Assoc. Prof Deon Bezuidenhout

Co-supervisor: Assoc. Prof Neil Davies

August 2015

The financial assistance of the National Research Foundation (NRF) towards this research is hereby acknowledged. Opinions expressed and conclusions arrived at, are those of the author and are not necessarily to be attributed to the NRF.

Declaration

I, Aliza Janse van Rensburg, hereby declare that the work on which this dissertation/thesis is based is my original work (except where acknowledgements indicate otherwise) and that neither the whole work nor any part of it has been, is being, or is to be submitted for another degree in this or any other university.

I empower the university to reproduce for the purpose of research either the whole or any portion of the contents in any manner whatsoever.

Signed by candidate

Signature

15 August 2015

Date

Acknowledgements

The completion of this thesis was only possible with the help, support and guidance of the people at the Cardiovascular Research Unit of UCT. I would like to express my sincere thanks to the following people and institutions in particular:

My supervisor, **Assoc. Prof Deon Bezuidenhout**, for the successful completion of not only my thesis dissertation, but also for the interest that he had awakened in me for medical research, biomaterials and tissue engineering; for the distinction I have received for my final year project at Stellenbosch University; for the guidance, time, advice and financial support during the last three years; as well as the patience with which he has mentored me throughout my studies. I would also like to thank my co-supervisor, **Dr Neil Davies**, for the assistance with my growth factor incorporation and release studies, as well as for his assistance in analysing histological data.

I would like to express a special thank you to **Anel Oosthuysen** for performing the initial studies for the project and for teaching me safe laboratory practices and several experimental procedures. I would also like to thank her and **Joel du Toit** for the assistance with the synthesis of different chemicals needed for the project. I would like to extend a special thank you to **Helen Ilsley**, **Cindy Chokoza**, **Liezl Immelman** and **Pete Roberts** for the performance of histological processing, ELISA assays, TEGs and ROTEMs, as well as NMRs spectroscopy, respectively. Thank you for not only performing these tests, but also sharing your knowledge, skills and time with me in your respective fields of expertise.

Another notable thank you to the FHS Animal Unit, in particular **Rodney Lucas**, **Emma Alsop**, **Janet McCallum** and **Kim Tutt** for their assistance with the animal study. I would like to thank **Jandré De Villiers** for explaining several aspects of chemistry and polymer science to me, as well as helping me plan several of the experiments for my project.

Lastly I would like to thank my family and friends for encouraging and supporting me to follow my dreams and to complete my Master's degree. A special thanks to **Jason Voorneveld** for all the help, advice and encouragement during the last two years.

Funding for this study were provided through the Competitive Program for Rated Researchers (CPRR) awarded to Assoc. Prof Deon Bezuidenhout by the National Research Foundation (NRF), the Scholarship for Full-time Master's or Doctoral Study at a South African University by the NRF, the University of Cape Town Merit Award Bursary, as well as the Medical Research Council of South Africa.

Abstract

Heparin (Hep) and heparan sulfate (HS) have been shown to possess anti-coagulative properties, inhibit smooth muscle cell proliferation, moderate inflammation and control angiogenesis by stabilization and potentiation of growth factors (GF). These properties are potentially very useful for the treatment of cardiovascular diseases, especially when delivered as injectable hydrogels that can form in situ. This project focused on developing Hep and HS hydrogels for localized GF delivery.

Hep and HS were acrylated, characterized and crosslinked with PEG tetra-thiols, either directly (10m% Hep/HS-Ac, Type 1) or by copolymerization with 20PEG8Ac or 20PEG8VS (4m% copolymer; 1.5% Hep/HS-Ac) to form degradable (Type 2D) or non-degradable (Type 2N) gels, respectively. Gelation times, viscoelasticity, swelling, mesh size, Hep/HS elution and activity, as well as GF incorporation and release were studied *in vitro.* Type 2D gels with covalently incorporated (CI) Hep and GFs were evaluated *in vivo* as ingrowth matrices in porous polyurethane (PU) scaffolds for healing response in a rat subcutaneous model.

Forty percent acrylation was readily achieved and Type 1, 2D and 2N gels formed after approx. 4, 7 and 3 minutes (37 °C, PBS, pH = 7.4), with storage moduli (G′) 4-5 kPa, 6-8 kPa and 9-11k Pa, respectively. Type 2N gels had faster gelation times and higher G' than Type 2D gels due to the higher relative reactivity of VS towards Michael-type addition reactions than Ac. After rapid initial swelling caused by equilibrium water uptake, Type 2N gels were stable for more than 6 months, while Type 1 and 2D gels showed increasing swelling ratios, which resulted in disintegration after 22 days in the case of Type 2D gels due to hydrolysis. Gel properties of Type 2 gels were not significantly influenced by the addition of non-covalently incorporated (NI) or CI Hep/HS.

The sustained Hep/HS release from Type 1 and Type 2D CI gels can be described by zero ($R^2 \geq 0.96, 0.93$; Hep-Ac, HS-Ac) order kinetics, while Type 2N CI gels followed first ($R^2 \geq 0.90, 0.84$) order release kinetics due to the absence of the secondary release mechanism. Conversely simple incorporation led to release of essentially all the Hep/HS within the initial two days. Anticoagulative activities of Hep and HS were retained in the original form, after chemical modification and after the

incorporation and release from Type 1 and 2 gels. Type 2D CI gels achieved 78% (PEG-Ac/SH/Hep-Ac) and 51% (PEG-Ac/SH/HS-Ac) more bonding of GF than in Type 2D control gels (PEG-Ac/SH). GF release from Type 2D CI and control gels followed zero ($R^2 \geq 0.91$, 0.99; Hep-Ac, HS-Ac) and first ($R^2 \geq 0.96$) order kinetics, respectively.

Gel incorporation limited tissue ingrowth after the first week of implantation, due to gel presence, while scaffolds without gel allowed full infiltration during this time. After 28 days the degrading gels were completely displaced by tissue. The use of Type 2D control gels in scaffolds resulted in the formation of fewer blood vessels than scaffolds without gel due to the gel presence causing a delay in tissue ingrowth. However, the capillary relative to ingrown area in scaffolds containing PEG-Ac/SH/Hep-Ac gels with and without GF were respectively 119% and 50% higher than scaffolds without gel. The controlled and localized delivery of CI Hep from Type 2D gels thus overcame the ingrowth inhibition, led to a significant and marked increase in angiogenesis *in vivo* and was even more profound when pro-angiogenic GFs (VEGF) were additionally delivered.

These Hep gels are potentially very useful for vascular graft applications where their potent anticoagulative properties could help retain patency while the GF binding and anti-inflammatory properties facilitate angiogenesis and healing. For cases where strong anti-coagulation may not be as desirable (such as myocardial infarction therapy) analogous HS gels may be more suitable.

Graphical Abstract

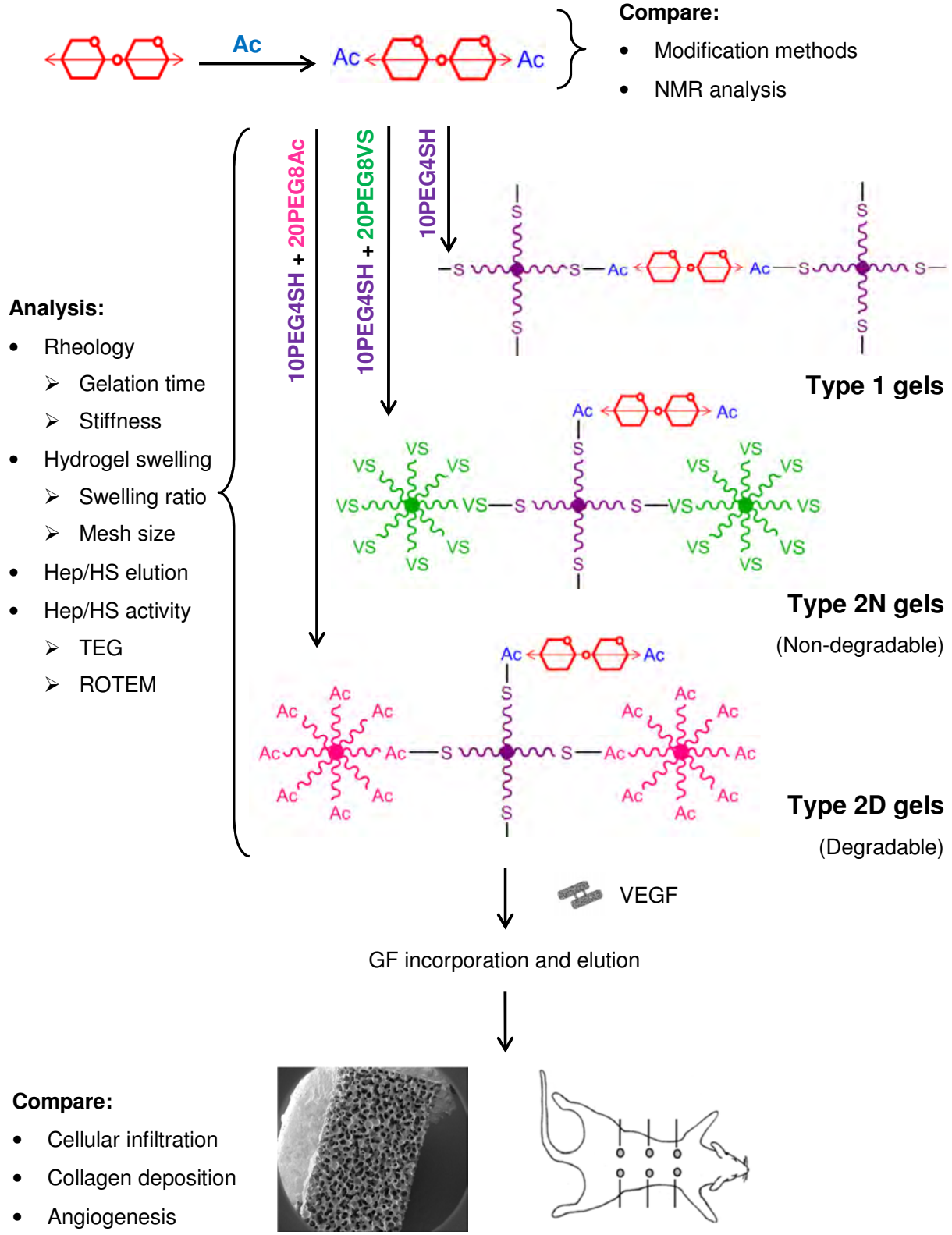

Table of Contents

List of Abbreviations

10PEG4SH	4 armed thiolated (SH) PEG with a molecular weight of 10 kiloDalton (kDa)
^{13}C	carbon-13
^{1}H	hydrogen-1 or proton
20PEG8Ac	8 armed acrylated (Ac) PEG with a molecular weight of 20 kDa
20PEG8OH	8 armed polyethylene glycol (PEG) with a molecular weight of 20 kDa
20PEG8VS	8 armed PEG vinyl sulfone (VS) with a molecular weight of 20 kDa
1D	one-dimensional
2D	two-dimensional
3D	three-dimensional
Ac	acrylate/acrylated
AcCl	acryloyl chloride
ADH	adipic acid dihydrazide
AEM	N-(2-aminoethyl) maleimide trifluoroacetate salt
APMMA	N-(3-aminopropyl) methacrylamide hydrochloride
AT	antithrombin
bFGF	basic fibroblast growth factor
BMP-2	bone morphogenetic protein-2
$CDCl_3$	deuterated chloroform
CI	covalent incorporation/covalently incorporated
–COOH	carboxyl groups
COSY	correlation spectroscopy
CVD	cardiovascular decease
d	doublet
D_2O	deuterium oxide
DCM	dichloromethane
dd	doublet of doublets
DI	deionised water
DMAP	4-dimethylaminopyridine
DMF	dimethylformamide
DMPA	2,2-dimethoxy-2-phenyl acetophenone
DTP	3,3'-dithiobis(propionic hydrazide)
DTT	dithiothreitol
EDC	1-ethyl-3-(3-dimethylaminopropyl)carbodiimide
EDTA	ethylenediaminetetraacetic acid
EGF	epidermal growth factor
ELISA	enzyme-linked immunosorbent assay
EPO	erythropoietin
EtOH	ethanol

GF	growth factor
GlcA	β-D-glucopyranosyluronic acid
GlcNAc	2-acetamido-2-deoxy-α-D- glucopyranose
$GlcNSO_3$	2-deoxy-2-sulfamino- α -D-glucopyranose
$GlcNSO_3$-3S6S	2-deoxy-2-sulfamino-α-D-glucopyranose 3,6-O-disulfate
$GlcNSO_3$-6S	2-deoxy-2-sulfamino- α -D-glucopyranose 6-O-sulfate
GMA	glycidyl methacrylate
H&E	haematoxylin and eosin
HA	hyaluronic acid
Hep	heparin
Hep/HS	heparin or heparan sulfate
Hep/HS-Ac	acrylated heparin or acrylated heparan sulfate
Hep-Ac	acrylated heparin
Hep-MA	methacrylated heparin
HGF	hepatocyte growth factor
HIP	heparin interacting protein
HMBC	heteronuclear multiple bond correlation
hMSC	human mesenchymal stem cell
HOBt	hydroxybenzotriazole
HS	heparan sulfate
HS-Ac	acrylated heparan sulfate
HS-MA	methacrylated heparan sulfate
HSQC	heteronuclear single quantum coherence
IdoA	α-L-idopyranosyluronic acid
IdoA-2S	α-L-idopyranosyluronic acid 2-O-sulfate
IGF-1	insulin-like growth factor-1
kDa	kiloDalton
KGF	keratinocyte growth factor
m	multiplet
MA	methacrylate/methacrylated
MAAn	methacrylic anhydride
Mal	maleimide functionalized
MBTH	3-methyl-2-benzothiazolinone hydrazone hydrochloride monohydrate
MI	myocardial infarct(ion)
n	sample size
$–NH_2$	primary amines
NHS	N-hydroxysuccinimide
NI	non-covalent incorporation/non-covalently incorporated
NMP	N-methylpyrrolidone
NMR	nuclear magnetic resonance

NVP	N-vinyl-2-pyrrolidone
OD	outside diameter
–OH	hydroxyl groups
PBS	phosphate buffered saline (pH=7.4)
PDGF	platelet-derived growth factor
PEG	polyethylene glycol
pH	$-\log[H^+]$
pK_a	$-\log[K_a]$, K_a =acid dissociation constant
ppm	parts per million
PU	polyurethane
PVA	polyvinyl alcohol
RGD	tripeptide Arg-Gly-Asp
RT	room temperature
s	singlet
SBA-PEG-SBA	N-hydroxysuccinimide ester of PEG-bis-butanoic acid
SD	standard deviation
SDF-1α	stromal cell-derived factor-1α
SH	thiol/thiolated
TEA	triethylamine
TGF-β2	transforming growth factor-β2
THF	tetrahydrofuran
TLC	thin layer chromatography
TOCSY	total correlation spectroscopy
Trizma	2-amino-2-hydroxymethyl-propane-1,3-diol
UV	ultraviolet
VEGF	vascular endothelial growth factor
VS	vinyl sulfone
WB	whole blood

Nomenclature/Glossary

in vitro	In an artificial environment such as a test tube rather than inside a living organism
in vivo	Existing or carried out inside a living organism, as in a test or experiment
anastomosis	A cross-connection between adjacent channels, tubes, fibres, or other parts of a network
angiogenesis	The development of new blood vessels
antithrombin	A small protein molecule that inactivates several enzymes of the coagulation system
atherosclerosis	A disease of the arteries characterized by the deposition of fatty material on their inner walls
autologous	Obtained from the same individual
bio-adhesives	Natural polymeric materials used for sticking objects or materials together
biodegradable	A substance capable of being decomposed by bacteria or other living organisms
bioprosthetic valve	An implanted device of non-synthetic origin designed to replace a defective heart valve
bradycardia	Abnormally slow heart action
cardiomyocyte	Cardiac muscle is a type of involuntary striated muscle found in the walls and histological foundation of the heart
cardioverter defibrillator	A device implantable inside the body, able to perform both cardioversion, defibrillation and pacing of the heart
chemokines	A family of small cytokines, or signaling proteins secreted by cells
chondrogenesis	The process by which cartilage is developed
collagen	A fibrous protein found in skin, bone, cartilage, tendon and other connective tissue
COSY	2D NMR that show correlation between adjacent protons within a given spin system
cytokines	Any of a number of substances, such as interferon, interleukin, and growth factors, which are secreted by certain cells of the immune system and have an effect on other cells
cytotoxic	Toxic to living cells
defibrillators	An apparatus used to control heart fibrillation by application of an electric current to the chest wall or hear
differentiation	To make or become different in the process of growth or development
edema	A condition characterized by an excess of watery fluid collecting in the cavities or tissues of the body
electrophile	A reagent attracted to electrons
endothelium	A layer of cells that lines the inside of certain body cavities, for example, blood vessels
fibrin	An insoluble fibrous protein produced by the polymerization of fibrinogen during the blood clotting process

fibroblasts	A type of cell that secretes the proteins that form collagen and elastic fibers and the substance between the cells of connective tissue
fibrosis	An abnormal thickening and scarring of connective tissue most often following injury, hypoxia, or surgery
glycosaminoglycans	Any of a group of compounds occurring chiefly as components of connective tissue; complex polysaccharides containing amino groups
haemorrhage	The loss of blood from a ruptured blood vessel
HMBC	2D NMR which shows correlations between carbons and protons that are separated by two or three bonds
HSQC	2D NMR which shows correlation between the aliphatic carbon and its attached protons
hyperkalaemia	A condition that occurs when your blood contains too much potassium
hypertrophy	The enlargement of an organ or tissue from the increase in size of its cells (of a body or an organ)
hypotension	Abnormally low blood pressure
immunogenicity	The ability of a particular substance to provoke an immune response in the body of a human or animal
immunohistochemistry	An assay that shows specific antigens in tissues by the use of markers that are either fluorescent dyes or enzymes
infarct	A small localized area of dead tissue resulting from failure of blood supply
ischemia	An inadequate supply of blood to a part of the body, caused by partial or total blockage of an artery
leucocytes	A colourless cell which circulates in the blood and body fluids and is involved in counteracting foreign substances and disease; a white (blood) cell
lipolysis	The breakdown of fats and other lipids by hydrolysis to release fatty acids
lyophilised	Freeze-dry
macrophage	A cell present in the blood, lymph, and connective tissues, removing waste products, harmful organisms and foreign material
mesenchymal	A type of tissue characterized by loosely associated cells that lack polarity and are surrounded by a large extracellular matrix
myocardial infarction	Destruction of heart tissue resulting from obstruction of the blood supply to the heart muscle
neurotrophic	Relating to the growth of nervous tissue
neovascularization	The formation of functional micro-vascular networks with red blood cell perfusion
nucleophiles	A chemical species that donates an electron pair to an electrophile to form a chemical bond in relation to a reaction
osteogenesis	A disease that causes weak bones that break easily
patency	Used to describe an artery, duct or other tube in the body that is naturally open and unblocked
pathology	The scientific study of the nature, origin, progress, and cause of disease
perfusion	Pumping a liquid into an organ or tissue (especially by way of blood vessels)
pericarditis	Inflammation of the pericardium

progenitor cell	A biological cell that, like a stem cell, has a tendency to differentiate into a specific type of cell, but is already more specific than a stem cell and is pushed to differentiate into its target cell
proliferation	Rapid reproduction of a cell, part, or organism
proteases	An enzyme which breaks down proteins and peptides
proteinase	An enzyme which breaks peptide bonds other than terminal ones in a peptide chain
proteoglycan	A compound consisting of a protein bonded to glycosamino-glycan groups, present especially in connective tissue
proteolysis	The breakdown of proteins into smaller polypeptides or amino acids
subcutaneous	Situated or applied under the skin
thrombin	An enzyme in blood plasma that causes the clotting of blood by converting fibrinogen to fibrin
thrombomodulin	An integral membrane protein expressed on the surface of endothelial cells and serves as a cofactor for thrombin
thrombosis	The formation or presence of blood clots that may partially or completely block an artery or vein
tissue engineering	The culture of living cells to form viable structures or organs
TOCSY	2D NMR which shows correlations between all protons within a given spin system
transanastomotic	An event that occurs across the anastomosis (juncture between the natural vessel and the prosthesis)
transcription factor	Proteins involved in the process of converting, or transcribing, DNA into RNA
transdermal	Relating to or denoting the application of a medicine or drug through the skin, typically by using an adhesive patch, so that it is absorbed slowly into the body
transmural	An event that occurs through the wall of the prosthesis
vascular graft	Vascular prosthesis or artificial blood vessel
vascularization	The organic process whereby body tissue becomes vascular and develops capillaries

List of Figures

List of Tables

1 Introduction

Since the discovery of the anticoagulative properties of heparin (Hep) in 1916,[1] the polysaccharide has been shown to possess numerous other advantageous properties. These include inflammation moderation, cell adhesion promotion and smooth muscle cells proliferation,[2–4] and the ability to control angiogenesis through the sequestration and potentiation of growth factors (GF),[5,6] which is the main focus of this project. Local, controlled and sustained GF delivery is known to induce localized growth of healthy vessels and to prevent undesirable side effects adverse to healing.[7–11] Therefore the incorporation of Hep into a suitable delivery device that can elicit specific biological responses, such as survival, proliferation and differentiation, is of interest in regenerative medicine.[12]

Hydrogels have proven themselves useful for drug delivery applications and several delivery routes have been developed over the years. Some of the favourable properties of hydrogels as controlled release systems include their drug protection ability, physical integrity and network structure provided by the crosslinks. The particular interest in this work was to synthesise spontaneously forming Hep eluting hydrogels, which have the potential to improve healing in the treatment of cardiovascular diseases, the second-biggest killer in South Africa and the leading killer worldwide.[13] However, in some instances the GF binding and anti-inflammatory properties of Hep are more important than its anticoagulative properties,[2] and therefore the use of a less antithrombotic agent, heparan sulfate (HS), was also considered.[14]

The remainder of this chapter will be dedicated to reviewing literature pertaining Hep/HS hydrogels, formed through Michael-type addition reactions in particular, for GF delivery, as well as their potential use in cardiovascular applications. Finally, the aims of the thesis together with novelties of the project will be presented in more detail.

1.1 Glycosaminoglycans

Proteoglycans and glycosaminoglycans (GAGs) are components of the extracellular matrix (ECM) and interact with a variety of molecules and ligands. These interactions are associated with coagulation, growth, inflammation, fibrinolysis and lipolysis.[15–17]

Since proteoglycans are formed by GAGs covalently attached to core proteins, their major function depends on the GAG component of the molecules. Most GAGs have the ability to stabilize GFs, cytokines and chemokines; signal molecules in response to cellular damage during wounding/infection; and regulate enzyme activity.[7,18–20] Glycosaminoglycans are negatively charged molecules constituting of long, unbranched heteropolysaccharides with alternating disaccharide units (dimers) and contain either of two modified sugars (*N*-acetylgalactosamine or *N*-acetylglucosamine) and uronic acid (such as glucuronate or iduronate). Hyaluronic acid (HA), dermatan sulfate, chondroitin sulfate (CS), Hep, HS, and keratan sulfate are GAGs of physiological significance, with specific focus on Hep and HS.

1.1.1 Introduction to Heparin and Heparan Sulfate

Heparin and HS are highly sulfated, anionic and heterogeneous GAGs of which the polysaccharide backbones constitute linear, alternating sequences of 1→4-linked uronic acid (I) and glucosamine (A) residues (as summarized in Table 1).[21,22] The backbones can be represented by $(I\text{-}A)_n$, where n varies from 10 – 200,[23] and the amino sugars of the residues may be N-acetylated or N-sulfated (of which the latter substituent is unique to Hep and HS).[2,24] Although Hep is polydispersed in nature, the major disaccharide repeating unit consists of iduronic acid 2-sulfate (1→4) glucosamine-2,6-sulfate (IdoA-2S – GlcNSO3-6S), that accounts for at least 85% and 70% of the dimers in Hep from bovine and porcine intestinal mucosa, respectively (see Fig. 1).[25–27] Heparan sulfate is similar in structure to Hep, except that it is less sulfated, contains higher acetylated glucosamines than Hep and the relative proportions of N-ester and N-sulfate content of the iduronic and glucuronic acids differ between Hep and HS.[14,28]

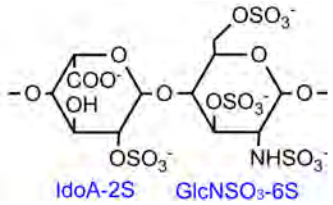

Figure 1: Major disaccharide repeating unit of Hep

Table 1: Abbreviations and chemical formulae for residues forming Hep/HS (red indicates the position(s) sulfated)

Compound	Name	Structure	Specification	Abbreviation
Uronic Acid (I)	β-D-glucuronic acid	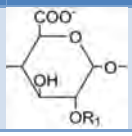	$R_1 = H$ $R_1 = SO_3^-$	GlcA GlcA-2S
	α-L-Iduronic acid	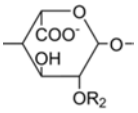	$R_2 = H$ $R_2 = SO_3^-$	IdoA IdoA-2S
Glucosamine (A)	N-sulfo-α-D-glucosamine	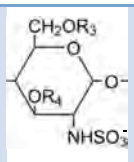	$R_3 = R_4 = H$ $R_3 = SO_3^-$, $R_4 = H$ $R_3 = R_4 = SO_3^-$ $R_3 = H$, $R_4 = SO_3^-$	$GlcNSO_3$ $GlcNSO_3$-6S $GlcNSO_3$-3,6S $GlcNSO_3$-3S
	N-acetyl-α-D-glucosamine	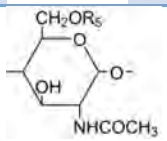	$R_5 = H$ $R_5 = SO_3^-$	GlcNAc GlcNAc-6S

Heparin is abundant in the liver and granules of mast cells lining blood vessels, while HS is found in the ECM and on the surface of most eukaryotic cells.[29] Their biological effects depend on specific and nonspecific ionic interactions mediated by charge density/distribution, sequence composition and molecular size. The acidic nature and extremely high negative charge of Hep and HS mediate their biological roles as multivalent binding agents for many proteins.[30–32] More than 100 proteins with heparinoid-binding domains have been identified in various studies, such as proteins involved in coagulation (primarily antithrombin III), fibrinolysis and lipid metabolism, various GFs, ECM proteins related to cell binding (laminin, fibronectin, vitronectin),[33] proteins associated with osteogenic differentiation (bone morphogenetic proteins and pleiotrophin), the cell-adhesion molecule protein family,[34] as well as mediators of the immune response (pro-inflammatory cytokines and chemokines).[2,35]

1.1.2 Anti-thrombotic Properties of Heparin and Heparan Sulfate

The anti-coagulative properties of Hep are mediated through a pentasaccharide sequence (see Fig. 2) contained in approximately one third of the chains. This sequence is known to bind antithrombin (AT) III which subsequently complexes thrombin.[28,36–39] The middle residue of the pentasaccharide, 3-O-sulfated glucosamine (in red), is key to high-affinity binding of AT III.[28]

Figure 2: Pentasaccharide antithrombin-binding sequence. The residue in red marks the typical 3-O-sulfated glucosamine residue and the circled sulfate groups are essential (full circle) or marginally essential (dotted circle) for high affinity

Blood coagulation is initiated by tissue factor exposed during vascular injury and leads to the generation of thrombin. Since thrombin is known to convert fibrinogen to fibrin, activate factors V and VIII (key cofactors in coagulation) and activate platelets, which leads to generation of more thrombin, tight regulation of thrombin activity is essential to prevent excessive thrombosis.[40] Two anticoagulant pathways exist to regulate thrombin, namely the protein C and AT pathways. The protein C pathway is initiated when thrombin binds to thrombomodulin and converts it from a pro-coagulant enzyme to a potent protein C activator.[38] The AT pathway, on the other hand, inhibits thrombin and other clotting enzymes in a slow, progressive fashion through interaction with AT III.[28,38] Once Hep is released, in response to injury, it enters the serum and its pentasaccharides complex AT III. This results in conformational changes at the reactive centre loop of the AT and enhances its reactivity with thrombin, which has shown to accelerate the rate at which all the serine proteases of the coagulation cascade are inhibited by two to three orders of magnitude.[28,38,41]

Although there are many structural and functional similarities between Hep and HS, an important difference lies in their anticoagulative activities. Similar to Hep, HS binds AT III via a unique pentasaccharide sequence containing the 3-O-sulfated glucosamine residue, but the pentasaccharide only comprises one to ten percent of the glycosaminoglycan side-chains. Heparan sulfate is therefore known to be less antithrombotic than Hep. Hoppensteadt et al. (1990) confirmed this with a rabbit model of stasis thrombosis which had shown that a five to ten time's higher dose of HS was required to produce an equal antithrombotic effect as Hep and, regarding the haemorrhagic effects, Hep had also shown much stronger platelet interactions than HS.[14,42,43] However, an investigation by Weitz et al. (1996) had shown that HS is not completely non-antithrombotic.[38] They generated mice deficient in 3-*O*-

sulfotransferase-1 (an enzyme responsible for 3-*O*-sulfation of the glucosamine residue within the pentasaccharide sequence) and showed that the ability of HS to bind to AT was only attenuated.[28,38,44]

Even though Hep is a common antithrombotic agent, there are bleeding side effects associated with its use in certain biomedical applications - especially when administered at high doses to fully exploit the heparinoid's anti-inflammatory and GF binding properties.[14,28,45] Due to the reduced amount of AT binding pentasaccharides present in HS, little to no bleeding side effect has been observed at HS dosages in the antithrombotic range.[14] Heparan sulfate will therefore be used as an alternative to Hep to develop solutions to applications where anticoagulation are not needed or may even be detrimental, but which still have the need for GF binding and anti-inflammatory properties.

1.1.3 Growth Factor Binding Properties of Heparin and Heparan Sulfate

Heparin and HS have also attracted a lot of research attention due to their ability to bind GFs, potentiate and retain their activities, stabilize their active conformations, and protect them from immediate clearance, degradation or thermal/proteolytic inactivation and limit their activity to cells liberating the GF during proteolytic remodelling of ECM.[46–53] Interactions between Hep/HS and GF's occur by shape recognition, as well as electrostatic attractions between N- and O-sulfated residues of Hep/HS and the lysine and arginine residues of the GFs.[16] To date Hep has shown high specific binding towards fibroblast GFs (FGF), vascular endothelial GFs (VEGF), platelet-derived GF (PDGF), glial-derived neurotrophic factor (GDNF), human growth hormone and transforming GFs beta (TGF-β).[54–59] Heparan sulfate has also shown to modulate the binding and signalling of GFs, including FGF, VEGF and heptocyte GF (HGF).[60,61]

1.1.4 Need for Controlled Heparin and Heparan Sulfate Delivery

For certain tissue engineering and biomedical applications Hep/HS delivery should be localized and controlled to maintain optimum Hep/HS concentrations in the target tissues and minimize side effects. Although Hep/HS can be introduced to the blood circulation through several ways, such as directly via intravenous injection or via transdermal or oral routes (secondary) from where the drug is absorbed into the circulation, its delivery should be controlled to obtain the optimal concentration (not

too high or too low) at the area of interest. Furthermore, when Hep/HS enters the circulation many different cells and organs accessible to the blood system are exposed to unnecessary treatment. It is therefore important for certain applications that Hep/HS should be administered by means of a drug delivery system which releases it over a specified period of time and at a rate which is determined by the needs of the body. Since drug delivery using hydrogels is well known for meeting the demands of both controlled and local release, these will be discussed for Hep and HS release.

1.2 Hydrogels

1.2.1 Introduction to Hydrogels and Applications

Hydrogels are insoluble, three-dimensional (3D) polymer networks that are swollen by and capable of absorbing/retaining a significant amount of water.[62] Due to the ability to control certain properties of hydrogels they are used in contact lens production, controlled release matrices, bio-adhesives and various other biomedical applications.[63,64] Since mechanical, solute permeability, elasticity, swelling, and hydrophilic/hydrophobic properties of a hydrogel can be tailored by choice of polymers and synthesis method,[65] it is possible to create gels that fulfil the demands of biomaterials with physical integrity and network structure suitable to be used as wound covers, implant coatings or materials that mimic *in vivo* functionality.[66,67]

In tissue engineering, hydrogels are also increasingly being used as cell carriers because of the structural and mechanical similarity between the ECM and a highly swollen hydrogel network (consisting of over 96% water).[68] Since these porous hydrogel scaffolds permit circulating cells to infiltrate them and allow diffusion of respiratory gases, nutrients and therapeutic agents through the gel, they are optimal vehicles for drug delivery, cell implantation, and regrowth of new tissue.[69] Hydrogels are particularly conducive to releasing water-soluble drugs due to their drug protection ability, rapid mass transport and highly predictable degradation (if tailored to be) conditions.[70] Controlled release mechanisms include diffusion, swelling, chemically controlled systems as well as environmentally responsive systems.

1.2.2 Polymeric Building Blocks and Crosslinked Networks

Since hydrogels are created when a sufficient number of crosslinks form between polymeric building blocks, their properties are mainly dependant on the nature (natural or synthetic), functionalization and geometry of polymeric building blocks, as well as the nature of the crosslinks formed between these polymers. This should all be taken into account when developing hydrogels suitable for localized and controlled drug delivery.

1.2.2.1 Natural and Synthetic Polymers

Natural polymers used as building blocks for hydrogel formation contain inherent biological properties, such as charged groups, signalling peptides and/or other functionalities, which make them useful for many tissue engineering applications.[16,71,72] These polymers include several polysaccharides (alginate, chitosan, collagen, dextran, fibrin, HA, Hep and HS) and proteins (collagen, fibrin, gelatine).[46,65] Moreover, polysaccharide-based hydrogels are known to be non-cytotoxic and biodegradable.[70] However, due to variation in composition and substitution pattern between different batches and polymer sources, hydrogel formation through natural polymers often deliver unpredictable results and potential risks of infectious pathogens and immunogenicity (especially in the case of animal-derived substances) exist.[73]

Synthetic polymers, on the other hand, offer greater control over the material properties of the gels and good repeatability. To date a wide range of synthetic polymers have been used to create hydrogels for utilization in cell scaffolds and drug delivery devices, including polyacrylic acid, polyethylene glycol (PEG), polylactic acid, poly-*N*-isopropyl acrylamide, poly-*N*-vinyl-2-pyrrolidone, poly-*N*-isopropylacrylamide (PIPAM) and polyvinyl alcohol (PVA). [52,65,74,75] In recent studies, natural and synthetic materials have been combined to form scaffolds providing not only mechanical stability and structural support, but also bio-functionality.[76,77] With this broad register of choices gels can be created with very specific properties that fulfil the strict demands of biomaterials.[65]

Polyethylene Glycol Hydrogels

One of the most studied and widely applied synthetic polymers for hydrogels is polyethylene glycol (PEG), prepared by polymerization of ethylene oxide.[68,78–80] Due to its widely reported low immunogenicity, biocompatibility, hydrophilicity, platelet/bacterial repellence and resistance to protein adsorption, it is often used in biomedical applications.[62,74] It is also non-reactive towards proteins, receptors and other parts of cell membranes and generally has a very low reactivity toward tissue due to its extensive interaction with water.[68] Moreover, hydrogels formed by PEG have been approved by the Food and Drug Administration in the United States for various medical uses such as valves, biosensors and surface mono layers in microarray devices.[77]

Although PEG by itself is nonreactive, the abundant hydroxyl pendant groups on the chains can be substituted with various reactive, functional groups that are able to form crosslinks and insoluble networks.[81] Polyethylene glycol functionalized with acrylates, methacrylates, vinyl sulfones, amines, sulfhydryls, maleimides, N-hydroxysuccinimide (NHS) esters, aldehydes and carbodiimides, among others, are well documented.[6,12,47,68,80,82–84] The PEG geometry is also important to obtain desired gel properties and to facilitate crosslinks, since it has an extreme effect on the swelling, mechanical strength, solute permeability and drug diffusion properties.[85–87] Common geometries of building blocks include linear, branched, star-shaped and dendritic structures.

1.2.2.2 Physical and Chemical Crosslinks

The mechanisms responsible for producing the crosslinks between the building blocks categorize hydrogels into either physical or chemical gels, while drug incorporation into the crosslinked network can also be of physical or chemical nature. Physical crosslinking occur either due to non-covalent interactions between polymers or as a result of entanglements between dynamic macromolecules. These gels form by crosslinking polymers functionalized with charged groups with species of the opposite charge, associating blocks to minimise contact with the surrounding media, hydrogen bonding, metal-ligand interactions, or through stereo-complexation.[62,88] The connections are generally electrostatic or solvent induced and reversible, allowing systematic re-establishment of the non-covalent bonds.[89,90] Chemical gels, on the other hand, are fabricated by the formation of covalent bonds between

functionalized polymers.[91] These gels are stronger, easier to adapt/modify and have greater mechanical properties than physical gels.

Delivery of drugs incorporated physically into gels (physical of chemical) constitutes systems where the drug is stored or dispersed within the gel and release is controlled by the design of physical parameters, such as crosslink density, degree of swelling and degradation rate. The release of drugs chemically incorporated into gels is dependent on the breaking of covalent bonds between the drug and hydrogel (through hydrolysis, enzymatic digestion or reduction of disulfide bonds) and is therefore potentially much more controlled than when physically incorporated.

Well known methods used for the chemical formation of covalent PEG crosslinked networks, which are capable of local, controlled drug delivery, include free radical polymerization, amide coupling reactions, enzyme-catalysed reactions, Michael-type addition reactions, thiolene chemistry and other click chemistries.[92,93] The focus of this thesis was however on Michael-type addition reactions.

Michael-type Addition Reactions

The Michael-type addition reaction (also known as 1,4-nucleophilic addition reaction) is a spontaneous reaction between α,β-unsaturated carbonyl compounds (Michael acceptors) and nucleophiles (Michael donors) which does not rely on radical chemistry.[94] The conjugating feature of the double bond renders the terminal carbon electrophilic and liable for a nucleophilic attack.[95] The nucleophiles deprotonate and react with the electrophiles, whereafter proton abstraction from the protonated solvent occurs. The reaction mechanism is illustrated in Fig. 3, an example of thiolated PEG (nucleophile) reacting with an α,β-unsaturated acrylate (electrophile):

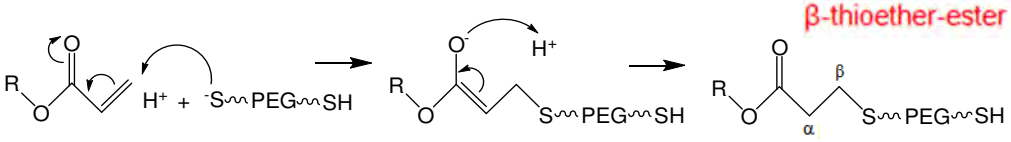

Figure 3: Reaction mechanism of Michael-type (1,4 nucleophilic) addition reaction

Michael-type addition reactions hold many potential advantages over other gel formation chemistries: hydrogels form spontaneously at physiological pH and temperature (pH = 7.4 and 37 °C), without the need for initiation by chemical agents or radiation and without producing leaving groups or undesirable side-

products.[7,12,23,96] In addition, these gels have the ability to form in situ by preparing an admixture of two components and injecting it directly into the treatment area, in close contact with biological molecules or tissue.[69,80] This allows the gels to conform to complex shapes and sizes *in vivo*, alleviating the need for further manipulation, and allows large amounts of material to be delivered through minimally invasive surgery. Since biological molecules (such as proteins, drugs and living cells) can be safely encapsulated by in situ forming gels[73,97] and the physical properties of the gels can be varied by functionality, molecular weight and crosslinker type, drugs can be released from the gels, with or without gel degradation.[80]

1.2.2.3 Degradable or Non-degradable Crosslinked Networks

Depending on the nature of the crosslinks formed between functionalized building blocks the resulting gels may be degradable or non-degradable, while the drug incorporation can also be of degradable or non-degradable nature. For many *in vivo* applications it is desired that the applied hydrogel degrades, since shorter exposure to the gel will lower its risk to cause a long-term inflammatory response. While acting as a temporary, mechanical 3D support for cell growth,[62] certain PEG gels can be degraded and the products dissolved into the circulatory system, whereafter it can be cleared via renal and hepatic pathways.[51] Although degradable gels decrease the occurrence of long-term inflammatory responses, the degradation process and resorption into the body can also initiate an inflammatory response.[80,98,99] Gel degradation through hydrolysis is therefore preferred, since it can be designed to occur over days to months, depending on the desired application.

There are instances, however, where more persistent gels are required and therefore injectable, non-degradable gels are developed which can act as mechanical support during heart remodelling (for example).[100] Our group applied such hydrogels in a rat infarction model in order to improve pathological remodelling in the early healing phase.[80] Although it successfully led to an increase in wall thickness and reduction in wall dilatation, a substantial inflammatory response was caused by the material. Gels that are able to release drugs over an extended period of time to influence the body's response to their presence were therefore required. Degradable and non-degradable gels suitable for drug delivery were therefore developed through Michael-type addition by Hubbell and co-workers,[47,68,101–105] and ever since several researchers have adopted and developed the methodology to obtain variations for a variety of applications.[81,86,94,99]

1.3 Growth Factor Delivery

1.3.1 The Role of Growth Factors in Angiogenesis

For many tissue engineering and biomaterial applications, in particularly cardiovascular tissue regeneration, treatment should ideally include the stimulation of angiogenesis. Angiogenesis is important for many physiologic processes, such as wound healing, tissue/organ development and female reproductive functions. The outgrowth of new capillary blood vessels from existing micro-vessels is however extremely complex and regulated by more than twenty known cytokines that appear in complex series. The process begins with secretion of GFs, followed by emergence of proteinase activity and the breakdown of the ECM (i.e. plasminogen activators; matrix metalloproteinase enzymes, MMPs; tissue inhibitors of MMPs; heparinise; chymase; and tryptase) and parent capillary basement membrane, which in turn cause further ECM-bound GF release.[106] Consequently endothelial cells migrate into the matrix to form capillary sprouts, which grow by continuing endothelial proliferation and organize into tubules to form a lumen. Contiguous tubules anastomose to form a new basement membrane which finally result in mature micro-vessels.[107]

Neo-vessel formation is crucial for regeneration of lost or diseased tissues, to ensure a functional vascular network for adequate integration into biomaterials and/or tissue engineered constructs.[108–112] However, a large obstacle for tissue regeneration is that the innate angiogenic response is either too slow or inadequate to sustain prolonged cell survival.[113] Many researchers have therefore concentrated on enhancing angiogenesis by the administration of molecular regulators of angiogenesis, such as genes, recombinant proteins or factor-overexpressing genetically engineered cell transplants. Recombinant proteins include prototypic angiogenic proteins such as GFs, which are the focus in this project.

Every step of the angiogenic process is regulated by a balance between stimulatory and inhibitory cytokines, of which the most important are the prototypic angiogenic GFs, namely vascular endothelial GF (VEGF) and acidic/basic fibroblast GF (aFGF, bFGF).[112] Preclinical and clinical investigations have shown that the therapeutic delivery of angiogenic GFs through bolus injection (intra-arterially or directly into the sites of ischemia) and by sustained release from polymeric implants, could improve regional blood flow.[62,114–118] It has however been seen that serious complications can result from bolus delivery of high doses of GFs, such as severe vascular leakage into

the circulation or ischemic zone, which can lead to severe nitric oxide-dependent hypotension or edema, respectively.[119,120] Moreover, GF overdose can induce formation of highly fenestrated and non-functional capillary vessels due to the unregulated exposure of freely diffusible GFs, while the sustained exposure can result in malformed vessels.[121–123] On the other hand, early withdrawal of GFs can lead to ablation of new, immature vessels and prevention of lasting tissue vascularization. A further disadvantage of bolus injection is the short half-lives of GFs in the body - if delivered without stabilization the GFs diffuse rapidly, undergo proteolysis and consequently lose their bioactivity.[124]

1.3.2 Controlled Growth Factor Release

Controlled GF release systems have therefore been developed to avoid burst release and provide sustained exposure to low GF concentrations, which can support the localized growth of new, functional and lasting vasculature while preventing undesirable side effects adverse to healing. Since the ECM is known to store angiogenic GFs, regulate their release, localize their activities and prevent their degradation, biomaterials that share functionalities with the ECM are favourable to develop release systems in promotion of tissue repair and new tissue growth.[62] To date many polymeric biomaterials have been studied for GF delivery, including gelatin, alginate, ethylene-vinyl acetate, polyglycolic acid, PEG, chitosan, dextran, and different GAGs.[7] However, many of these materials have no or limited sites for biologically specific molecular interaction with the GFs or for specific signalling interactions with cells of the target tissue. Growth factor delivery is therefore either driven by diffusion or degradation and not always in tune with the healing process. The use of Hep for GF incorporation is however a very promising approach due to its high affinity for GFs. The Hep-GF interaction avoids GF damage, maintains biological activity upon release and relies on chemical degradation for GF release.[16]

Since the delivery of Hep through hydrogels is well known for meeting the demands of both controlled and local release, as well as the numerous advantages for tissue engineering applications stated before, these gels are ideal GF delivery vehicles. It combines a synthetic component (PEG) to modulate bulk properties, such as modulus, biodegradability, crosslinking, and an ECM component (Hep) to sequester, stabilize and protect GFs. Simultaneously the gel serves as provisional ingrowth matrix to guide cell migration and regenerate functional tissue in the place of the hydrogels. This conjugation does not only bring the GF into solution but also

increases the persistence of GF at the disease site, confining its availability to a targeted region and thus avoiding angiogenesis at unwanted sites.[35] The presence of Hep is crucial since PEG hydrogels are normally resistant to cell adhesion, while evidence exists that Hep can promote cell adhesion.[12,16,69,72,125,126] Functionalization with Hep further enables the gels to actively and selectively stimulate desired cell functions and maintain the functionality of the embedded GF during bulk material fabrication and release.[62] Since the rate of Hep hydrogel degradation can be tailored by varying the extent of crosslinking and the breakdown products have active, pro-angiogenic properties, the hydrogels actively participate in the tissue response, rather than merely serving as passive delivery mechanisms.[112]

1.4 Heparinoid/PEG Hydrogels

In order to ensure the controlled release and prolonged *in vivo* residence time of Hep/HS modification different approaches have been reported to covalently incorporate Hep/HS into hydrogels. These methods include modification of free amine groups,[52,127] carboxylic acid groups[7–9,23,35,59,97] or hydroxyl groups[12,69,128] on the polysaccharide. Literature regarding the functionalization and crosslinking of GAGs, specifically Hep and HA, which can be copolymerized/crosslinked with PEG to form hydrogels suitable for controlled GF delivery, have been investigated, as discussed below and summarized in Table 2. Together, these works demonstrate the utility of covalently incorporating Hep into PEG-based hydrogels to promote cell adhesion, proliferation, differentiation and the controlled delivery of GFs for clinical applications in tissue regeneration.[129]

1.4.1 Hyaluronic Acid: Hydroxyl Group Modification

Smeds et al. methacrylated HA (HA-MA) by targeting the hydroxyl groups of HA with methacrylic anhydride (MAAn), whereafter they crosslinked it through photo-polymerization with N-vinyl-2-pyrrolidone (NVP), 2,2-dimethoxy-2-phenylacetophenone (DMPA) and ultraviolet radiation.[73] Modification of HA hydroxyls was also performed in various other studies by making use of acrylic acid/acryloyl chloride/methacryloyl chloride, with or without the presence of phase transfer catalysts. Thereafter these precursors were capable of hydrogel formation through enzyme mediated crosslinking.[128,130]

1.4.2 Hyaluronic Acid: Carboxyl Group Modification

Peattie et al. functionalized the HA carboxyls with adipic dihydrazide (ADH), after activation with 1-ethyl-3-(3-dimethylaminopropyl) carbodiimide (EDC), and crosslinked it with PEG-dialdehyde. These hydrogels were capable of sequestering and releasing VEGF or bFGF, which successfully promoted a controlled angiogenic response *in vivo*.[83,112] In another study dual GF-induced angiogenesis was obtained *in vivo* by preloading hydrogels with VEGF and keratinocyte GF (KGF).[111] Hyaluronic acid was thiolated (HA-SH) by a reaction with 3,3-dithiobis(propionic hydrazide) (DTP), in the presence of the EDC, followed by reduction with dithiothreitol (DTT). Thereafter the HA-SH was crosslinked with acrylated PEG (PEG-Ac) through Michael type addition.[111,131,132] Hahn et al. developed hydrogels capable of the sustained release of erythropoietin (EPO) by reacting the carboxylic acid groups of HA (activated by EDC) with ADH, followed by either MAAn or traut's reagent to obtain methacrylated HA (HA-MA)[96] or HA-SH,[98] respectively. Thereafter the HA-MA was crosslinked with DTT by Michael-type addition, and HA-SH with sodium tetrathionate.

1.4.3 Heparin: Hydroxyl Group Modification

Polyethylene glycol (PEG) hydrogels functionalized with Hep were utilized by Benoit et al. as a 3D synthetic scaffold for osteogenic differentiation of human mesenchymal stem cells (hMSCs): Hep-MA, formed by reacting MAAn with Hep, whereafter it was crosslinked by photo-induced polymerization with methacrylated PEG (PEG-MA) and analysed as a localized delivery vehicle for bFGF to promote cell adhesion and proliferation.[12,16] A study performed by Nilasaroya et al. also made use of Hep-MA (Hep hydroxyl groups functionalized with glycidyl methacrylate, GMA), but crosslinked it with methacrylated polyvinyl alcohol (PVA-MA) through UV irradiation.[69,133] Yamaguchi et al. also synthesised hydrogels capable of binding and releasing bFGF in a controlled manner, but through Michael-type addition of maleimide (Mal) functionalized Hep (Hep-Mal) with end-terminated star PEG.[52] In this study the amine groups on Hep were N-deacetylated with hydrazine and reacted with succinimidyl 4-(*N*-maleimidomethyl)cyclohexane-1-carboxylate to obtain Hep-Mal, which was crosslinked with thiolated PEG (PEG-SH) and copolymerized with heparin-binding peptides (HIP) attached to vinyl sulfone functionalized PEG.[52,127]

1.4.4 Heparin: Carboxyl Group Modification

Several researchers investigated the modification of the carboxylic groups on Hep. Recently Oliviero et al. developed hydrogels to elicit new micro-vessel growth *in vivo* through the sustained delivery of VEGF. Heparin was methacrylated, using N-(3-aminopropyl) methacrylamide hydrochloride (APMMA), and crosslinked with PEG-MA via photo-induced radical copolymerization.[134] Similar to the approach of Peattie et al., Cai and co-workers thiolated Hep, HA and CS (Hep-SH, HA-SH and CS-SH, respectively) and covalently linked them, separately, to 20PEG8Ac via Michael-type addition reactions. These GAG-based hydrogels were investigated to stimulate *in vivo* angiogenesis through the slow release of non-covalently incorporated bFGF.[7] Similar hydrogels were synthesized and evaluated by Pike et al. and Elia et al., but for the controlled release of VEGF[8] and combinations of the cytokine GFs (VEGF, angiopoietin-1, Ang-1, KGF and platelet-derived GF, PDGF),[9] respectively. Both showed improved localized angiogenic responses to implanted Hep hydrogels *in vivo.*

Vascular endothelial GF was non-covalently incorporated into hydrogels developed by Tae et al., who crosslinked modified Hep (through carbodiimide chemistry) with the NHS ester of PEG-bis-butanoic acid (SBA-PEG-SBA).[23] In another study GF-loaded hydrogels were also formed by copolymerization of SBA-PEG-SBA with hydrazide-functionalized heparin (Hep-ADH), to promote cartilage formation and chondrogenesis through the controlled release of bone morphogenetic protein-2 (BMP-2), transforming GF-β2 (TGF- β2) and insulin-like GF-1 (IGF-1).[135]

Successful sequestering and controlled release of bFGF for different wound-healing and vascular therapies were also achieved in various studies by crosslinking Hep-Mal with PEG-SH through Michael-type addition.[35,136–138] These studies utilized chemical methods that permit controllable modification of Hep with aminoethyl maleimide groups (AEM) by employing EDC and 1-hydroxybenzotriazole hydrate (HOBt) as catalysts.[35] Cell responses and adhesiveness of the gels were also studied using human aortic adventitial fibroblasts.[138] In another example of carboxylate modification, Hep was thiolated with DTT, using cysteamines and carbodiimide chemistry, whereafter it was crosslinked with PEG-Ac using Michael-type addition to form hydrogels capable of cell encapsulation, proliferation and GF release.[59,97,139–141] Kim et al. and Tae et al. successfully encapsulated primary rat hepatocytes[142] and fibroblast cells,[97] respectively, within these hydrogels and

dedifferentiated chondrocytes were used to show that these hydrogels are further capable of inducing cartilage regeneration.[139]

1.4.5 Heparin: Amine Group Modification

To date many researchers have also made use of amide coupling for crosslinking injectable PEG-based hydrogels.[10,11,84,143–147] Freudenberg et al. developed hydrogels by copolymerizing thiolated Hep with amino end-functionalized star-PEG (PEG-Amine), after modification of the Hep carboxylic acid groups with sulfo-NHS.[10,11,84] These gels had shown to be successful at binding and delivering several GFs, including bFGF, VEGF, epidermal GF (EGF), PDGF and hepatocyte GF (HGF),[84,144] as well as dual GF delivery[10,11,146] to promote angiogenesis and cell proliferation. More recently Baumann et al. and Prokoph et al. also employed these gels for the localized release of stromal cell-derived factor-1α (SDF-1 α), to promote stem/progenitor cell recruitment.[143,145]

1.5 Release kinetics

Since drugs can be physically or chemically incorporated into hydrogels through various methods, attached drugs may be controlled by different mechanisms and released with different kinetics. The most commonly considered mechanisms for drug release are swelling, diffusion, degradation and the breaking of covalent bonds. To significantly ascribe experimentally obtained release data to any of these mechanisms, mathematical models are used. However, to assign an elution profile there are multiple parameters to consider and since each model makes certain assumptions it is only suitable for systems that fit those criteria.[148]

A commonly used model to describe diffusion controlled elution is the Higuchi equation, but is only valid for non-swelling and non-degrading thin films and is therefore not applicable to describe elution from hydrogels.[149,150] Models that consider swelling and degradation include the Hixson-Crowell and Korsmeyer-Peppas equations.[151] If experimentally obtained release data fits to the latter equation it may also be possible to distinguish whether the drug elution is primary controlled by the diffusion, swelling or a combination of the two mechanisms. [152] These equations were developed to describe the elution of physically incorporated drugs.[153,154] The release of chemically incorporated drugs is generally determined by

the degradation rate of the covalent linker. These links are commonly designed to degrade through hydrolysis, giving rise to unique zero or first order elution profiles.[86,154–156] Release data can be compared to representative equations to determine whether the release rate is dependent (first order) or independent (zero order) on the drug concentration.[153]

Only a limited number of the studies regarding Hep or HA containing PEG hydrogels discussed in Section 1.4 (summarized in Table 2), investigated release kinetics. Luo et al. loaded hydrogel films with anti-bacterial and anti-inflammatory drugs and found that pilocarpine, hydrocortisone, prednisolone and cortisone followed rapid first order release kinetics (released approximately whole amount in 10 min), while slow first-order release kinetics (1-24 hours) were observed for dexamethasone and prednisone.[83] Hydrogels comprising PEG-SH and Hep-Mal by Balwin et al. degraded via hydrolysis and released Hep, which also followed first-order kinetics.[136] In a study by Benoit et al. bFGF released from Hep-MA gels followed zero order release kinetics,[16] and in other studies with Hep hydrogels the release of VEGF[6] and BMP-2[140] also followed near linear sustained profiles. Since GFs are connected to Hep via electrostatic forces, the release profiles are however not due to covalent linkages. Although GF release from Hep hydrogels developed by Elia et al. occurred in part through diffusion and in part through gel breakdown, release models were not investigated in the study.[9]

Other factors influencing the release kinetics have also been reported in these studies, but were however not modeled. Yamaguchi et al. found that bFGF delivery from hydrogels was primarily matrix erosion controlled,[52,127] while release test from HA-MA hydrogels by Hahn et al. showed that the EPO release profile was dependent on the crosslinking reaction time and temperature.[96] Nie et al. showed that both the polymer concentration and Hep:GF ratio affected the release of bFGF.[35] Several of the other studies also included release experiments and found that covalently crosslinked Hep significantly retarded GF release from hydrogels, which therefore resulted in more controlled and sustained delivery.[7,8,10,59,69,84,134,141,143,144]

Table 2: Summary of literature decribing the functionalization and crosslinking/copolymerization of GAGs with PEG to form hydrogels

Functional group	Reactions summary	Gelation Reaction	Biomedical Aspects and Applications	GF/drugs released
HA-OH *Smeds et al. 2001; Kumar et al. 2009*	• HA + MAAn → HA-MA • HA-MA + initiator + UV → gel[73]	Photo-polymerization[73]	Sealing wounds & reconstructing soft tissues; sutureless surgery[73]	-
	• HA + Acrylic acid→ HA-Ac • HA-Ac + initiator + enzyme → gel[128,130]	Enzyme-mediated[130]	Potential cosmetic, biomedical & pharmaceutical applications[128,130]	-
HA-COOH *Peattie et al 2004; Peattie et al. 2006; Hahn et al. 2006a; Hahn et al. 2006b*	• HA + ADH + EDC → HA-ADH • HA-ADH + PEG-dialdehyde → gel[83,112]	Hydrazide-aldehyde reaction[83,112]	Stimulation of localized, synergistic angiogenic response *in vivo*;[112] sustained release of anti-bacterial & anti-inflammatory drugs[83]	VEGF/bFGF;[112] Dexamethasone, cortisone, ect[83]
	• HA + DTP + EDC + DTT → HA-SH • Hep-SH + PEG-Ac → gel[111,131,132]	Michael-type addition[111,131,132]	Dual GF-induced angiogenesis;[111] supports cell proliferation & growth;[132] wound healing & tissue repair[131]	VEGF & KGF;[111] fibroblast[131,132]
	• HA + ADH + EDC + MAAn → HA-ADH-MA • HA-ADH-MA + DTT → gel[83,96]	Michael-type addition[83,96]	Sustained release of EPO for the treatment of patients with anemia[83,96]	EPO[83,96]
	• HA + ADH + EDC + traut's reagent → HA-ADH-SH • HA-SH + tetrathionate → gel[83,98]	Michael-type addition[83,98]	Sustained release of EPO for the treatment of patients with anemia[83,98]	EPO[83,98]
Hep-OH *Benoit et al. 2007; Nilasaroya et al. 2008;*	• Hep + MAAn → Hep-MA • Hep-MA + PEG-MA + initiator + UV → gel[12,16]	Photo-polymerization[12,16]	Promote adhesion, proliferation & osteogenic differentiation[12,16]	bFGF & hMSCs[12,16]
	• Hep + GMA→ Hep-MA • Hep-MA + PVA-MA + initiator + UV → gel[49,69,157–159]	Photo-polymerization[49,69,157–159]	Presenting & activating GFs to promote cell proliferation;[69] development of salivary gland[157–159]	bFGF;[69] Salivary cells[157–159]
Hep-NH_2 *Yamaguchi et al. 2005*	• Hep + hydrazine-*N*-deacetylate + Mal-NHS ester → Hep-Mal • Hep-Mal + PEG-SH + PEG-HIP → gel[52,127]	Michael-type addition[52,127]	Bind & permit controlled release of GFs on the basis of specific peptide-heparin interactions[52,127]	bFGF[52]
Hep-COOH *Oliviero et al. 2012; Cai et al. 2005; Tae et al.2006; Nie et al. 2007;Tae et al.2007; Fredenberg 2009;*	• Hep + APMMA + EDC + HOBt → Hep-MA • Hep-MA + PEG-Ac + NVP + DMPA + UV → gel[134]	Photo-polymerization[134]	Stimulation of *in vivo* angiogenesis[134]	VEGF [134]
	• Hep + DTP + EDC + DTT → Hep-SH • Hep-SH + HA-SH + PEG-Ac → hydrogel[7–9]	Michael-type addition[7–9]	Stimulation of *in vivo* angiogenesis;[7–9] dual GF-loaded[9]	bFGF;[7] bFGF/VEGF;[8] VEGF, KGF&PDGF[9]
	• Hep + ADH + EDC + HOBt → Hep-ADH • Hep-ADH + SBA-PEG-SBA → gel[23,135]	Hydrazide-NHS ester reaction[23,135]	Stimulation of *in vivo* angiogenesis;[23] promote cartilage formation & chondrogenesis, dual GF-loaded[135]	VEGF;[23] IGF-1, TGF-β2 & BMP-2[135]
	• Hep + AEM + EDC + HOBt/NHS → Hep-Mal • Hep-Mal + PEG-SH → gel[35,136–138]	Michael-type addition[35,136–138]	Sustained & controlled release of GFs;[35,136–138] improved cell adhesiveness[138]	bFGF;[35] bFGF, fibronectin[138]
	• Hep + Cysteamine + EDC + HOBt → Hep-SH • Hep-SH + PEG-Ac → gel[59,97,139–141]	Michael-type addition[59,97,139–141]	Improved cell proliferation;[97] encapsulation & cultivation of primary hepatocytes;[59] regenerate cartilage in partial-thickness defects[139]	Fibrinogen;[97] HGF;[59] BMP-2;[140] TGF-β2[139]
	• Hep + EDC + sulfo-NHS → Hep-SH • Hep-SH + PEG-Amine → gel[10,11,84,143–147]	Amide coupling[10,11,84,143–147]	Neuronal differentiation & axo-dendritic outgrowth;[84] cell recruitment;[143,145] stimulation of *in vivo* angiogenesis;[10,11] cell proliferation[144]	bFGF;[84] SDF-1α;[143,145] bFGF& VEGF;[10,11] EGF/bFGF;[144] PDGF[146]

1.6 Anti-inflammatory Effects of Heparin

Although the anti-inflammatory properties of Hep are not the focus of this project it is important to understand the effects of Hep on the inflammatory response since the bulk fabrication of the gels, the chemical modification of the Hep and/or the presence of the GFs, among other factors, may interfere with the Hep and alter its properties. Since the hydrogels in this project (especially the degradable gels) are inert and formed in situ they are not expected to elicit a long-term inflammatory response. The gels are however in close contact with surrounding cells and therefore the anti-inflammatory properties of Hep should not be reduced during modification, incorporation or release.[68] The use of Hep as anti-inflammatory agent has previously been hindered because these activities were only expressed at high Hep concentrations, where the anticoagulant effects predominate.[2,160] Therefore HS hydrogels will also be developed for applications where strong anticoagulation is not desired.

An inflammatory response is usually characterized by the recruitment and activation of leucocytes, which account for destruction of foreign pathogens and remodelling of inflamed tissues.[161–164] Although leukocyte adhesion and activation are important components in wound healing, excessive adherence to the vascular endothelium may lead to intravascular aggregation and the release of undesirable oxygen radicals and proteolytic enzymes, which contribute to vascular and tissue damage. Inflammation is triggered and sustained by pro-inflammatory cytokines, prostaglandins and gaseous radicals.[164–166] Pro-inflammatory mediators and enzymes can, once stabilized by their receptors, activate a range of inflammatory cells responsible to direct and promote leukocyte migration and activation[167,168] and therefore most anti-inflammatory drugs target their production.[2,169]

However, due to the high negative charge of Hep/HS, it is also known to moderate inflammation by binding and neutralising many different positively charged proteins involved in the inflammatory cascade.[170] Heparin, therefore, either prevents the mediators and enzymes to interact with their respective receptors (inhibiting the activation of the inflammatory cells)[171–174] or inhibits the actions of enzymes and cytotoxic mediators released from these activated cells.[175–178] Other anti-inflammatory mechanisms of Hep/HS include its ability to inhibit adhesion of leukocytes (especially

neutrophils) to endothelial cells, as well as to limit their accumulation in inflamed tissues.[3,170,172,179–182] On a molecular level Hep/HS has also shown to bind nuclear factor kappa B, a transcription factor responsible for the regulation of a series of cytokine and adhesion molecules.[183,184]

When taking the different mechanisms responsible for the favourable anti-inflammatory properties of Hep/HS into account and since there is at present no evidence of a specific sequence of the Hep chain needed to exert an anti-inflammatory response (unlike its antithrombotic properties), these properties are not expected to be influenced significantly during Hep/HS modification and hydrogel formation.[2,3]

1.7 Cardiovascular Applications

As this work forms part and contributes to a large research project concerning vascular grafts and myocardial infarction (MI) treatment a short section on cardiovascular disease (CVD) is given for additional context.

Cardiovascular disease is a term used for a number of pathologies concerning the heart, its vascular network and the general vascular system throughout the body. Research conducted by Steyn and Fourie (2007) has shown that it is the second-biggest killer in South Africa by stating that, between 1997 and 2004, 195 people died per day due to CVD.[185] It is however not just a problem in South Africa, but exists in all populations of the world, remaining the leading global cause of death.[186,187] In a report from the American Heart Association it has been indicated that CVD accounts for 17.3 million deaths per year, representing 30% of all global deaths, and that this number is expected to grow to more than 23.6 million by 2030.[13] Since more than half the deaths caused by CVD are premature (80% of deaths caused by CVD in 2008 occurred before the age of 65 years), it not only has a major impact on people's lives, but also on the workforce, the economy and a country as a whole.[13,185–187]

Cardiovascular disease is often referred to as a "medical hydra" with no easy solution.[188] The first line of treatment is through non-pharmacological management - decreasing risk factors such as an unhealthy diet, use of tobacco, lack of exercise, stress, obesity, hypertension, diabetes, as well as high blood cholesterol.[185] As the condition progresses,

more advanced treatment options for CVD are needed. Therapeutic approaches for CVD are multiple and include pharmacological therapy, mechanical devices and surgical interventions.[189] However, most of the drugs used during these treatments (angiotensin enzyme inhibitors, beta-blockers, digoxin, diuretics, blood vessel dilators and calcium channel blockers, among others) have adverse effects, including worsening renal function, hyperkalaemia, hypotension, bradycardia and pericarditis.[190] Surgical interventions currently used include bypass surgery, pacemakers, ultrafiltration, cardioverter defibrillators, heart valve surgery, infarct exclusion surgery, as well as heart transplantation.[189,190] Although these methods are often successful, there are high risks and financial implications associated with them.[189]

Despite the treatments currently available there is still an urgent need for improved therapeutics for CVD, especially to avoid progression of the disease which leads to the need of heart transplantation or invasive surgery. This project is therefore aimed at the synthesis, optimisation and use of degradable and non-degradable Hep and HS containing PEG hydrogels for the tissue regenerative treatment of CVDs, in general, and in vascular graft applications and MI treatment, in particular. These hydrogels will be utilized in collaborative projects to facilitate spontaneous transmural endothelialisation in vascular grafts, by making use of the proven anticoagulative and angiogenic GF binding ability of Hep, while the latter ability will be employed in the treatment of MI though HS hydrogels.

1.7.1 Vascular Graft Application

Atherosclerosis is the slow, systemic build-up of plaque (fatty deposits, inflammatory cells and scar tissue) within the walls of arteries, which leads to compaction and loss of elastic tissue, calcification, ulceration, mural thrombosis, slow wall lysis, and consequently the cause of nearly three quarters of all CVDs.[191] At present the most effective method to treat atherosclerosis is by surgical intervention during which the afflicted arteries are replaced or bypassed with vascular grafts.[191,192] These grafts are therefore used for the treatment of numerous CVDs, such as ischemia, coronary heart disease and peripheral artery disease among others, through abdominal/thoracic aortic replacement or aortocoronary/pheripheral bypass surgery.[192]

Vascular grafts can be classified into two groups, namely bioprosthetic and synthetic grafts. Bioprosthetic grafts include autologous, homologous or heterologous tissues used in their untreated or modified form during bypass grafting procedures. However, due to the limited availability of healthy autologous vessels, grafts made either predominantly or completely of synthetic material are used as substitutes in vascular engineering. Since implantation of synthetic grafts often elicits a sequence of events, including acute and chronic inflammation, foreign body response, formation of granulation tissue, as well as fibrosis and fibrous encapsulation,[193] long-term patency can only be achieved if these grafts are developed to be biocompatible. Synthetic grafts made of polymeric biomaterials are often favoured in tissue engineering applications, as long as they allow complete integration or silent acceptance within the body. Pennel et al. showed that synthetic vascular grafts with increased porosity and pore-size allow for transmural endothelialisation which allows tissue to populate the outer and inner surface of the graft, without resulting in increased intimal hyperplasia.[194,195]

To further ensure graft patency the biocompatibility of these grafts can be improved by making use of hydrogels. Injection of these gels into the pores of a vascular graft will improve constructive interaction between the graft and the host tissue, causing functional incorporation and healing.[84,192,196] The use of degradable Hep hydrogels in vascular graft applications is based on several reasons: slow released Hep will decrease the thrombogenicity of the material, inhibit thrombogenesis inside the graft and attenuate inflammation. The PEG hydrogel, on the other hand, will ensure interaction with the host tissue by mimicking the ECM, serve as an ingrowth matrix to increase proliferation and migration of desired cell types into the material and minimize the long-term inflammatory response by degrading at the ingrowth rate.[197] Moreover, the release of pro-angiogenic GFs will improve cell proliferation, angiogenesis and endothelialisation in the graft as well as in surrounding tissue, ensuring adequate and rapid vascularization to achieve tissue regeneration.[8,9,110]

1.7.2 Myocardial Infarction Treatment

The most common cause of heart failure is a CVD known as MI. In 2005, 8.1 million patients suffered an MI, while approximately one third of these patients developed heart failure.[188] The heart responds to an MI by undergoing left ventricular remodelling,[198,199]

during which the left ventricle dilates to form a more spherical shape. This leads to an increase in left ventricular volume, elevated wall stress and, consequently, wall thinning.[198,200,201] Although the initial remodelling may be compensatory for the damaged pump, by preserving stroke volume via the Starling mechanism, the increasing wall stress leads to further remodelling.[198] This results in increasing interstitial fibrosis, cardiomyocyte hypertrophy, infarct expansion and/or further eccentric ventricular enlargement, which finally provokes heart failure.[202,203] Although heart transplantation remains the "gold standard treatment" for heart failure, the need for donor hearts far exceeds their availability and therefore an urgent need for alternative therapies, which can prevent the progression of the disease to the extent that a transplantation is needed, exists.[203]

The injection of hydrogels within the ventricular wall has been shown to be successful at increasing wall/scar thickness in the infarct zone,[204–206] counteracting elevated wall stress within the infarcted heart,[207] decreasing the infarct size,[205] and reducing unfavourable left ventricular remodelling.[206,208] Dobner et al. showed that the injection of a synthetic non-degradable PEG hydrogel as a permanent tissue integrated scaffold in a rat infarction model reduced left ventricular dilation post-infarct.[80] However, due to its non-degradability the PEG gel caused an on-going foreign body response.[203] The need for fully or partially degradable hydrogels, engineered to break down over several months, exists in order to potentially overcome the macrophage based inflammatory response, while still providing mechanical support for an extended period.

Since heart failure is a very complex pathology, it is desirable that injected hydrogels have additional functionalities above that of stress relief. Although Hep has previously shown to inhibit smooth muscle cell proliferation, moderate inflammation and control angiogenesis by potentiation of GFs,[5,6] these activities were only expressed at high Hep concentrations, where the anticoagulant effects predominate.[2,160] Bleeding side effects are therefore often associated with its use in some cardiovascular implementations, particularly in the left ventricle of the heart.[14,203] Heparan sulfate hydrogels can however be developed to provide mechanical strength for the critical early stages of the infarct (where strong anticoagulation is not desired), while locally delivering pro-angiogenic GFs which will reduce left ventricular remodelling by increased angiogenesis.[209–212]

1.8 Aims and Strategies

1.8.1 Aims

The objective of the study was to design, synthesise, optimise and evaluate injectable degradable and non-degradable Hep and HS containing PEG hydrogels capable of controlled, localized GF delivery for improved angiogenesis in tissue regeneration applications. This will be achieved by:

1. Modifying Hep and HS by covalent attachment of α,β-unsaturated groups, using controlled nucleophilic acyl substitution chemistry to achieve controlled and repeatable degrees of modification.
2. Preparing hydrogels from the modified Hep/HS by Michael-type addition reactions with multithiol crosslinkers, either directly (to compare Hep versus HS effect) or by copolymerization with functionalized PEGs (to include degradability/non-degradability and control over the Hep/HS content).
3. Retaining desired gel properties (crosslink density, degradation, stiffness and mesh size) when adding Hep/HS, while achieving controlled, extended and localized release of Hep/HS from the hydrogels.
4. Controlling the anticoagulative properties of the gels and their eluates from highly to reduced anticoagulation by the use of Hep and HS, respectively, while retaining GF binding capability and anti-inflammatory properties.
5. Binding pro-angiogenic GFs to the Hep/HS hydrogels and achieving controlled, extended and localized release of active GFs *in vitro*.
6. Evaluating and achieving improved vascularization *in vivo* when Hep/HS hydrogels containing GF are used in regenerative scaffolds.

1.8.2 Novelty of Project

The novelties in this thesis include the development of a controlled and repeatable approach for the functionalization of Hep/HS hydroxyl groups using acrylate moieties, with optimal degrees of modification. This guaranteed gelation through spontaneous Michael-type addition with multithiols at physiological pH and temperature (pH = 7.4 and 37 °C) in the absence of initiators or free radical polymerization, while retaining its activity and GF binding/delivery abilities. Since the specific Hep/HS modification method

does not produce leaving groups or spacers, Hep/HS is rendered in its original, unmodified form upon degradation of the relatively labile β-thio-ether ester linkages through hydrolysis.

Limited studies regarding the modification, crosslinking, polymerization and the evaluation of rheological, swelling and anticoagulant properties of HS hydrogels; comparison with Hep gels; as well as the modelling of the controlled, slow release mechanism of Hep/HS from PEG hydrogels have been performed. This work is therefore valuable to expand the understanding of the *in vitro* properties of these gels.

Determination of retained antithrombotic activities of eluates from Hep/HS containing PEG gels through rotational thromboelastometry (ROTEM) and its comparison with thromboelastography (TEG) results are novel, as well as the incorporation of pro-angiogenic GFs into these gels evaluated *in vitro* using enzyme-linked immunosorbent assay (ELISA). The evaluation of these specific degradable, Hep containing hydrogels *in vivo* in a rat subcutaneous model using scaffolds provides valuable information for future implementation in certain cardiovascular regenerative applications, specifically vascular grafts and myocardial infarct therapy.

2 Materials and Methods

2.1 Materials

All reagents were obtained from Sigma-Aldrich (Pty) Ltd. (Johannesburg, RSA), Fluka (Buchs, Switzerland) and Merck Millipore (Midrand, RSA), unless otherwise specified. Heparin (Hep) and heparan sulfate (HS) (both sodium salt, from porcine intestinal mucosa) were purchased from Celsus Laboratories (Cincinnati, Ohio, USA), while 8 armed polyethylene glycol (PEG) with a molecular weight of 20 kDa (20PEG8OH) and 4 armed PEG thiol (SH) with a molecular weight of 10 kDa (10PEG4SH) were obtained from Nektar Therapeutics, Huntsville, USA and Creative PEGworks, Winston Salem, USA, respectively.

2.2 Nuclear Magnetic Resonance Spectroscopy

1D (one-dimensional: ^{1}H and ^{13}C) and 2D (two-dimensional: Correlation Spectroscopy, COSY; Heteronuclear Single Quantum Coherence, HSQC; Total Correlation Spectroscopy, TOCSY; and Heteronuclear Multiple Bond Correlation, HMBC) Nuclear Magnetic Resonance (NMR) spectra were recorded using a Bruker DRX-400 spectrometer under standard quantitative conditions (RT, 10 s recycle delay, 128 scans). The ^{2}HOH signal (peak at 4.79 ppm) in proton experiments was suppressed by pre-saturation for 3 s. All samples were dissolved at 4 mg/mL in $CDCl_3$ and D_2O (as indicated) and filtered (0.45 µm) prior analysis. MestreNova 10.0 software was used for phase correction, baseline subtraction and integration.

2.3 Derivatization of Multi-arm PEG copolymers

Branched 20PEG8OH was derivatized with either acrylate (Ac) or vinyl sulfone (VS) to form 20PEG8Ac (**I**) or 20PEG8VS (**II**), respectively by following protocols adapted from literature as briefly described below.[47,80,213]

Synthesis of 20PEG8Ac: 20PEG8OH (10 g) was dissolved in 100 mL toluene. The solution was dried by azeotropic distillation (110 °C, 1 hr, Ar flow 1 L/min), cooled to 30 °C and diluted with dichloromethane (DCM, 37.5 mL). After further cooling (< 4 °C),

Triethylamine (TEA, 0.836 mL, 50 mole eq of OH groups) was added to the reaction solution, followed by the addition of acryloyl chloride (AcCl, 0.487 mL, 50 mole eq of OH groups) over 5 min. The reaction proceeded with stirring in the dark (overnight, RT). Purification was performed by filtration (to remove TEA/HCl salt), precipitation in diethyl ether (0 °C, 10 x excess volumes) and vacuum drying (RT, 750 mmHg, overnight). Re-precipitation was performed twice from DCM (2-3 mL DCM/g) in diethyl ether (0 °C, 10 x excess volume). The product was re-dissolved in 5 mL deionized water (DI), dialyzed (cut off value = 1 kDa, 24h) against DI and freeze dried to obtain a slightly off white powder (66% yield, 93% acrylation, see Fig. 4).

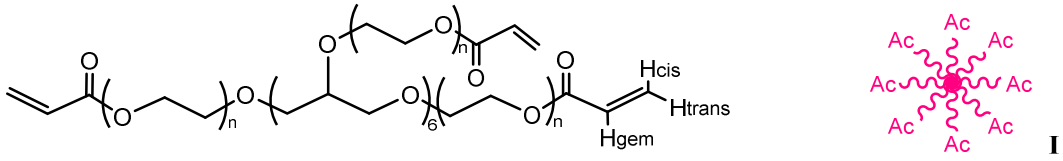

I

Figure 4: Structure of 20PEG8Ac (I, n≈54) 1H NMR (400 MHz, $CDCl_3$): δ = 3.39-3.67 (m; PEG), 4.30 (t, J = 5.5 Hz; PEG-OCH_2CH_2Ac), 5.82 (dd, J = 10.4, 1.5 Hz; H_{cis}), 6.14 (dd, J = 17.3, 10.4 Hz; H_{gem}) and 6.41 (dd, J = 17.3, 1.5 Hz; H_{trans}) ppm

Synthesis of 20PEG8VS: 20PEG8OH (10 g) was dissolved in 100 mL DCM. The solution was dried on 4 nm molecular sieves (overnight, RT) and purged (Ar flow 2 L/min). Thereafter anhydrous DCM (400 mL) was added with subsequent addition of sodium hydride (NaH, 65% in oil, 0.74 g, 5 mole eq of OH groups) and additional DCM (100 mL). After divinyl sulfone (DVS, 20 mL, 50 mole eq of OH groups) was added, the reaction solution was purged again (30 min, Ar flow 0.5 L/min) and left to react in the dark (48 hr, inert atmosphere). Glacial acetic acid (3.5 mL) was used to quench the remaining NaH. The resulting solution was filtered to remove precipitated acetate salt and its volume was reduced (to 100 mL) by rotary evaporation at RT. The product was purified as with **I** (30% yield, 94% modification, see Fig. 5).

Percentage modification for both copolymers was calculated from the integration of vinyl proton peaks of Ac or VS groups and proton peaks of the PEG repeat unit (OCH_2CH_2) for **I** or **II**, respectively (see Appendix B, Fig. 44 or Fig. 45).

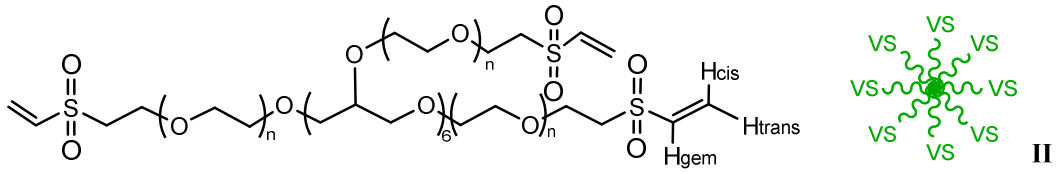

Figure 5: Structure of 20PEG8VS (II, n≈54); 1H NMR (400 MHz, $CDCl_3$): δ = 3.24 (t, J = 5.7 Hz, PEG-OCH_2CH_2VS), 3.44-3.73 (m; PEG), 3.89 (t, J = 5.7 Hz, PEG-OCH_2CH_2VS), 6.07 (d, J = 9.9 Hz, H_{cis}), 6.38 (d, J = 16.6 Hz, H_{trans}) and 6.80 (dd, J = 16.6, 9.9 Hz, H_{gem}) ppm

2.4 Molecular Weight Analysis of Heparin/Heparan Sulfate

Determination of the molecular weight (MW) of Hep/HS (**III**) is complex due to its structural heterogeneity. An experiment performed by 20 participating labs used gel permeation chromatography (GPC) with a single broad standard calibrant to determine the MW of Hep (sodium salt, from porcine intestinal mucosa) from Celsus Laboratories and since the same Hep was used in this project a MW of 15900 g/mole was used.[214–218] A molecular weight of 15000 g/mole was used for HS, as indicated by the supplier. The average MW of a disaccharide unit (dimer) was determined by using the following information from literature: (i) The major repeating dimer in Hep (see Fig. 6) accounts for at least 70% of dimers,[25,26] (ii) combination of dimers making up the unique hexasaccharide sequence (which contains the pentasaccharide binding site for AT III) occurs in 33% of the chains[219–225] and (iii) 85% of the glucosamines in Hep are N-sulfated. [221,226]

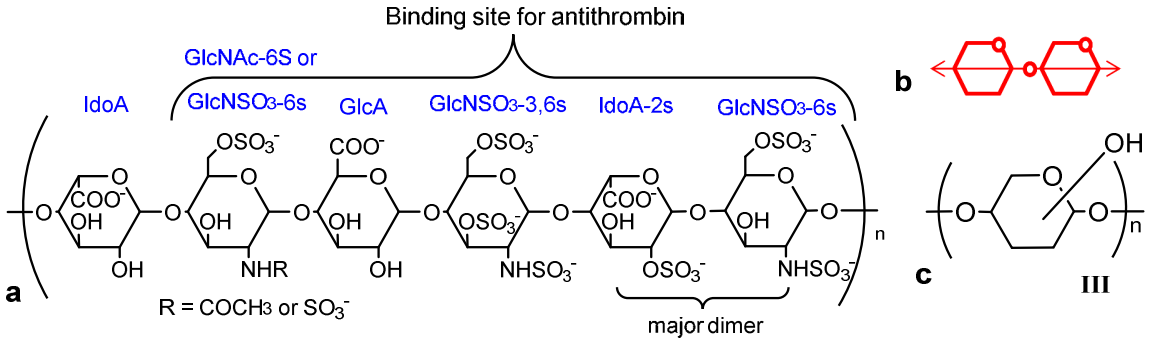

Figure 6: Hexasaccharide sequence, containing the pentasaccharide binding site for antithrombin (a); schematic for Hep/HS (b); abbreviated structure for Hep/HS (c)

Since (IdoA-2S)-($GlcNSO_3$-6S) in the hexasaccharide already accounts for 70% of the dimers, it can be estimated that (IdoA)-(GlcNAc-6S or $GlcNSO_3$-6S) and (GlcA)-

($GlcNSO_3$-3,6S) accounts for the other 30%, of which only 15% can be N-sulfated. The average MW of a Hep dimer was therefore calculated to be 550 g/mole using Eq. 1.

$$MW_{\text{Hep dimer}} = \left[0.7MW_{\text{IdoA}-2S} + 0.3MW_{\text{GlcA/IdoA}}\right] + \left[0.7MW_{\text{GlcNSO3}-6S} + 0.15MW_{\text{GlcNAc}-6S} + 0.075MW_{\text{GlcNSO3}-6S} + 0.075MW_{\text{GlcNSO3}-3,6S}\right] \quad \textbf{Eq. 1}$$

Heparan sulfate is considered to be similar in structure to Hep, but is less sulfated than Hep and has more than 20% N-acetylated glucosamine residues (GlcNAc and GlcNAc-6S).[227,228] This is confirmed by the comparison of Hep and HS spectra in Fig. 7, where the major signals appear in both spectra although they differ slightly in intensity and thus monosaccharide concentration. The integration of the signal of the N-acetylmethyl group (2.05 ppm) is also significantly higher in the HS than Hep spectra, confirming higher N-acetylation of HS glucosamines.

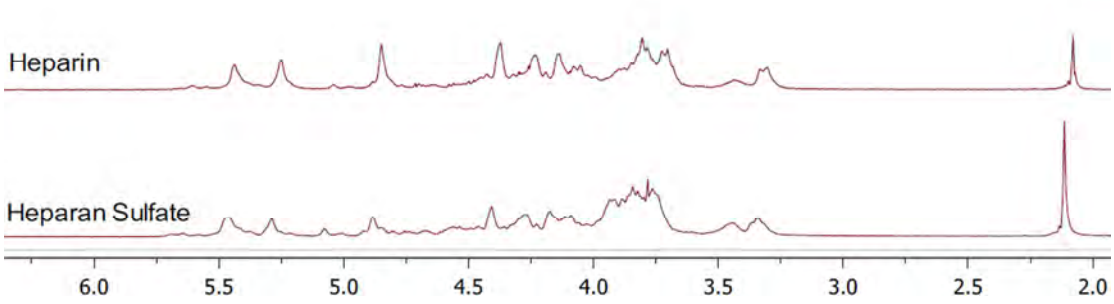

Figure 7: ^{1}H NMR spectra of Hep and HS

Based on the assumption that the major dimer is still most abundant (70%), the average MW of a HS dimer was calculated to be 515 g/mole using Eq. 2.

$$MW_{\text{HS dimer}} = \left[0.7MW_{\text{IdoA}-2S} + 0.3MW_{\text{GlcA/IdoA}}\right] + \left[0.7MW_{\text{GlcNSO3}-6S} + 0.2MW_{\text{GlcNAc/GlcNAc}-6S} + 0.05MW_{\text{GlcNSO3}-6S} + 0.05MW_{\text{GlcNSO3}-3,6S}\right] \quad \textbf{Eq. 2}$$

2.5 Synthesis of (Meth)acrylated Heparin/Heparan Sulfate

Three different electrophilically activated acrylating reagents, acryloyl chloride (AcCl, **1**); methacrylic anhydride (MAAn, **2**) and glycidyl methacrylate (GMA, **3**), were investigated for the modification of Hep and HS hydroxyl groups. Acrylation percentage (Ac %) was calculated by integration of three acrylate peaks representing vinyl protons (H_{cis}, H_{gem}, and H_{trans}, δ = 6.08, 6.21-6.35 and 6.53 ppm, respectively, see Fig. 13 or Fig. 47 in Appx.

B) over six peaks representing anomeric protons (A_1, I_1 and I_5, δ = 4.87-5.61 ppm, see Fig. 11 or Fig. 47 in Appx. B) of Hep/HS, which is represented by Eq. 3.[69,97,128]

$$Ac\ \% = \frac{\int(H_{trans}+H_{gem}+H_{cis})}{\int(A_1+I_1+I_5)} \text{ x } 100 \qquad \textbf{Eq. 3}$$

While methacrylation percentage (MA %) by integration of two methacrylate peaks (H_{cis} and H_{trans}, δ = 5.7 and 6.1 ppm, respectively) over the Hep/HS anomeric protons (see Eq. 4).[69]

$$\boldsymbol{MA\ \% = \frac{\int(H_{trans}+H_{cis})}{\int(A_1+I_1+I_5)} \text{ x } \frac{3}{2} \text{ x } 100} \qquad \textbf{Eq. 4}$$

2.5.1 Synthesis of Acrylated Hep/HS using Acryloyl Chloride

Syntheses using AcCl (see Fig. 8) were performed by: **1a**) controlled addition of AcCl, **1b**) interfacial reactions, **1c**) phase transfer catalysts inclusion, **1d**) buffer utilization and **1e**) usage of alternative solvents. Some of these methods were adapted from literature.[229,230]

1a: Hep/HS was dissolved in DI (0.02 g/mL) and stirred for 30 min (0 °C, pH = 9.5, 0.5 mL 0.1 M NaOH) to deprotonate the hydroxyl groups. Thereafter AcCl (2.5 mL, 20 mole eq of OH groups, 2.5 mL/h) was added to the Hep/HS solution with a syringe pump, ensuring controlled addition.[130] The reaction solution was allowed to stir for another hour (< 5 °C, pH = 8-9, 10 mL 1-5 M NaOH). Purification was performed by filtration of the reaction solution, precipitation of the filtrate in ethanol (0 °C, 10 x excess volume) followed by centrifugation (5 min, 2000 rpm, 0 °C), and vacuum drying of the resulting precipitate (RT, 750 mmHg, overnight). The product was re-dissolved in DI (5 mL), dialyzed (cut off value = 1 kDa, 24 hr) against DI and freeze dried (61-94% yield, 20-80%

1b: Three different interfacial reactions were performed: (i) N-hexane (Hex, 10 mL) was poured onto a Hep/HS solution (0.02 g/mL in DI) which had been stirred for 30 min (0 °C, pH = 9.5). Once an interface stabilized, AcCl (2.5 mL, 20 mole eq of OH groups) was added over 30 min. The solution was stirred for another hour (< 5 °C, pH = 8-9, 7 mL 1 M NaOH) whereafter the Hex was poured off and the resulting Hep/HS solution was purified, as with **1a** (52% yield, 8% acrylation). (ii) A similar procedure to (i)

was followed, but dichloromethane (DCM) was used instead of Hex (58% yield, 6% acrylation). (iii) A mixture of AcCl (2.5 mL, 20 mole eq of OH groups) and DCM (2.5 mL) was added to a Hep/HS solution (0.02 g/mL in DI) over an hour, stirred for another hour (< 5 °C, pH = 8-9, 1 M NaOH) and purified as with **1a** (58% yield, 12% acrylation).

1c: A solution of Hep/HS in DI (0.02 g/mL) was stirred for 30 min (0 °C, pH = 9.5). AcCl (2.5 mL, 20 mole eq of OH groups), DCM (2.5 mL), 4-dimethylaminopyridine (DMAP, 0.07 g, 6.4 mole eq of OH groups) and tetra-n-butylammonium bromide (TBAB, 0.08 g, 2.7 mole eq of OH groups) were mixed together and added to the Hep/HS solution over an hour.[231–234] Thereafter the solution was stirred for another hour (< 5 °C, pH = 8-9, 1 M NaOH) and purified as with **1a** (71% yield, 14% acrylation).

1d: Hep/HS (0.5 g) was dissolved in a phosphate buffer (pH = 8, 0.5 M, 1.65 g Na_2HPO_4 and 0.1 g NaH_2PO_4 in 25 mL DI, 0 °C) and stirred for 30 min. AcCl (2.5 mL, 20 mole eq of OH groups) was added to the Hep/HS solution over an hour, stirred for another hour (< 5 °C, pH = 8-9, 1 M NaOH) and purified as with **1a** (45% yield, 1% acrylation).

1e: Hep/HS (50 mg in 100 µL water) was dissolved in dimethyl sulfoxide (DMSO, 25 mL, 12 °C, pH = 11.4), whereafter AcCl (250 µL, 500 µL or 1000 µL; 10, 20 or 40 mole eq of OH groups) and triethylamine (TEA, 431 µL, 862 µL or 1724 µL; 1:1 ratio of AcCl) were added over an hour (8-12 °C, pH = 8-9). Purification was performed as with **1a**, but precipitation was performed using acetone instead of ethanol (56-63% yield, 0%, 3% and 9% acrylation for 10, 20 or 40 mole eq, respectively).

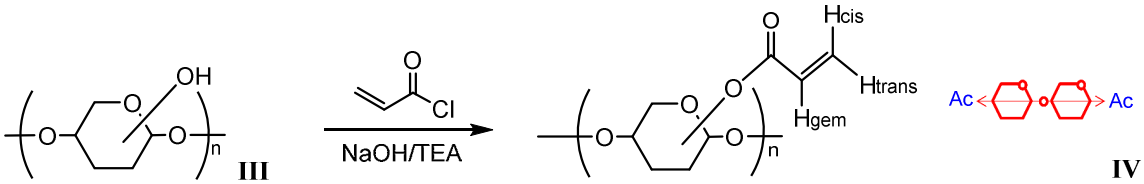

Figure 8: Reaction of Hep/HS (III) with AcCl to form Hep/HS-Ac (IV); 1H NMR (400 MHz, D_2O): δ = 6.08 ppm (dd, J = 18.6, 9.0 Hz, H_{trans}), 6.21-6.35 (m, H_{gem}), 6.53 (d, J = 17.4 Hz, H_{cis}) ppm

2.5.2 Synthesis of Methacrylated Hep/HS using Anhydride Chemistry

Hep/HS (0.02 g/mL in DI, 4 °C) was reacted with MAAn (2.5 mL, 20 mole eq of OH groups) for 2, 5, 8 or 16 hours (pH = 8.5, 5 mL 1M NaOH) as in Fig. 9 and followed by thin layer chromatography (TLC; ether), as adapted from literature.[12,16,73] Purification was

performed as with **1a**, with an additional re-precipitation step from DI into ethanol (51-60% yield, 11-13% acrylation).

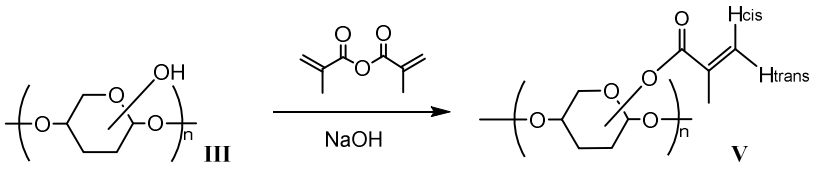

Figure 9: Reaction of Hep/HS (III) with MAAn to form Hep/HS-MA (V); 1H NMR (400 MHz, D_2O): δ = 5.84 (d, J = 21.3 Hz, H_{trans}), 6.24 (d, J = 22.9 Hz, H_{cis}) ppm

2.5.3 Synthesis of Methacrylated Hep/HS using Epoxy Chemistry

Hep/HS (0.1 g/mL in PBS_2, pH = 7.4, RT, see Appendix A for PBS_2) was reacted (RT, 14 days, Fig. 10) with GMA (127 µL, 318 µL or 636.5 µL; 2, 5 or 10 mole eq of OH groups) subjected to vigorous stirring. The reaction was followed by TLC (toluene), as adapted from literature.[49,69] Purification was performed as with **1a**, but re-precipitation was performed from DI into acetone (44-61% yield, 11-19% acrylation).

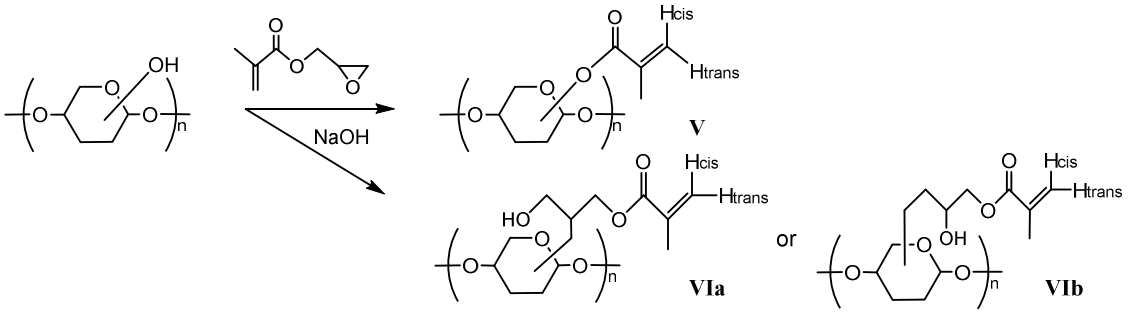

Figure 10: Reaction of Hep/HS (III) with GMA to form Hep/HS-MA (V) through transesterification or epoxy ring opening (3-methacryloyl-1-glyceryl ester, VIa, or methacryloyl-2-glyceryl ester, VIb). 1H NMR (400 MHz, D_2O): δ = 5.83 (s, H_{trans}), 6.27 (s, H_{cis}) ppm

2.6 Analysis of Heparin/Heparan Sulfate Hydroxyl Groups

The number and position of Ac groups on modified Hep/HS were evaluated by performing a thorough study of the compositional analysis of Hep/HS using NMR. Based on the analysis of spectra COSY (Fig. 48 and 49, Appx. B), HSQC (Fig. 50 and 51, Appx. B), TOCSY (Fig. 52, Appx. B) and HMBC (Fig. 53, Appx. B) of Hep and HS,

assignments were made for the major signals in the ^{1}H and ^{13}C NMR spectra, as displayed in Fig. 11 and 12, respectively. The signals respond to the main constituent monosaccharide residues of Hep/HS and are assigned as follow: A1: H_1 of $GlcNSO_3$-6S linked to GlcA; A1: H_1 of $GlcNSO_3$-6S linked to IdoA-2S; A1: H_1 of $GlcNSO_3$ linked to IdoA-2S; I1: H_1 of IdoA-2S; I1: H_1 of IdoA; I5: H_5 of IdoA-2S linked to $GlcNSO_3$-6S; A6: H_{6a} of $GlcNSO_3$-6S; I2: H_2 of IdoA-2S; A7: H_{6b} of $GlcNSO_3$-6S; I3: H_3 of IdoA-2S; I4: H_4 of IdoA-2S; A5: H_5 of $GlcNSO_3$-6S; A4: H_4 of $GlcNSO_3$-6S; A3: H_3 of $GlcNSO_3$-6S; A2: H_2 of $GlcNSO_3$-6S; A2: H_2 of GlcNAc; Ac: N-acetylmethyl protons. The positions of the signals for the ^{13}C NMR spectra are similar, but refer to the carbon instead of the proton (due to structure similarity only Hep spectra are further shown in this project; see Fig. 47 in Appendix B for proof of structure similarities).

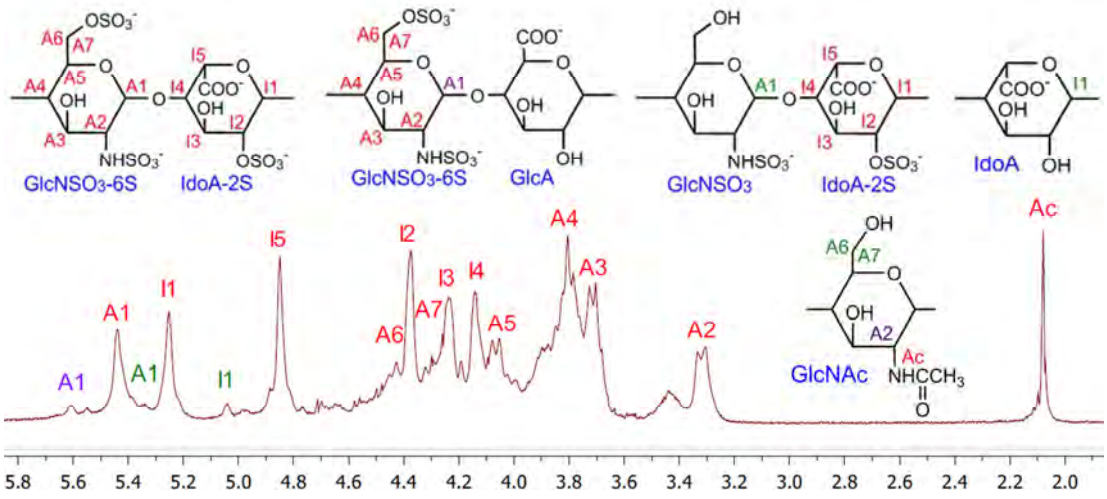

Figure 11: ^{1}H NMR spectrum of Hep with major signals

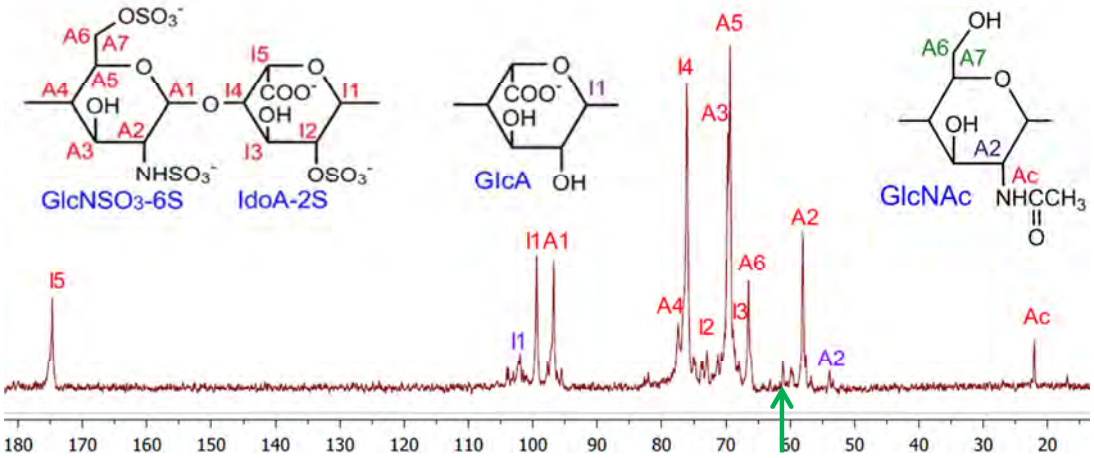

Figure 12: ^{13}C NMR spectrum of Hep with major signals

Since Hep and HS contain primary and secondary hydroxyl groups it was necessary to determine whether the primary and/or secondary hydroxyl groups were modified. Primary hydroxyls of most polysaccharide are less sterically hindered and more nucleophilic than secondary hydroxyl groups, therefore the reaction of acrylates with primary hydroxyls was expected to be faster in comparison to secondary hydroxyls.[235,236] The peak at 61 ppm (indicated by green arrow) in the Hep spectrum (Fig. 12) represents the methylene carbon (A6 and A7) of GlcNAc (see Fig. 46 in Appendix B for more detail). This peak is absent in the Hep-Ac spectrum, showing that all free primary hydroxyl groups were modified. However, since the signal is very small it implies that a small concentration of free primary hydroxyl groups is present in Hep, as confirmed by Toida et al. who found that only 4.8% of Hep dimers contained a primary hydroxyl group.[20,237]

After investigating acrylation percentages (reaching up to 80%) it was apparent that secondary hydroxyl groups were modified as well, since more modification occurred than primary hydroxyl groups present in Hep. Monosaccharide residues present in Hep were identified by using scalar connectivities in COSY (Fig. 48 and 49, Appendix B), but due to the structural complexity the peaks overlapped to a great extent. This resulted in similar coupling constants obtained for different Hep-Ac modification sites.[238,239] However, HSQC of Hep-Ac in Fig. 13 clearly showed the correlation between vinyl proton (H_{trans}, H_{gem}, H_{cis}) and carbon peaks (C_a, C_c, C_b) at 6.53/133.4, 6.28/127.1 and 6.08/133.4 (indicated in red box).

Cross peaks also appeared at 5.4/70.1 and 4.5/73.4 (circled in green) after acrylation which suggest deshielding of the protons on carbons at A3 and I2. Deshielding these protons resulted in the shielding of neighbouring carbons, which caused their proton signals to shift to the anomeric region. This systematic deshielding effect of the ring carbon at the position of attachment is characteristic of acrylation reactions, among others,[240,241] which suggest that the secondary hydroxyl attached to the carbon at A3 and I2 was acrylated. TOCSY and HMBC of Hep-Ac were also investigated to determine the number and position of Ac groups, but could not provide additional information due to partial esterification and the heterogeneous structure of Hep causing resonance overlaps.

Differentiation between the nucleophilicity of the different secondary hydroxyl groups in a polysaccharide is often difficult and almost impossible in a heterogeneous structure such as Hep.[236,242,243] It can therefore only be suggested that most modification occurred at the secondary hydroxyl attached to the carbon at A3 and I2 of the major dimer.[240,241] It can further be suggested that more modification occurred on glucosamine (at A3) than uronic residues (at I2), since the steric space occupied by the carboxyl groups on the uronic residues restricts modification. If carbon-13 enriched AcCl is used, which has been targeted at position C_a trough neutron activation, the exact modification positions might be determined. This process is however very specialized, expensive and unnecessary regarding the scope of this study.

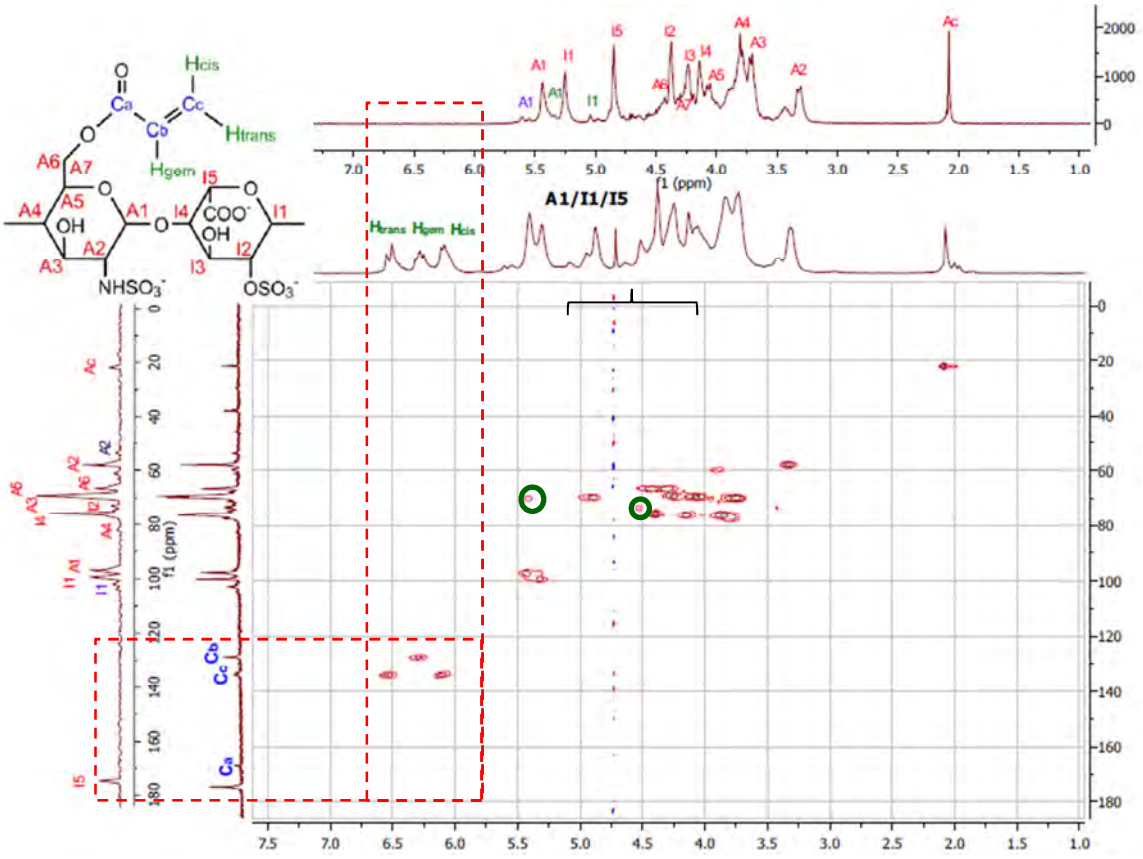

Figure 13: HSQC spectrum of Hep-Ac, with ^{1}H and ^{13}C NMR of Hep and Hep-Ac for comparison. Acrylate proton (H_{trans}, H_{gem}, H_{cis}) and carbon peaks (C_a, C_c, C_b), as well as correlation indicated in red boxes, crosspeaks due to deshielding shown by green circles

After determination of the position of Ac groups, it is possible to calculate the number of Ac moieties per Hep/HS chain after modification. The number of dimers per chain was calculated as 29 for Hep and HS, using Eq. 5.

$$\text{Dimers per chain} = \frac{MW_{Hep/HS}}{MW_{Hep/HS\ dimer}} \qquad \textbf{Eq. 5}$$

Since primary and/or secondary hydroxyls were modified the major dimer has two possible modification sites (hydroxyl groups) and the rest of the dimers either have one, two or three. A Hep chain therefore has approximately 58 hydroxyl groups (on average two per dimer). Thus, 40% acrylation represents approx. 11 Ac groups per Hep/HS chain, 10% acrylation represents approx. 3 Ac groups per Hep/HS chain, and 3% acrylation represents less than 1 acrylate group per Hep/HS chain.

2.7 Gel Formation

Two gel formation methods were investigated as briefly described below, i.e. photo-polymerization and Michael-type addition reaction. Although both methods were used to test the viability of Hep/HS-Ac and Hep/HS-MA to form gels when reacted with PEG crosslinkers, photo polymerization was not further investigated after the determination of gel formation due to the many advantages Michael-type addition reactions hold over photo-polymerization for the proposed applications of this study.[7,12,23,80,96]

2.7.1 Photo-polymerization

Gels (100 µL, 10m% nominal Hep/HS-Ac concentration) were formed by mixing 10 mg of Hep/HS-MA (**V**) or Hep/HS-Ac (**IV**) in 50 µL PBS_2 with 19.5 µL of 2,2-dimethoxy-2-phenylacetophenone (DMPA; 4.7 mg in 5 mL NVP; 1 mole% DMPA and 1000 mole% NVP regarding Ac groups). Thereafter it was irradiated by UV light (100 W, 5 min) at a distance of 15 cm. Control gels were made by UV irradiation of modified Hep/HS, a mixture of modified Hep/HS and DMPA (1 mole%), a mixture of modified Hep/HS and NVP, as well as a solution of DMPA in NVP (0.94 mg/mL); all in 100 µL PBS_2.

2.7.2 Michael-type addition reaction

Two different gel formulation groups were investigated for gels formed through Michael-type addition reactions and are referred to as Type 1 and 2 gels. Type 1 gels were formed by crosslinking 10% mass per volume Hep/HS-Ac with a stoichiometric amount of star-shaped PEG tetra thiol crosslinker (10PEG4SH, **VII**, see Fig. 14). Since Hep has previously been incorporated into similar hydrogels by our group, as well as various authors,[8,16,35,69,97,127] Type 1 gels were formed to compare the effect between Hep and HS in hydrogels. However, the large amount of Hep/HS present in these gels can be detrimental for the particular *in vivo* application and was therefore only tested *in vitro*.

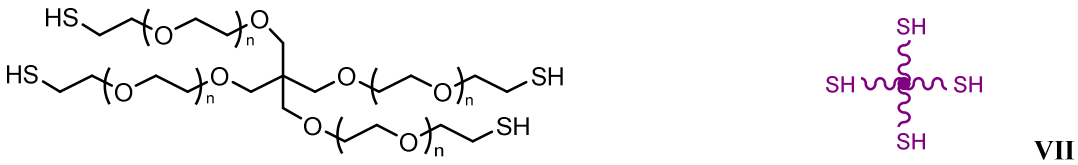

Figure 14: Structure of 10PEG4SH (VII, n≈54) used as crosslinker in Michael-type addition reaction

Type 2 gels were formed by crosslinking 4% mass per volume copolymer with a stoichiometric amount of PEG crosslinker (10PEG4SH). The copolymers were either 20PEG8Ac or 20PEG8VS (to form Type 2D and 2N gels, respectively) and Hep/HS-Ac (1.5 mass% of the copolymer). Type 2 gels provided more control over the Hep/HS content and the degradable nature of the gels - the reduction in solid content was based on faster ingrowth *in vivo* (as seen by Bracher et al.[244]) and the amount of Hep/HS-Ac was reduced based on the minimal Hep concentration capable of effective control of release,[8] as well as the potential of this amount of Hep/HS in a 100 µL gel to cause anticoagulation in a rat model without causing excessive bleeding or adversely affecting mechanical properties of the gels.[69] Since the effect of the covalent incorporation (CI) of Hep/HS into gels were investigated (*in vitro* and *in vivo*), control gels (without Hep/HS-Ac) and non-covalently incorporated (NI) gels (with unmodified Hep/HS instead of Hep/HS-Ac) were also formed.

The different gel formulations of Type 1 and 2 (D and N) gels are summarized in Table 3 followed by a brief description of their formation methods. It is important to note that only

Hep and HS modified by 40% acrylation was used, because that functionality has been determined to be high enough to guarantee gelation through Michael-type addition (previously seen by our group), while taking Hep/HS activity and its ability to sequester and release GFs into account.[35,69]

Table 3: Summary of the different gel formulations of Type 1 and 2 gels with their contents and abbreviations

				Copolymers (%**)***					
Categories			**Abbreviation**	**Hep**	**HS**	**Hep-Ac**	**HS-Ac**	**PEG-Ac**	**PEG-VS**
Type 1			**Hep-Ac/SH**	-	-	10	-	-	-
			HS-Ac/SH	-	-	-	10	-	-
Type 2	**Type 2D**	**Control**	**PEG-Ac/SH**	-	-	-	-	4	-
		NI gels	**PEG-Ac/SH/Hep**	0.06*	-	-	-	3.94	-
			PEG-Ac/SH/HS	-	0.06	-	-	3.94	-
		CI gels	**PEG-Ac/SH/Hep-Ac**	-	-	0.06	-	3.94	-
			PEG-Ac/SH/HS-Ac	-	-	-	0.06	3.94	-
	Type 2N	**Control**	**PEG-VS/SH**	-	-	-	-	-	4
		NI gels	**PEG-VS/SH/Hep**	0.06	-	-	-	-	3.94
			PEG-VS/SH/HS	-	0.06	-	-	-	3.94
		CI gels	**PEG-VS/SH/Hep-Ac**	-	-	0.06	-	-	3.94
			PEG-VS/SH/HS-Ac	-	-	-	0.06	-	3.94

*1.5m% of 4m% copolymer; Type 2D: degradable gels; Type 2N: non-degradable gels **mass percentage of copolymer present in the gel; *** 1:1 mole ration of crosslinker (10PEG4SH) added in comparison to copolymer

Type 1 gels: Gels were made (100 µL, n = 3, 10m% nominal Hep/HS-Ac concentration) by reacting Hep/HS-Ac (**IV**, 10 mg in 50 µL PBS_2) with 10PEG4SH (**VII**, 17.9 mg in 50 µL PBS_2) in a 1:1 mole ratio of SH to Ac groups (according to Eq. 6), and was allowed to react for 2 hr at 37 °C.

$$n_{SH} = n_{Ac} = \text{Ac \% x 2 x} \frac{m_{Hep/HS}}{MW_{Hep/HS\ dimer}} \qquad \textbf{Eq. 6}$$

Where n_{SH} is the mole of thiol groups, n_{Ac} is the mole Ac moieties, Ac % is the percentage acrylation, $m_{Hep/HS}$ is the mass of Hep/HS and $MW_{Hep/HS\ dimer}$ is the molecular

weight of a Hep/HS dimer. Type 1 gels are specifically referred to as **Hep-Ac/SH** and **HS-Ac/SH** throughout the thesis and the reaction is illustrated in Fig. 15.

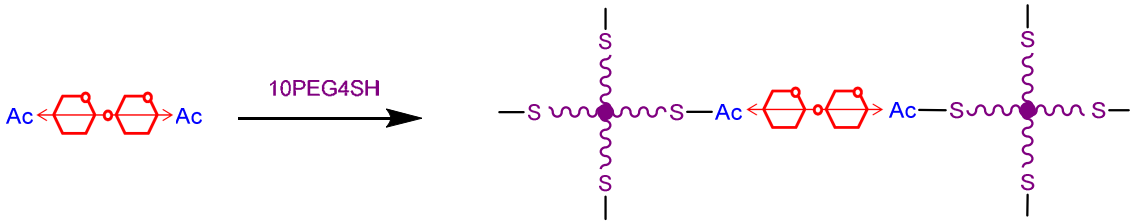

Figure 15: Reaction scheme of Type 1 gel formation through Michael-type addition reaction using Hep/HS-Ac and stoichiometrically equivalent amounts of 10PEG4SH crosslinker

Type 2 gels: Covalently incorporated (CI) gels (100 µL, n = 4, 4m% nominal copolymer concentration) were made by reacting 0.06 mg of Hep/HS-Ac (**IV**, 1.5m% of 4m% copolymer) in 10 µL PBS_2 with 10PEG4SH (**VII**, 4.04 mg in 50 µL PBS_2), followed by the addition of 20PEG8Ac (**I**) or 20PEG8VS (**II**) (3.94 mg of in 40 µL PBS_2) at 37 °C to form degradable (Type 2D) and non-degradable (Type 2N) gels, as illustrated in Fig. 16. The ratio of SH to total functional groups was 1:1, and determined using Eq. 7.

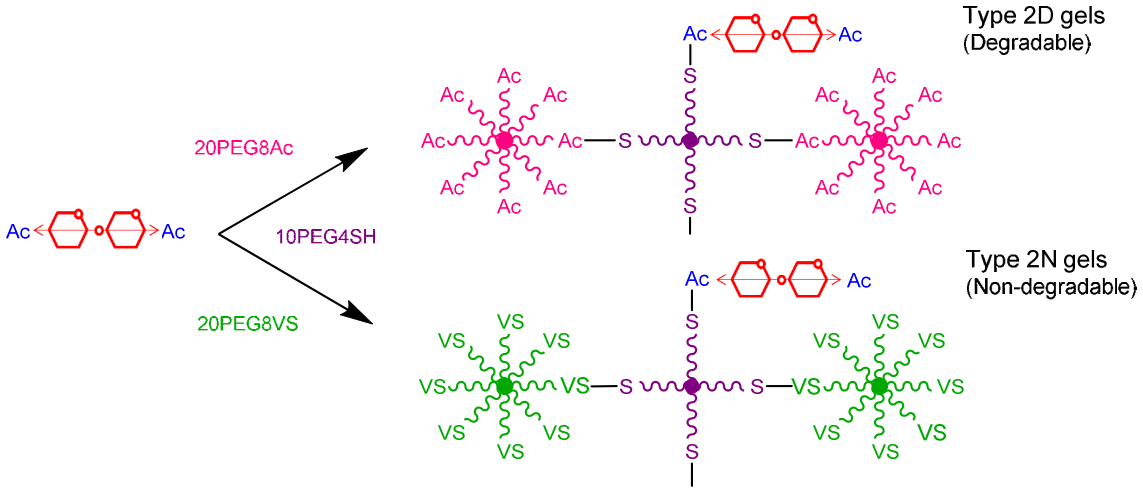

Figure 16: Reaction scheme for the pegylation and copolymerization of Type 2 CI gels using Hep/HS-Ac, 20PEG8Ac or 20PEG8VS (degradable or non-degradable gels, respectively) and stoichiometrically equivalent amounts of 10PEG4SH crosslinker

$$n_{SH} = \mathrm{n}_{I\ or\ II} + \mathrm{Ac}\ \%\ \mathrm{x}\ 2\ \mathrm{x}\frac{m_{Hep/HS}}{MW_{Hep/HS\ dimer}} \qquad \textbf{Eq. 7}$$

Where $n_{I \text{ or } II}$ is the mole Ac or VS moieties. Non-covalently incorporated (NI) gels (100 µL, n = 4; 4m% nominal copolymer concentration) were made similarly to CI gels, but Hep/HS was used instead of Hep/HS-Ac. Control gels (100 µL, n = 4, 4m% nominal copolymer) were made by reacting 10PEG4SH (**VII**, 4 mg in 50 µL PBS_2) with **I** or **II** (4 mg in 50 µL PBS_2) at 37 °C. In all cases the gels formed within 10 min, but were allowed to crosslink for 2 hr. The complete gel study design is represented in Table 4.

Table 4: Schematic representation of gel study design

Chemistry	Type of gel, contents and abbreviations				Analyses performed
Photo-Polymerization	Hep/HS-MA or Hep/HS-Ac + initiator + UV				Gel formation
Michael-type Addition	Type 1			Hep-Ac/SH	Gel formation, gelation times, viscoelasticity, swelling, Hep/HS elution and activity *in vitro*
				HS-Ac/SH	
	Type 2	Type 2D	Control	PEG-Ac/SH*	Gel formation, gelation times, viscoelasticity, swelling, mesh size, Hep/HS elution and activity, GF incorporation and release *in vitro; * in vivo*
			NI gels	PEG-Ac/SH/Hep*	
				PEG-Ac/SH/HS	
			CI gels	PEG-Ac/SH/Hep-Ac*	
				PEG-Ac/SH/HS-Ac	
		Type 2N	Control	PEG-VS/SH	Gel formation, gelation times, viscoelasticity, swelling, mesh size, Hep/HS elution and activity *in vitro*
			NI gels	PEG-VS/SH/Hep	
				PEG-VS/SH/HS	
			CI gels	PEG-VS/SH/Hep-Ac	
				PEG-VS/SH/HS-Ac	

2.8 Porous Scaffold Production

Porous polyurethane (PU) rods (5 mm OD) were produced via phase inversion/porogen extraction.[110,245] Cylindrical columns of sized gelatin beads (125–180 µm, Thies Technologies, St Louis) were infiltrated with a 20% (m/m) solution of segmented PU (M48) in N-methylpyrrolidone (NMP, 4 hr, 1000 kPa). Resultant polymer/solvent/porogen rods were solidified and precipitated in ethanol (2 days in a rotating precipitation tube). Porogen extraction, extensive washing and drying resulted in porous scaffolds. Disks were uniformly sliced (2 mm thick) and sterilized in ethylene oxide, whereafter pore sizes were measured using scanning electron microscope (SEM) images (Image J software; n = 3). In Fig. 17, SEM images of PU disks revealed macro-pores and interconnecting

windows of 156.9 ± 1.2 µm and 76.4 ± 2.0 µm, respectively, with a porosity of 82.3 ± 2.4%.

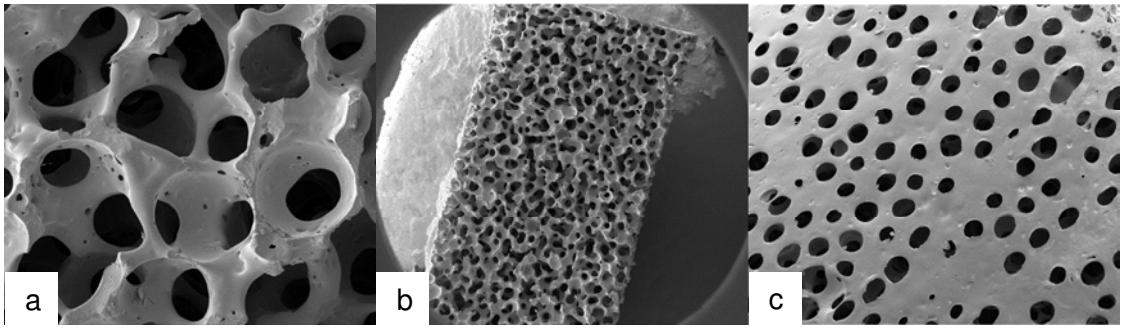

Figure 17: SEM of pores and interconnecting windows (a), the hemi-cylindrical shape as cut during explantation (b) and the outside surface (c) of the PU disk at 500x, 75x and 200x magnification, respectively, before hydrogel infiltration and implantation

2.9 Rheology

An AR-1500 rheometer (TA Instruments Inc.) with 20 mm diameter standard steel parallel-plate geometry was used for the characterization of all samples. Oscillatory time, stress and frequency sweep tests were employed. Time sweep monitored the in situ gelation of gels (100 µL, n = 3) over 30 min (50 µm gap thickness) at constant strain (2%), temperature (25 °C) and frequency (1 Hz). Storage (G′) and loss moduli (G″) were recorded over time. Gelation time was defined as the crossover between G' and G'', which is in compliance with the criteria of Chambon and Winter who found G' and G'' to be congruent over a wide range of frequencies at gel point and corresponds to a constant phase angle of 45°.[68,246,247]

Gels (200 µL, n = 3, 22 mm diameter, 0.5 mm thick) used in stress and frequency sweep tests were formed between siliconized (Sigmacote) glass coverslips (2 hr, 37 °C). Formed gels were detached after gelation and individually immersed in PBS_1 (see Appendix A) to swell to equilibrium (37 °C, overnight). To prevent slippage the plate height was adjusted, starting from the original sample height and compressing the sample to reach a normal force of 30% compression (0.75-1 mm gap thickness). Stress sweep (G' as a function of oscillatory stress) was performed by shearing the gels (1-2000 Pa) at constant frequency (1 Hz) and temperature (25 °C) until structure

breakdown. This was done to determine the ranges in which G' of swollen gels are constant when subjected to stress, which are regarded as the linear viscoelastic regions (LVR) of the gels and needed to evaluate the viscoelastic properties of different gels.[248,249]. Frequency sweep (G' and G'' as a function of oscillatory frequency) was performed at a constant shear stress (50% of the LVR) by varying frequency from 1 to 100 Hz, to determine the mechanical stiffness of the gels.[81,248]

2.10 Hydrogel Swelling

Two swelling ratios were determined in this project, namely swelling ratio 1 (Q, ratio of swollen over dried gel volumes determined through volumetric procedures) and 2 (SR, ratio of swollen over wet gel masses determined through gravimetric procedures). Although hydrogel swelling is normally defined as Q, which accounts for the loss of polymer during swelling,[64,81,133,250–252] SR mirrors the degree of swelling compared to the formed gel rather than to its dry content, which is an important parameter for *in vivo* applications.[99] Additionally, weighing the same gels repeatedly (for SR), instead of sacrificing gels through drying (for Q), is an efficient way to economise a limited amount of material. Due to the high water content both ratios are accurate representations of swelling. As per Flory-Rehner theory mesh sizes were determined to predict whether cellular invasion into gels could be achieved while facilitating the delivery of Hep/HS and GFs *in vivo*.[7,97,253]

2.10.1 Swelling ratio 1 (Q) using volumetric procedure

The volumes of gels (n = 3) were determined according to Archimedes' principle using a 5-decimal balance equipped with a density determination kit (Mettler Toledo). Gels were weighed (directly after crosslinking or after individually immersed in 1 mL PBS_1, pH = 7.4, incubated at 37 °C) in air and DI, dried (50 °C, overnight) and then weighed in air and DI again. Volumes of the formed (V_g), swollen (V_s) and dried (V_d) gels were calculated from the respective mass according to Eq. 8.

$$\mathbf{V} = \frac{\mathbf{m_{air} - m_{DI}}}{\mathbf{\rho_{DI}}} \qquad \textbf{Eq. 8}$$

$$\mathbf{Q} = \frac{\mathbf{V_s - V_d}}{\mathbf{V_d}} \qquad \textbf{Eq. 9}$$

Where V is volume of the gels, m_{air} is mass of the gel weighed in air, m_{DI} is mass of the gel weighed in DI and ρ_{DI} is the density of DI at RT. Thereafter Eq. 9 was used to calculate Q for hydrogels.

2.10.2 Swelling ratio 2 (SR) using gravimetric procedure

Gels (n = 4) were weighed directly after crosslinking to determine formed gel mass (W_g) by using a 5-decimal balance (Mettler Toledo). Thereafter the gels were individually immersed in PBS_1 (1 mL, pH = 7.4) and placed in an incubator (37 °C) for swelling and Hep/HS elution. Gels were removed at regular intervals and weighed in their swollen state (W_s) to follow swelling and degradation as a ratio of W_s/W_g over time. The eluates were collected and replaced by fresh PBS_1 at predetermined time points. The end points of Type 2D gels were considered to be reached when eluates could no longer be replaced without damaging the gels, which were substantially weakened by degradation. Since previous experiments in our laboratory for non-degradable gels similar to Type 2N gels did not show degradation while incubated for more than a year (not shown), these gels were measured until all the Hep/HS had theoretically been released, as determined through Hep/HS eluting experiments.

2.10.3 Mesh Size Calculations

The average molecular weight between crosslinks (M_c) in the gel network was calculated using Eq. 10,[254] with the molecular weight of the PEG building block (M_n = 20 kDa), the specific volume of the PEG building block before crosslinking ($\bar{u}$ = 0.861 mL/g), the molar volume of water (V_1 = 18.1 mL/mole) and the polymer-solvent interaction parameter for a PEG-water system (χ = 0.426) used as constants.

$$\frac{1}{\mathbf{M_c}} = \frac{2}{\mathbf{M_n}} - \frac{(\frac{\bar{\mathbf{u}}}{\mathbf{V_1}})\{\ln(1-\mathbf{u_{2,s}}) + \mathbf{u_{2,s}} + \chi \mathbf{u_{2,s}}^2\}}{\mathbf{u_{2,r}}\{\sqrt[3]{\frac{\mathbf{u_{2,s}}}{\mathbf{u_{2,r}}}} - \frac{1}{2}(\frac{\mathbf{u_{2,s}}}{\mathbf{u_{2,r}}})\}} \qquad \textbf{Eq. 10}$$

Experimental data is represented by $u_{2,s}$ and $u_{2,r}$ (as calculated by Eq. 11 and Eq. 12, respectively) using volumes of dried (V_d), swollen (V_s) and formed (V_g) gels.

$$\mathbf{u_{2,s}} = \frac{V_d}{V_s} \qquad \textbf{Eq. 11} \qquad\qquad \mathbf{u_{2,r}} = \frac{V_d}{V_g} \qquad \textbf{Eq. 12}$$

Thereafter Flory-Rehner calculations were used to calculate the average mesh size, ζ (Å), for the gels during degradation over time, (Eq. 13) with the characteristic ratio of PEG (C_n = 4) and the bond length of the gel's polymeric backbone (l = 1.48 Å) as contants.

$$\zeta = \alpha_s l \sqrt{C_n N} \qquad \textbf{Eq. 13}$$

Experimental data (α_s) is represented by Eq. 14 and the number of bonds between two crosslinks (N) was calculated according to Eq. 15 using the molecular weight of the PEG repeat unit (M_r = 44 g/mole).

$$\alpha_s = \frac{1}{\sqrt[3]{u_{2,s}}} \qquad \textbf{Eq. 14} \qquad\qquad N = \frac{3M_c}{M_r} \qquad \textbf{Eq. 15}$$

Since system specific constants for gels made predominantly from Hep/HS-Ac (i.e. Type 1 gels) were not available, average mesh size calculations were only performed for Type 2 gels. These gels were assumed to be similar to unmodified PEG gels, as the gels contained only a small amount of Hep/HS (1.5% of 4m% copolymer).

2.11 Heparin and Heparan Sulfate Elution

The eluates (n = 4), collected at different time points, were used to quantitatively determine Hep/HS elution over time by using a calorimetric method known as an MBTH (3-methyl-2-benzothiazoline hydrazone-hydrochloride) assay, adapted from literature.[255] Each eluate (250 µL) was reacted with a nitrous acid solution (500 µL, 0.025 M HNO_2, 1 M HCl) for 30 min (sonicate, RT) to cleave and deaminate N-sulfated glucosamine residues. Degradation was stopped by the addition of a 1 M ammonium sulfamate solution (250 µL). Thereafter the reaction solution was diluted with 1 M NaCl (300 µL) and reacted with 0.011 M 3-methyl-2-benzothiazolinehydrazone-hydrochloride (MBTH, 500 µL, 50 °C, 15 min), followed by the addition of 0.031 M $FeCl_3$ (500 µL, 50 °C, 20 min). Absorbances of the resultant solutions were determined by UV spectroscopy (660 nm, Shimadzu UV 1601-PC) using eluates from control gels (n = 4, pooled) as background readings to negate possible PEG effects. Standard Hep and HS solutions were made and treated in an identical manner (0–600 µg Hep/HS in 250 µL DI) to obtain a standard curve which was used to calculate the concentration of Hep/HS (mg/mL

eluate) released. The theoretical Hep/HS content (mg/g gel) was determined by normalizing the Hep/HS concentration released with W_g and coefficients of determination (R^2-values) of elution curves were determined by linear trend line fitting in Microsoft Excel.

2.12 Heparin and Heparan Sulfate Activity Assay

The activities of acrylated and unmodified Hep/HS (n = 3), as well as the activities of the eluates of all the gels (n = 3) were determined via thromboelastography (TEG) and rotational thromboelastometry (ROTEM). Both assays have the same fundamental principles and share many similarities, but differ in complexity, ease of use and cost.[256–258] The results obtained are also not completely interchangeable due to differences in operating characteristics.[259] Thromboelastography was performed based on previous studies in our laboratories, but studies were converted towards ROTEM because it is less sensitive to vibration, much more economical to use and it operates through automated pipetting which minimizes experimental error.[260] The use of human blood was approved by the Human Research Ethics Committee of the University of Cape Town (UCT) after informed consent.

2.12.1 Thromboelastography

Hep/HS or Hep/HS-Ac (110 µL, 0.01 mg/mL in PBS_1) was mixed with 1 mL citrated whole blood (WB, 3.2% sodium citrate tube; BD Medical, Johannesburg, RSA) and PBS_1 (110 µL in 1 mL WB) was used as control. The mixture (1 mL) was placed in a Kaolin-coated vial (BD Medical, Johannesburg, RSA), followed by the addition of CaCl (20 µL, 0.2 M). Of this solution, 340 µL was placed in a pre-warmed cup (37 °C) and the clotting parameters of the sample were determined by a TEG® haemostasis analyser (5000 series). These parameters are illustrated in Fig. 18 - clotting time (R, time from start to when the waveform reaches 2 mm above baseline); clot formation time (K, time from 2 mm above baseline to 20 mm above baseline); rate of clot strength build-up (α, alpha angle); and clot strength (maximal amplitude, MA). The activity of the eluates was determined in a similar way using 110 µL eluates (normalized to 0.01 mg/mL with PBS_1).

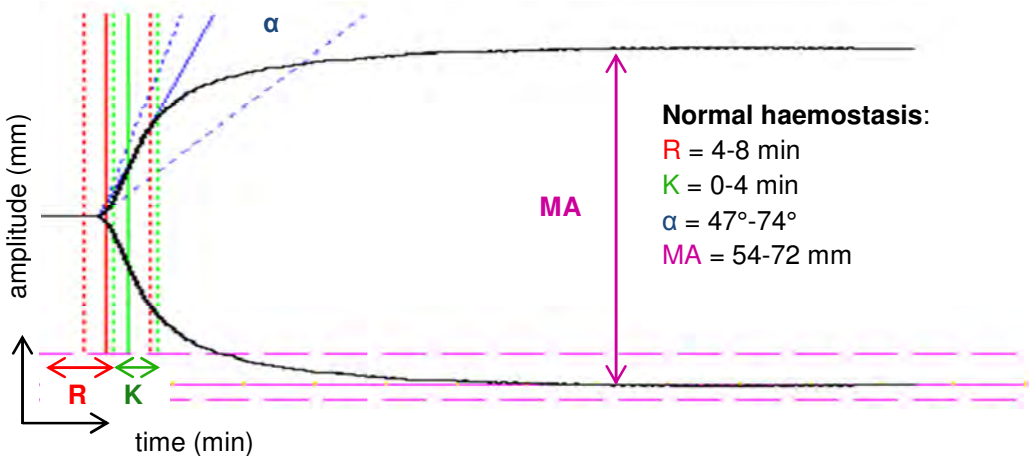

Figure 18: Characteristic TEG plot of whole blood. The clotting time (R), clot kinetics (K, α) and clot strength (MA) are drawn in solid lines while the range of normal haemostasis of these parameters are indicated through dashed lines.

2.12.2 Rotational Thromboelastometry

INTEM, EXTEM, HEPTEM, APTEM, FIBTEM and NATEM experiments were performed using a ROTEM® delta (Viking Medical & Surgical Pty. Ltd., Edenvale, RSA). Hep/HS (110 µL, 0.05 mg/µL in PBS_1) was mixed with 1 mL citrated WB and 300 µL thereof was placed in a cup, followed by the automated addition of initiators (summarized in Table 5). The activity of acrylated and modified Hep/HS (110 µL, 0.05 mg/µL in PBS_1) was evaluated by INTEM and the activity of eluates (normalized with PBS_1, 0.002 mg/mL) by NATEM (due to the lower concentration higher sensitivity was needed). For all ROTEM experiments PBS_1 (110 µL in 1 mL WB) was used as control.

Table 5: Summary of initiators for different ROTEM assays

INTEM	Intrinsic ROTEM	phospholipid and ellagic acid (star-tem® and in-tem®)
EXTEM	Extrinsic ROTEM	tissue factor (star-tem® and r ex-tem®)
HEPTEM	Heparinise ROTEM	lyophilised heparinase (in-tem® and hep-tem®)
APTEM	Aprotinin ROTEM	aprotinin (r ex-tem® and t ap-tem®)
FIBTEM	Fibrinogen ROTEM	cytochalasin D platelet inhibitor (r ex-tem® and fib-tem®)
NATEM	Native ROTEM	Re-calcifier (star-tem®)

2.13 Growth Factor Binding and Release

Only Type 2D gels were evaluated for GF binding and release *in vitro* and *in vivo*. Although both bFGF and VEGF have shown to possess pro-angiogenic properties and a binding site for Hep and HS, VEGF has been shown to be a stronger angiogenic promoter and was therefore used in this project. [122,261–265] Gels (50 µL, n = 4) were made by reacting Hep/HS-Ac (0.03 mg in 5 µL PBS_2) with VEGF (1 µL, 1 mg/mL), followed by the addition of 10PEG4SH (2.02 mg in 25 µL PBS_2) and 20PEG8Ac (1.97 mg in 20 µL PBS_2), and allowed to react for 1 hr at 37 °C. Gels were individually immersed in PBS_2 (500 µL, 1% BSA, pH = 7.4) with shaking (1 hr, 37 °C), whereafter the eluates were removed and stored at 4 °C. This was performed twice to remove GF that washed out after gelation. Gels were subsequently immersed in buffer (500 µL PBS_2, 1% BSA, 0.02% sodium azide) at 37 °C and eluates were collected and replaced by fresh buffer at regular intervals. Gels containing GF without Hep/HS and gels containing Hep/HS without GF (to validate the ELISA) were used as controls.

The concentration VEGF released during the wash-out phase and over time was quantified using a human VEGF enzyme-linked immunosorbent assay (ELISA) kit (R&D, Minneapolis, MN, USA), as per manufacturer's instructions. Briefly, a 96-well micro-plate was coated with mouse anti-human VEGF antibody (100 µL/well, 1.0 µg/mL in PBS_2) and incubated overnight at RT. Thereafter the plate was washed with 0.05% Tween®20 in PBS_2 (pH = 7.2-7.4, 400 µL, 3 times) and blocked by PBS_2 (300 µL, 1% BSA, pH = 7.2-7.4, RT, 1 hr). Each eluate (100 µL, collected over time or from wash steps) were placed in a separate well, followed by the addition of four different solutions: biotinylated goat anti-human VEGF antibody (100 µL/well, 100 ng/mL in 1% BSA PBS_2); streptavidin conjugated to horseradish-peroxidase (100 µL/well, 100 ng/mL in 1% BSA PBS_2); a H_2O_2 and Tetramethylbenzidine solution (1:1, 100 µL/well); and H_2SO_4 (2 M, 50 µL µL/well). Each addition was followed by incubation (RT, 2 hr or 20 min). Thereafter the optical density was determined by a micro-plate reader (450 nm, wavelength correction at 570 nm). Human VEGF standard solutions were made and treated in a similar manner (31.3–2000 pg/mL in 1% BSA PBS_2) to obtain a standard curve. The VEGF concentrations (ng/mL eluate) over time were calculated using the curve and R^2-values were determined by linear trendline fitting in Microsoft Excel.

2.14 Curve Fitting

In order to establish the release mechanism of covalently incorporated Hep/HS and GF the following mathematical models were investigated: Zero and first order release models represented by Eq. 16 and Eq. 17, respectively.[156]

$$\mathbf{Q_t = Q_0 + k_0 t} \qquad \textbf{Eq. 16} \qquad\qquad \mathbf{\ln Q_{rem,t} = \ln Q_0 - k_1 t} \qquad \textbf{Eq. 17}$$

Where Q_0 is the initial amount of Hep/HS, Q_t is the cumulative amount of Hep/HS released at time t, and k_0 and k_1 is the zero and first order rate constants, respectively. As $Q_{rem,t}$ relates to the amount of Hep/HS remaining at time t, Eq. 17 was modified to describe the amount released (Eq. 18).

$$\mathbf{Q_t = Q_0(1 - e^{-k_1 t})} \qquad \textbf{Eq. 18}$$

The coefficients of determination (R^2) were calculated by linear trendline fitting in Microsoft Excel and GraphPad Prism, either directly (cumulated release versus elution time) for zero order release or by using the natural logarithm of the amount versus elution time for first order release. Initial burst release data (day 1-2) and data obtained after gel disintegration (after day 22) were excluded and no Y-axis intersections were guided through zero.

2.15 *In Vivo* Evaluation in Rat Subcutaneous Model

Type 2D gels containing Hep (50 µL, n = 6) were prepared as for GF experiments, except that before polymerization it was absorbed into PU disks and incubated for 1 hr (37 °C), under sterile conditions. Sterility of the procedure was tested by incubating (37 °C, 3 days) disks, as prepared for implantation, in MCDB 131 medium (containing trace elements and L-glutamine) with 10% Fetal Bovine Serum (FBS). The absence of bacteria, viruses and fungi were determined through microscopic evaluation. The *in vivo* effects of the different samples (summarized in Table 6) were evaluated based on cellular infiltration, collagen deposition, angiogenesis and inflammation. [9,53,245] No *in vivo* tests were performed on HS and all samples were implanted per rat as internal controls.

Table 6: Different samples prepared for *in vivo* evaluation in rat subcutaneous model

Sample name	Content	Effect tested
PU	Control disk without gel	Surgical intervention and foreign body response caused by disk
PU + PEG-Ac/SH	Disk with Type 2D control gel	Gel swelling and degradation
PU + PEG-Ac/SH/Hep	Disk with Type 2D NI gel	NI Hep
PU + PEG-Ac/SH + GF	Disk with Type 2D control gel and GF	Release of GF from gel
PU + PEG-Ac/SH/Hep-Ac	Disk with Type 2D CI gel	Modified Hep CI into gel
PU + PEG-Ac/SH/Hep-Ac + GF	Disk with Type 2D CI gel and GF	GF release from gel through CI Hep

Animal experiments were approved by the Animal Research and Ethics Committee of UCT and complied with the Guide for the Care and Use of Laboratory Animals. Wistar rats (male) were obtained from the UCT Animal Unit and weighed to establish baseline weights for post-operative welfare monitoring. Anaesthesia was induced by placing the animal in an inhalation chamber with 5% isoflurane air flow for 3 min, and maintained throughout the procedure by nose cone delivery (1.5% Isoflurane, 1.5 l/min oxygen output, 750 mmHg, 21 °C). Body temperature was maintained by placing the animal on a custom made heating pad (37°C). The surgical area was shaved and sterilised with iodine, whereafter 0.05 mg/kg buprenorphine was given preoperatively as analgesic. All surgical procedures were performed using aseptic techniques.

Longitudinal incisions (6, 3 each side, 1 cm) were made on either side of the dorsal midline and pockets (1.5 cm in depth) were blunt dissected subcutaneously at each incision. Thereafter samples were placed each within its own pocket (each rat receiving only one disk of each group) and incisions were closed with monofilament nylon 4/0 stitches (interrupted sutures were placed in a subcuticular fashion with a buried knot). Rats were observed until fully conscious and received a buprenorphine injection (0.05 mg/kg, 24 hr after operation). Prior to retrieval of the tissue at predetermined time points (7, 14 and 28 days) the rats were killed whilst under general anaesthesia (inhalation of 5% halothane in air) and death was ensured by cardiac puncture (1 mL saturated KCl injection). The samples with surrounding tissue were explanted, halved into equal semi-cylindrical sections and fixed (one half of each disk in zinc fixative and the other in 10% buffered formalin, see Appendix A) for 5 days.

2.16 Histological Evaluation and Immunohistochemistry

Fixed samples were processed through a graded alcohol (15-100%) procedure and embedded in paraffin wax. Thereafter they were cut into 3 µm sections and baked on glass slides (60 °C, 30 min). These samples were dewaxed through 2,2,4-trimethylpentane (3 times, 20 min each), agitated in descending alcohol concentrations, stained and mounted in Canada Balsalm on coated slides. Stains performed were hematoxylin (Merck, Damstadt, Germany) and eosin (BDH; WWR International, Poole, England) (H&E) to identify nuclei; Sirius red F3B and picric acid (picrosirius red stain) to identify collagen; as well as mouse anti-rat CD31 antibodies for immunohistochemistry labelling endothelial cells.

Samples were observed and images captured with a Nikon eclipse 90i microscope with Digital Camera DXM-1200C (Nikon Corporation,Tokyo, Japan) and micrographs covering the entire disk were stitched together by automatic scanning (NIS Elements software). Image analysis was performed by training the Visiopharm Integrated Systems (Visiopharm A/S, Hørsholm, Denmark) software to automatically detect certain structures, but all analyses were assessed for accuracy by an observer and corrected manually where necessary. Tissue ingrowth was expressed as the **ingrown area** (tissue and nuclei) as a percentage of the available **ingrowth area** (excluding the PU); collagen deposition as the total **collagen area** relative to the **ingrowth area**; while angiogenesis was expressed as the number of capillaries and **capillary area** relative to the **ingrown area**.

2.17 Statistical Analysis

Results are expressed in text and represented in graphs as mean ± standard deviation (SD). Continuous data were tested for normality with a Shapiro-Wilk test (Stata/SE 12.1 software) and, where appropriate, analysed with a student's unpaired t-test and multiple-group analysis (one-way and two-way ANOVA) using GraphPad Prism. Significant levels for pairwise testing between categories were controlled by the Tukey's HSD studentized range test and a level of $p \leq 0.05$ was considered statistically significant

3 Results

3.1 Modified Heparin/Heparan Sulfate

Modified Hep/HS with acrylation percentages of 1-80% were obtained through different methods, with the largest degree of modification obtained through controlled addition of acryloyl chloride (AcCl) using a syringe pump. Methacrylated Hep/HS (Hep/HS-MA) of 11-13% and 11-19% were obtained through anhydride and epoxy chemistry, respectively. However, larger conversions of Hep/HS-MA were not achieved despite varying reaction conditions.

3.2 Gel Formation

Michael-type addition reactions (pH = 7.4, 37 °C) resulted in successful formation of Type 1 gels when Hep/HS-Ac (with acrylation percentages higher than 20%) were reacted with 10PEG4SH. Modified Hep/HS with acrylation lower than 20% did not form Type 1 gels through Michael-type addition reactions, despite varying temperatures (20-50 °C), pH levels (pH = 6-10) and Ac/SH ratios. Michael-type addition reactions (pH = 7.4, 37 °C) resulted in successful formation of Type 2 gels – when 20PEG8Ac or 20PEG8VS and 10PEG4SH were reacted together control gels (PEG-Ac/SH or PEG-VS/SH) formed, while the addition of either Hep/HS or Hep/HS-Ac (40% acrylation) to these formulations (PEG-Ac/SH or PEG-VS/SH) led to the successful formation of non-covalently (NI) and covalently incorporated (CI) gels, respectively.

Photo-polymerization through UV irradiation resulted in successful gel formation using Hep/HS-MA or Hep/HS-Ac (< 20% acrylation) in solution with DMPA and NVP, except when the degree of modification was 3% or lower. Controls: UV irradiation of modified Hep/HS, a mixture of modified Hep/HS and NVP, or a solution of DMPA in NVP did not result in gelation. A solution of modified Hep/HS and DMPA only showed initial gel formation after prolonged irradiation (30-40 min).

3.3 Rheological Characterization

3.3.1 Gelation time

The storage (G') and loss moduli (G'') of PEG-Ac/SH (as example) when subjected to oscillatory time sweep during gelation are shown in Fig. 19, as plotted over time. The crossover occurred at 7.2 ± 0.3 min, which was taken as the gelation time. This plot was characteristic for all gel formulations.[248,266]

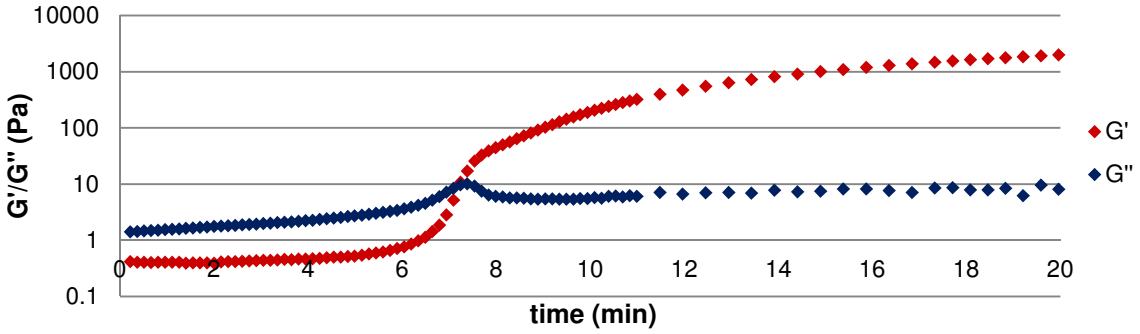

Figure 19: Characteristic plot of in situ gelation of all gels (Type 1 and 2 gels, PEG-Ac/SH in this case) during oscillatory time sweep (1 Hz; 2% strain; 25 °C)

Regarding Type 1 gels, the gelation time of HS-Ac/SH was 1.3 ± 0.2 min (p = 0.0112) shorter than Hep-Ac/SH (Fig. 20 a). Type 2D and 2N gels formed on average at 7.2 ± 0.3 min and 3.1 ± 0.1 min, respectively. Gelation time for Type 2N gels was therefore 58 ± 2% (p < 0.0001) shorter than Type 2D (Fig. 20 b). No significant difference was observed between gelation times of either different Type 2D or Type 2N gel formulations.

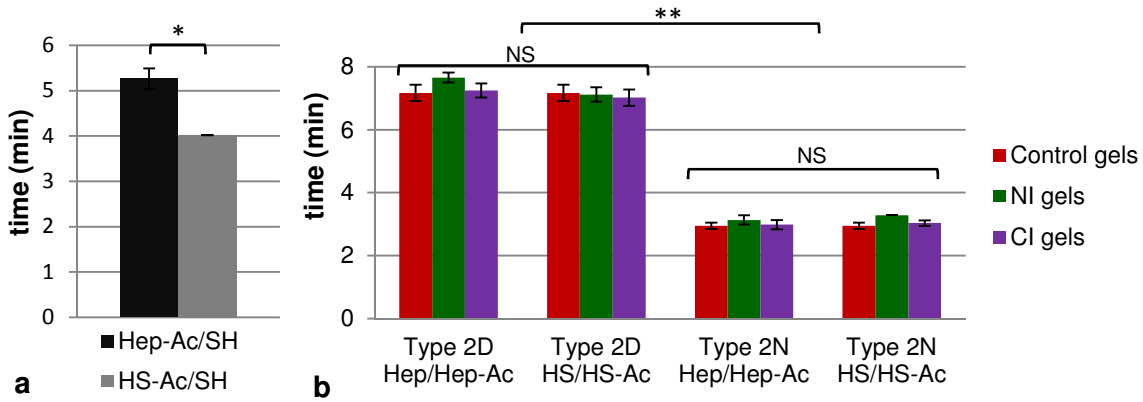

Figure 20: Gelation times of Type 1 (a) and Type 2 (b) gels obtained through oscillatory time sweep (n = 3; NS shows p > 0.05; * shows p < 0.05; ** shows p < 0.0001)

3.3.2 Viscoelasticity

When subjected to oscillatory stress sweep, the storage moduli (G') of Type 1 gels were constant at 4391 ± 441 Pa (Fig. 21 a), until the ultimate stress level (sharp decrease) was reached at 566 ± 92 Pa. Storage moduli for Type 2 gels were also constant, but at different G' values for different gel formulations (ranging from 6560 ± 27 Pa to 10460 ± 353 Pa). The ultimate stress level in Fig. 21 b was reached at 897 ± 145 Pa on average.

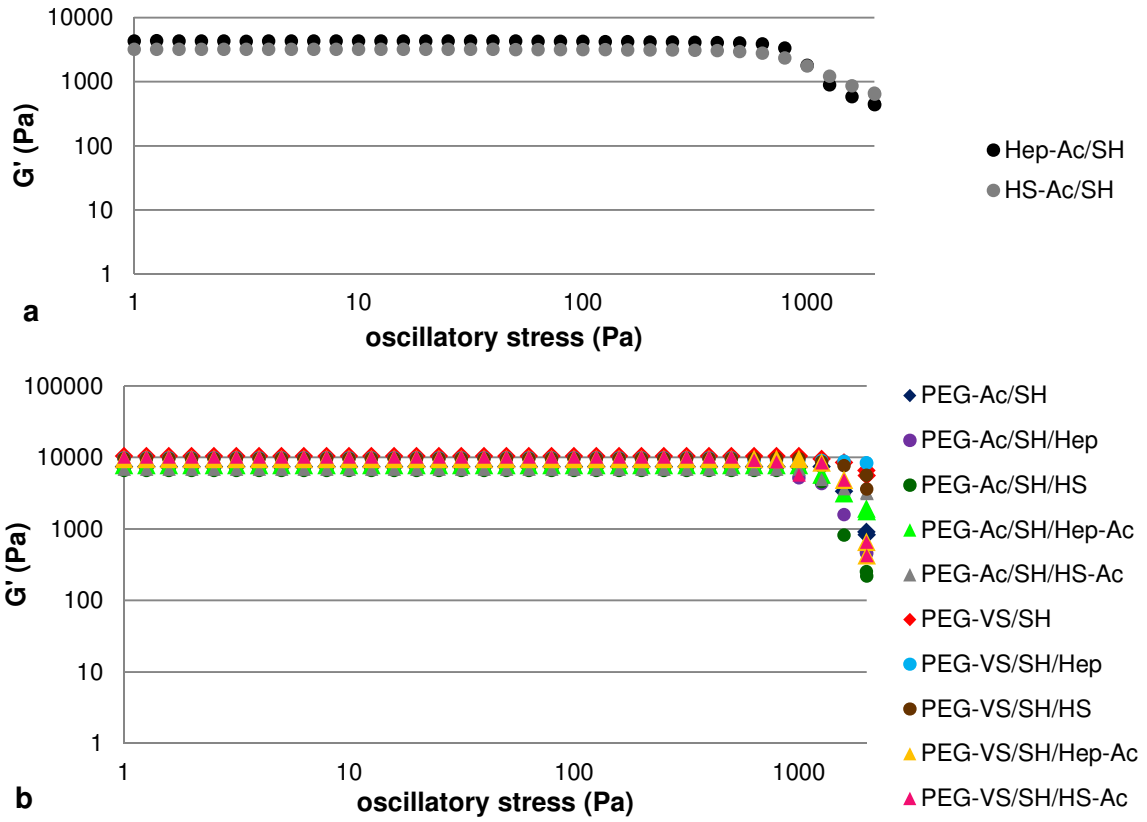

Figure 21: Linear viscoelastic region determination of Type 1 (a) and Type 2 (b) gels obtained through oscillatory stress sweep (1Hz; 25 °C)

The G' of Hep-Ac/SH (as example), subjected to frequency sweep at a constant shear stress (250 Pa), exhibited a plateau in the range 1-80 Hz (Fig. 22). This was followed by a slight increase at higher frequencies (80-100 Hz). Loss modulus (G''), slightly erratic in nature, was one to two magnitudes lower than G' over all measured frequencies and characteristic for all equilibrium swollen gels of different gel formulations.

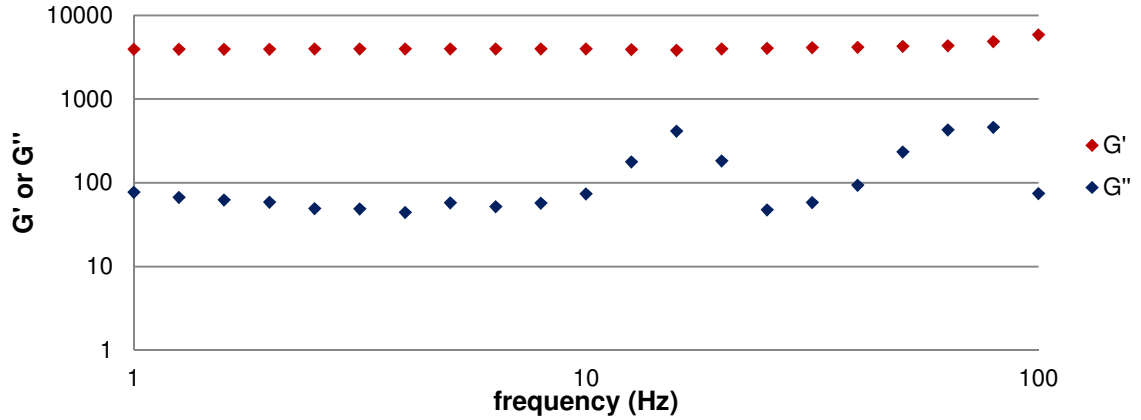

Figure 22: Characteristic plot of all equilibrium swollen gels (Type 1 and 2 gels, Hep-Ac/SH in this case) during oscillatory frequency sweep

Storage moduli of Type 1 gels showed that Hep-Ac/SH was 752 ± 105 Pa higher than HS-Ac/SH (19 ± 4%, p = 0.0064, Fig. 23 a). Regarding Type 2 gels, no significant differences were observed between either G' values of Type 2D control, NI and CI gels or between G' of Type 2N control, NI and CI gels. Type 2N gels had on average 40 ± 6% ($p < 0.05$) higher G' values than their corresponding Type 2D gels in Fig. 23 b.

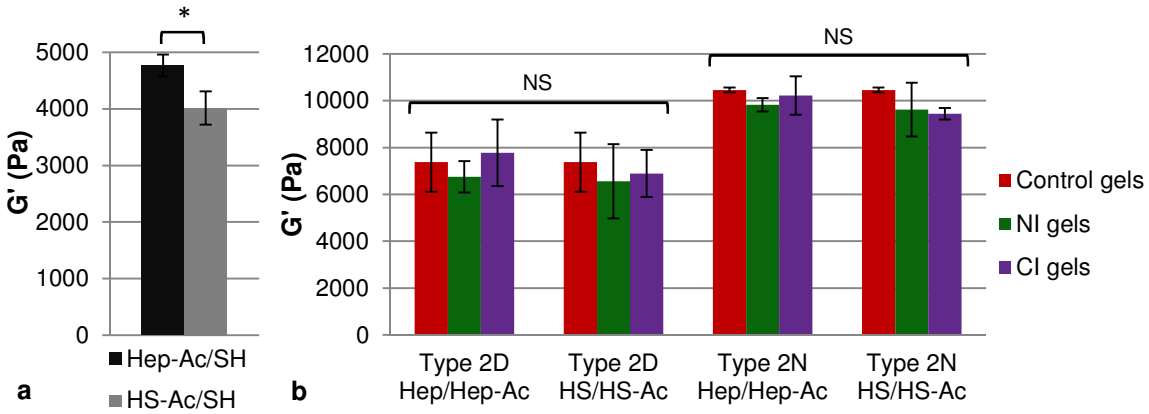

Figure 23: Storage moduli of Type 1 (a) and Type 2 (b) gels obtained through oscillatory frequency sweep. (n = 3; NS shows p > 0.05, * shows p < 0.05)

3.4 Hydrogel swelling

3.4.1 Swelling ratio 1

During the first three days Type 1 gels (Hep-Ac/SH and HS-Ac/SH) showed a 316 ± 13% (p = 0.0009) and 481 ± 3% (p = 0.0018) increase in swelling ratio 1 (Q), respectively followed by a significant increase to 34.5 ± 2.4 (on average) at 15 days, whereafter no

significant difference was observed in Fig. 24 a. No significant difference between Hep-Ac/SH and HS-Ac/SH was observed after day 3.

All Type 2 gels underwent an approximate 128 ± 37% ($p < 0.0001$) increase in Q between 0 to 3 days (Fig. 24 b). Type 2D gels continued to increase a further 145 ± 47% ($p < 0.0001$) on average between 3 and 17 days, whereafter gels were too disintegrated for further volume determination. There were no significant differences between different Type 2D gels. Swelling ratios (Q) of Type 2N gels stayed constant at 18.2 ± 1.1 from day 3 to 36, with no significant differences between different Type 2N gels. At 17 days the Q for Type 2D gels was, on average, 173 ± 30% ($p < 0.0001$) higher than Type 2N gels.

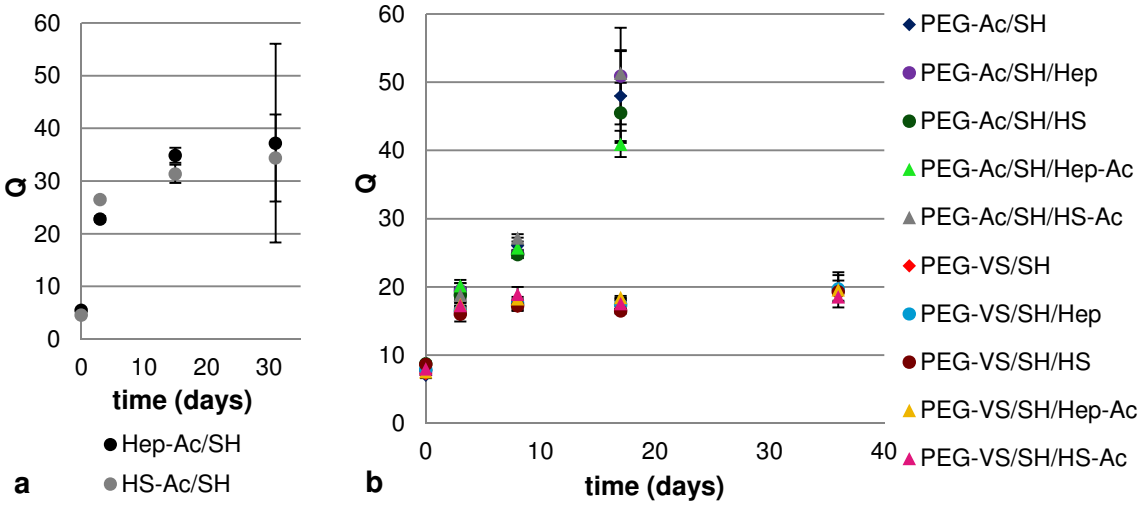

Figure 24: Swelling ratios (Q) of Type 1 (a) and Type 2 (b) gels during incubation at 37 °C in PBS (n = 3)

3.4.2 Swelling ratio 2

Type 1 gels showed rapid initial swelling during the first day (2.6 ± 0.1; $p < 0.0001$) subsequent steady increase to day 72 (Fig. 25). At day 15 and onwards, Hep-Ac/SH had significantly higher swelling ration 2 (SR) values than HS-Ac/SH and the final SR of Hep-Ac/SH was 50.5 ± 7.6% ($p < 0.0001$) higher than HS-Ac/SH at 72 days.

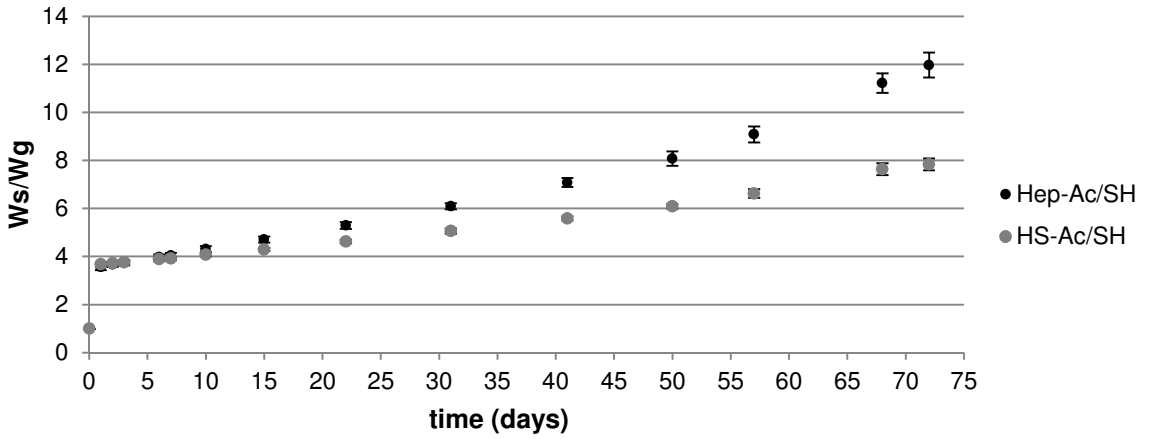

Figure 25: Swelling ratio (SR) of Type 1 gels during incubation at 37 °C in PBS (n = 4)

Type 2D gels showed rapid initial swelling within the first 6 hours ($p<0.05$), subsequent steady increase to 3.5 ± 0.9 at 21 days. Thereafter rapid degradation followed to such an extent that further accurate measurements were difficult (Fig. 26). These gels underwent a 252 ± 39% ($p < 0.0001$) increase in SR during day 0 to 21, with no significant differences between the different Type 2D gel formulations at any time point. Similarly, rapid initial swelling was observed with Type 2N gels, but the increase was only significant after 24 hours. Retention of equilibrium values at 1.2 ± 0.1 followed after the first day, with no significant differences between the different Type 2N gel formulations. These gels did not show signs of degradation for up to six months (data not shown). At day 21 the SR of Type 2D gels was 176 ± 29% ($p < 0.0001$) higher than Type 2N gels.

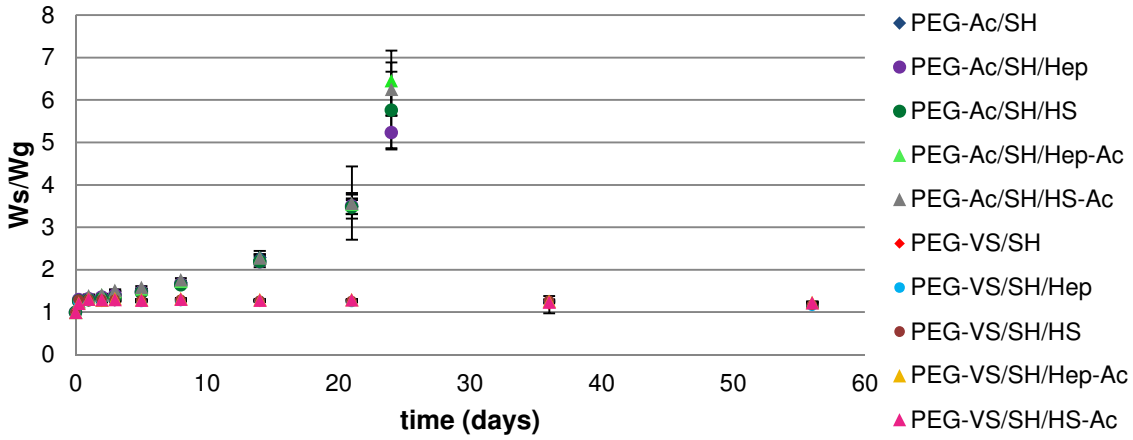

Figure 26: Swelling ratios (SR) of Type 2 gels during incubation at 37 °C in PBS (n = 4)

3.4.3 Mesh Size

The mesh sizes of Type 2 gels followed similar trends to Q over time. The average initial mesh size of the gels was 44.6 ± 3.1 Å, whereafter it increased by 170 ± 47% ($p < 0.0001$), on average, during the first three days (Fig. 27). Thereafter mesh sizes of Type 2D gels continued to increase a further 92 ± 14% ($p < 0.0001$) between 3 and 17 days towards an average mesh size of 245.6 ± 13.9 Å, There were with no significant differences between different Type 2D gels. Mesh sizes of Type 2N gels did not increase significantly between 3 and 36 days (average mesh size of 116.3 ± 7.1 Å during that time), and there were no significant differences between different Type 2N gels. At 17 days, the mesh sizes of Type 2D gels were, on average, 118 ± 16% ($p < 0.0001$) higher than Type 2N gels.

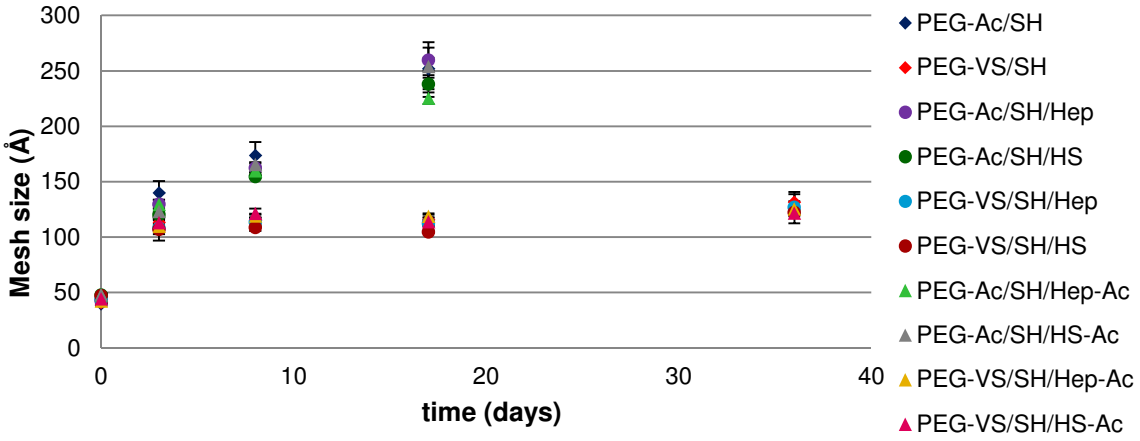

Figure 27: Mesh size of Type 2 gels during incubation at 37 °C in PBS (n = 3)

3.5 Heparin and Heparan Sulfate Elution

Eluates from Type 1 gels in Fig. 28 were characterized by initial burst releases of 2 ± 1% ($p = 0.0098$) Hep and 12 ± 2% ($p < 0.0001$) HS during the first day, whereafter the gels followed zero order Hep ($R^2 \geq 0.96$) and HS ($R^2 \geq 0.93$) release kinetics for the recorded period. Although the cumulative HS release was significantly higher than that of Hep between 1 to 41 days, there was no significant difference between the incremental amount of HS and Hep released during that period. Thereafter the incremental amount of Hep release was 41 ± 6% ($p = 0.025$) to 127 ± 7% ($p < 0.0001$) higher than the incremental HS release (41 to 72 days). During the recorded period Hep-Ac/SH and HS-

Ac/SH released 48 ± 5% Hep and 44 ± 5% HS of the initial amount, respectively ($p < 0.0001$).

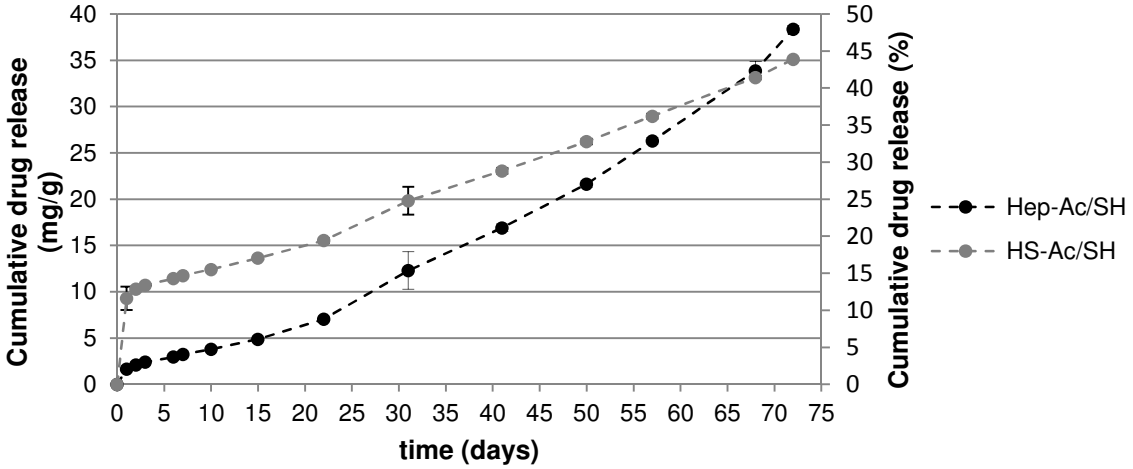

Figure 28: Cumulative release of Hep/HS from Type 1 gels during incubation in PBS at 37 °C over a 72 day period (n = 4)

Hep and HS release from Type 2 gels are shown in Fig. 29. NI gels showed rapid burst release, with over 90% of the initial amount of the Hep (93 ± 7%) and HS (92 ± 8%) eluted during the first 36 hours ($p < 0.0001$). No significant amount of Hep and HS were released from Type 2D NI gels (PEG-Ac/SH/Hep and PEG-Ac/SH/HS) between 2 to 21 days, whereafter a burst release was showed upon gel dissolution ($p < 0.0001$). Type 2N NI gels (PEG-VS/SH/Hep and PEG-VS/SH/HS) released no Hep and HS between 2 to 56 days ($p > 0.05$).

CI gels showed small initial burst release during the first day (but to a significantly smaller extent than the NI gels) since only 16 ± 3% ($p = 0.0074$) and 21 ± 2% ($p = 0.004$) of the initial amounts of Hep and HS eluted, respectively. Thereafter Hep/HS release from Type 2D CI gels (PEG-Ac/SH/Hep-Ac and PEG-Ac/SH/HS-Ac) followed a zero order ($R^2 \geq 0.88$ and $R^2 \geq 0.96$, respectively) release model. A further 57 ± 13% ($p < 0.0001$) Hep and 72 ± 7% ($p < 0.0001$) HS were released from these gels between 1 and 21 days. The cumulative HS release was 21 ± 16% ($p = 0.0008$) higher than the cumulative Hep release at day 21, whereafter a significant burst release of the remaining Hep/HS content occurred with natural gel dissolution. After the initial burst, the sustained Hep/HS release from Type 2N CI gels (PEG-VS/SH/Hep and PEG-VS/SH/HS) followed a first order ($R^2 \geq 90$ and $R^2 \geq 0.84$, respectively) fashion, with a total of 85 ±

12% ($p < 0.0001$) Hep and 90 ± 8% ($p < 0.0001$) HS released, respectively over the recorded period (56 days).

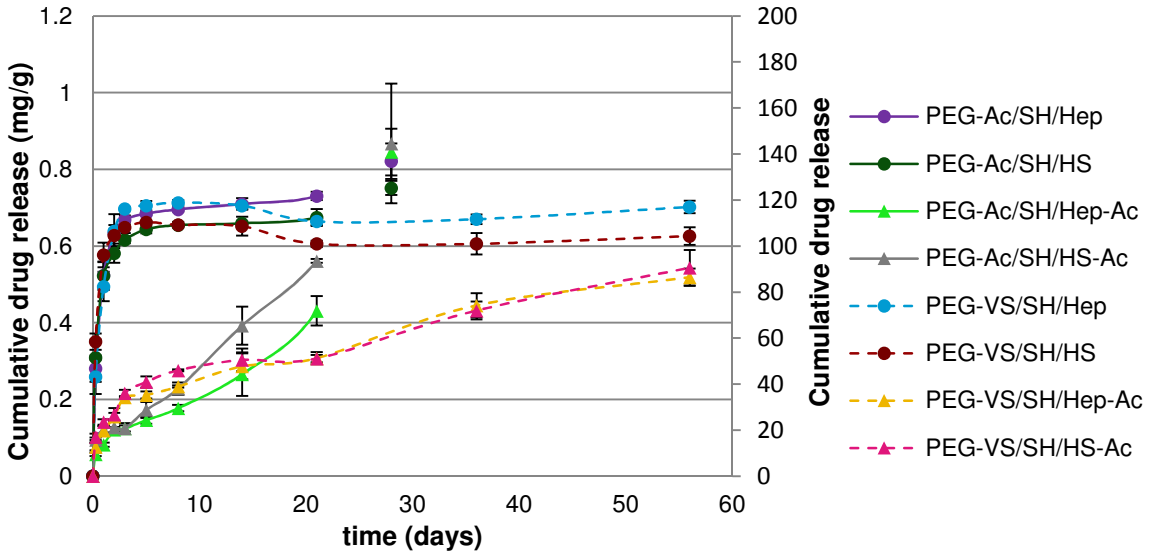

Figure 29: Cumulative release of Hep/HS from Type 2 gels during incubation in PBS at 37 °C (n = 4)

3.6 Heparin and Heparan Sulfate Activity

The clotting kinetic parameters in Fig. 30 showed no significant difference in clotting time (R), clot kinetics (K, α) or clot strength (maximal amplitude, MA) between whole blood (WB) containing PBS, HS in PBS or HS-Ac in PBS. Thromboelastography (TEG) of Hep and Hep-Ac showed 66 ± 10% ($p < 0.0001$) and 44 ± 7% ($p < 0.0001$) higher R times than PBS, respectively; K values were prolonged (869 ± 154% and 350 ± 38% higher than PBS; $p < 0.0001$); α values were 196 ± 10% and 86 ± 7% lower than PBS, ($p < 0.0001$); while MA of Hep and Hep-Ac were 27 ± 2% and 21 ± 1% lower than PBS, respectively ($p < 0.0001$). Although the addition of acrylated and unmodified Hep/HS to PBS affected R, K, α and MA significantly, only clotting time (R) was used to represent Hep and HS activity in the remainder of the study.

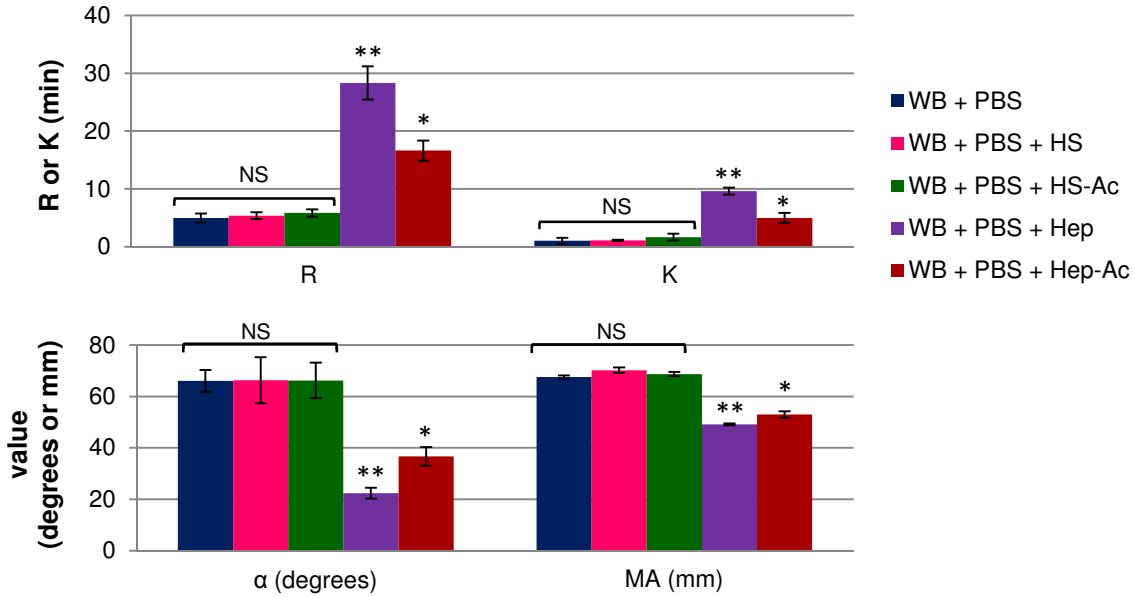

Figure 30: Clotting kinetic parameters of virgin and modified Hep/HS (0.01 mg/mL PBS) measured by TEG (n = 3; NS shows p > 0.05; * shows p < 0.0001 against PBS and eluates with HS; ** shows p < 0.0001 against Hep-Ac)

Of all the Rotational Thromboelastometry (ROTEM) assays that received initiators, the addition of PBS, Hep and HS to WB affected the coagulation profiles (Fig. 31 a) and clotting times (Fig. 31 b) of INTEM (intrinsic ROTEM) most significantly. Coagulation activity was therefore evaluated with INTEM for samples with Hep/HS concentrations of 0.05 mg/mL. Although results obtained through INTEM were approximately 4 to 15 times shorter than NATEM (native ROTEM), increased clotting times obtained through NATEM showed even larger differences. This made the discerning of small differences (at very low concentrations) possible. NATEM was therefore used for samples with Hep/HS concentrations of 0.002 mg/mL.

Unmodified and acrylated Hep/HS subjected to INTEM showed no significant difference in the clotting times between HS and HS-Ac, both of which were 1.8 ± 0.5 min (64 ± 17%; p = 0.0031) higher than PBS (Fig. 32). The clotting times of Hep and Hep-Ac were respectively 14.1 ± 1.3 min (535 ± 46%) and 5.5 ± 1.0 min (233 ± 38%) higher than PBS control (p < 0.0001). The clotting time of WB containing Hep was 91 ± 15% (p < 0.0001) higher than Hep-Ac.

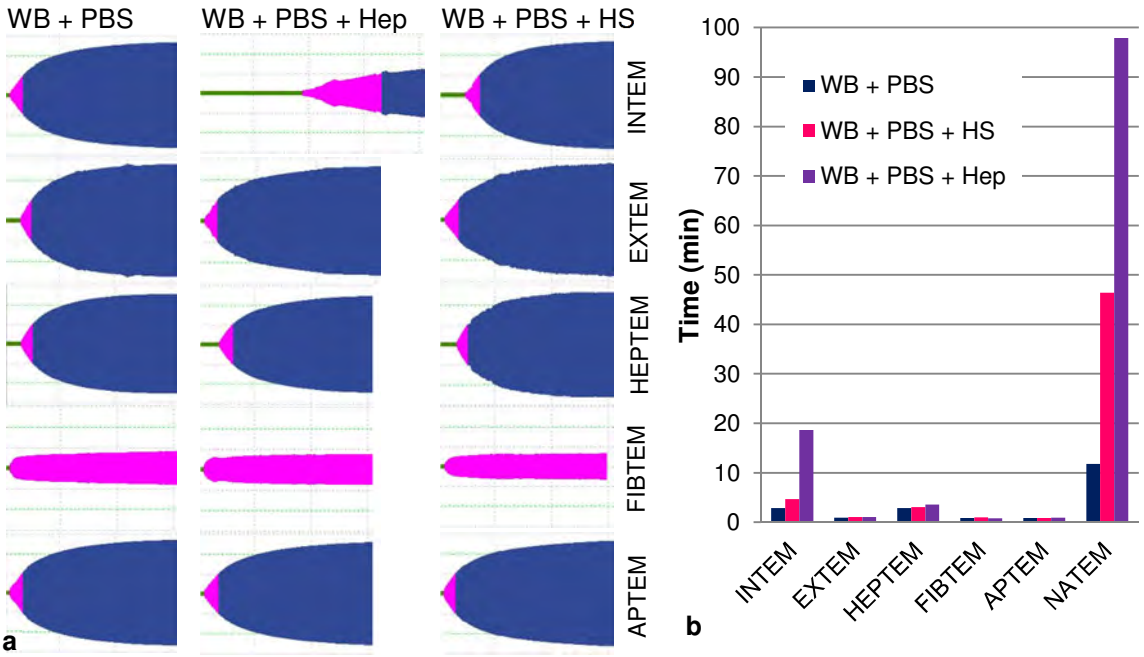

Figure 31: The coagulation profiles (a) and clotting times (b) of WB with PBS, Hep and HS (0.05 mg/mL PBS) subjected to ROTEM. NATEM profiles are not shown due to increased times

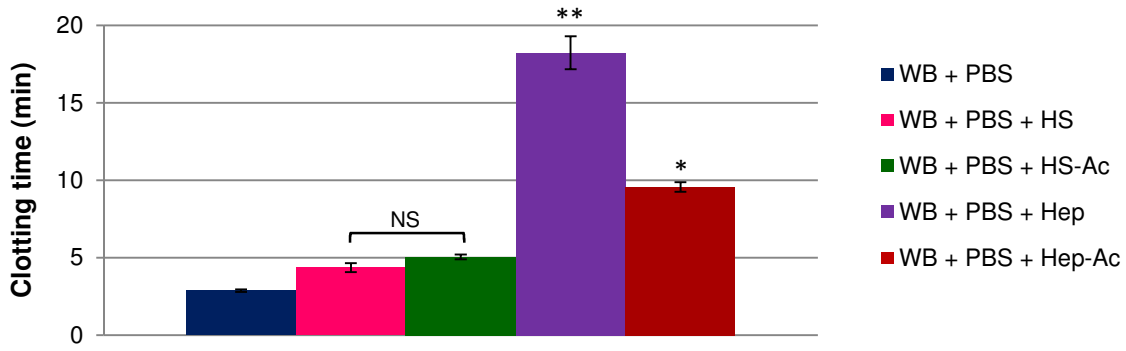

Figure 32: Clotting times of WB containing Hep/HS or Hep/HS-Ac (0.05 mg/mL in PBS) subjected to INTEM (n = 3; NS shows $p > 0.05$, * shows $p < 0.0001$ against PBS and eluates with HS; ** shows $p < 0.0001$ against Hep-Ac)

Clotting times of WB containing eluates from Type 1 gels showed no significant difference between the clotting times of eluates from HS-Ac/SH at different time points (day 3, 31 and 72). At day 3 and day 72, the clotting times were 32 ± 2% ($p = 0.01$) and 42 ± 17% ($p = 0.002$) higher than the PBS control, respectively (Fig. 33). The clotting times of eluates from Hep-Ac/SH were 74 ± 6%, 102 ± 16% and 148 ± 1% higher than the PBS control at 3, 31 and 72 days, respectively ($p < 0.0001$).

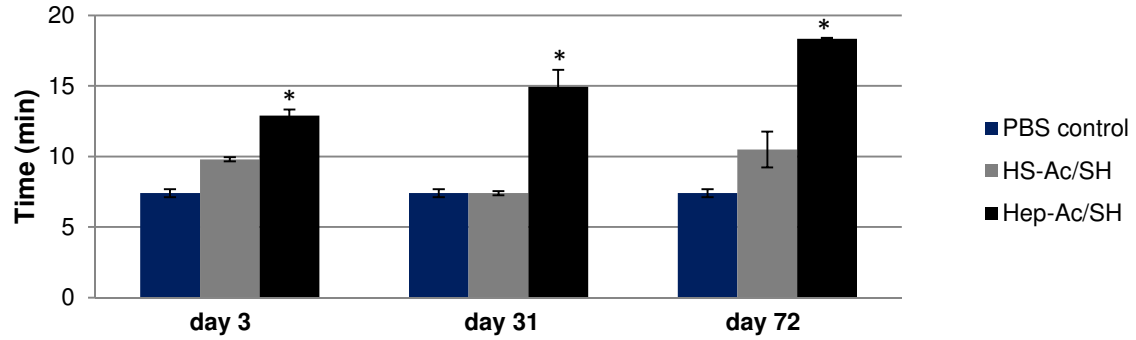

Figure 33: Clotting times of WB containing eluates of Type 1 gels subjected to TEG (n = 3; * shows p < 0.001 against PBS and eluates with HS)

Regarding eluates from Type 2 gels, no significant difference was observed between the clotting times of WB with eluates from PEG-Ac/SH/HS, PEG-VS/SH/HS and PBS at any of the time points (Fig. 34). Clotting times of eluates from PEG-VS/SH/Hep and PEG-Ac/SH/Hep were 9.9 ± 1.0 min ($p < 0.0001$) and 1.6 ± 0.1 min ($p < 0.0001$) higher than PBS, respectively at day 1 and increased significantly between day 1 and 3. However, at day 5 the clotting times of all NI gels were similar to the PBS control.

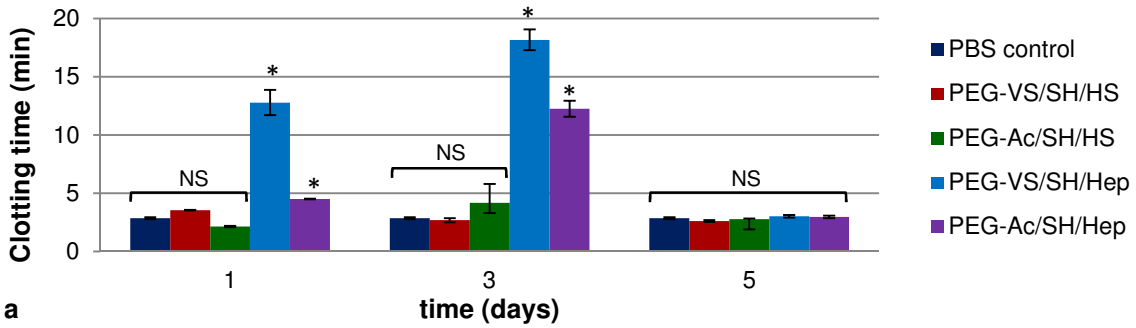

Figure 34: Clotting times of WB containing eluates from NI gels subjected to NATEM (n = 3; NS shows p > 0.05; * shows p < 0.05 against PBS and eluates with HS)

Similar to NI gels no significant differences were observed in the clotting times of PEG-Ac/SH/HS-Ac, PEG-VS/SH/HS-Ac and PBS over all time points (Fig. 35). Clotting times of PEG-Ac/SH/Hep-Ac were 81 ± 8% ($p = 0.004$) higher than PEG-VS/SH/Hep-Ac at day 1, but did not differ significantly thereafter. These clotting times were between 1.6 ± 0.6 min (56 ± 18%; $p = 0.047$) and 5.1 ± 1.9 min (183 ± 20%; $p = 0.0004$) higher than the PBS control.

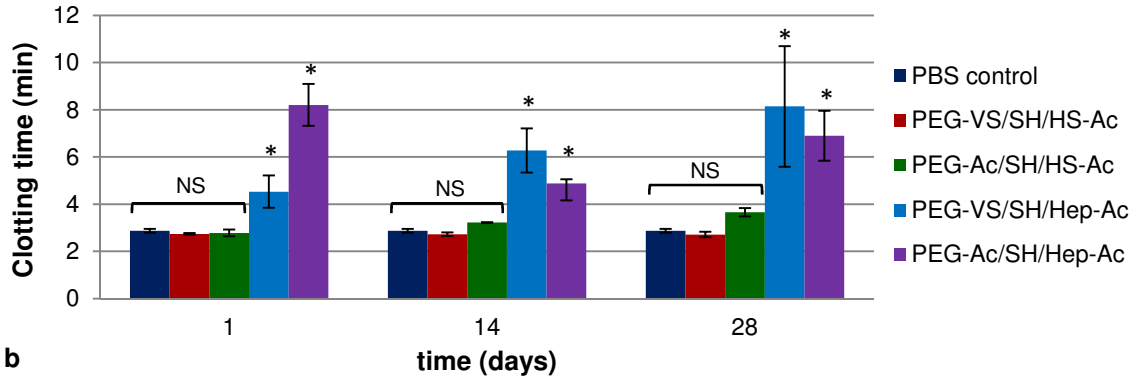

Figure 35: Clotting times of WB containing eluates from CI gels subjected to NATEM (n = 3; NS shows p > 0.05; * shows p < 0.05 against PBS and eluates with HS)

3.7 Growth Factor Binding and Release

Before swelling, 8.6 ± 1.2%, 0.8 ± 0.3% and 3.5 ± 0.4% of the growth factor (GF) added to the gels washed out of PEG-Ac/SH, PEG-Ac/SH/Hep-Ac and PEG-Ac/SH/HS-Ac, respectively (Fig. 36). Growth factor washout from Type 2D control gels (PEG-Ac/SH) was 1235 ± 7% and 149 ± 11% higher than from PEG-Ac/SH/Hep-Ac and PEG-Ac/SH/HS-Ac, respectively (Type 2D CI gels, $p < 0.0001$). PEG-Ac/SH/Hep-Ac without GF displayed an insignificant amount on the micro-plate reader (regarded as baseline noise).

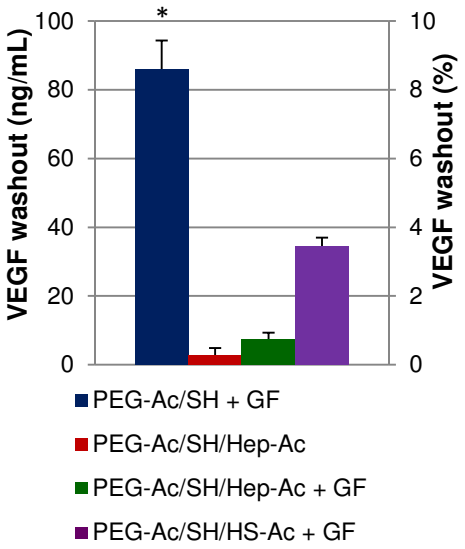

Figure 36: Growth factor washout from PEG-Ac/SH, PEG-Ac/SH/Hep-Ac and PEG-Ac/SH/HS-Ac (n = 4; * shows p<0.0001 against all other samples)

Growth factor (GF) release from PEG-Ac/SH/Hep-Ac and PEG-Ac/SH/HS-Ac (Type 2D CI gels) showed zero order ($R^2 \geq 0.91$ and $R^2 \geq 0.99$, respectively) release over the whole elution period recorded (Fig. 37). The GF release rate from PEG-Ac/SH/HS-Ac was on average 69 ± 11% ($p < 0.0001$) higher than PEG-Ac/SH/Hep-Ac over the recorded period (12 days). At day 12, 8 ± 1% and 13 ± 1% of the total amounts of incorporated GF were released from PEG-Ac/SH/Hep-Ac and PEG-Ac/SH/HS-Ac, respectively ($p < 0.0001$). GF release from PEG-Ac/SH (Type 2D control gels) showed

an initial burst (day 0-1), during which 3 ± 1% of incorporated GF was released, and was followed by a first order release profile ($R^2 \geq 0.96$). These gels released 11 ± 1% of the total amount of incorporated GF over the 12 day period. No release was observed from PEG-Ac/SH/Hep-Ac without GF (negative control).

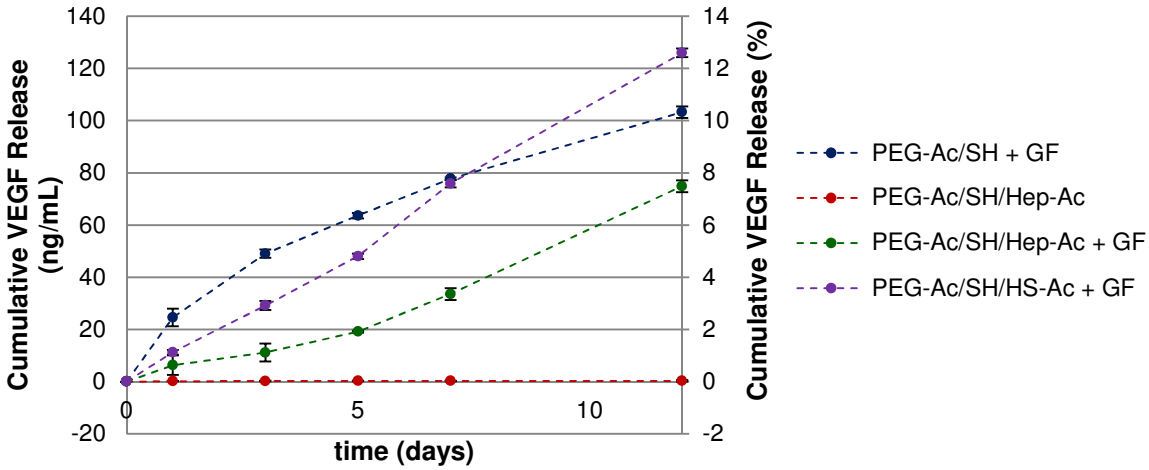

Figure 37: Growth factor elution from PEG-Ac/SH, PEG-Ac/SH/Hep-Ac and PEG-Ac/SH/HS-Ac (n = 4)

3.8 *In Vivo* Evaluation in Rat Subcutaneous Model

Qualitative assessment of hematoxylin and eosin (H&E) stains evinced that porous polyurethane (PU) disks without gel showed near-complete ingrowth at 7 days, while PU disks containing different gel formulations (for example PU + PEG-Ac/SH/Hep-Ac + GF in Fig. 38) suggested an increase in the area occupied by ingrown tissue relative to the available ingrowth area (scaffold area excluding the PU) over time. All samples were fully ingrown at 28 days. This was supported by quantitative data in Fig. 39 – explanted PU disks without gel were almost completely ingrown (97 ± 3%) at 7 days, while the disks with different gel formulations contained only 3 ± 2% to 35 ± 16% ($p < 0.0001$) tissue. At 14 days disks containing gels had 61 ± 16% to 95 ± 6% ingrown tissue, while all samples were fully ingrown (99 ± 1%) at 28 days. Between day 14 and 28 only PU + PEG-Ac/SH/Hep, PU + PEG-Ac/SH/Hep-Ac and PU + PEG-Ac/SH/Hep-Ac + GF (gel combinations with Hep) had a significant amount of ingrowth to complete.

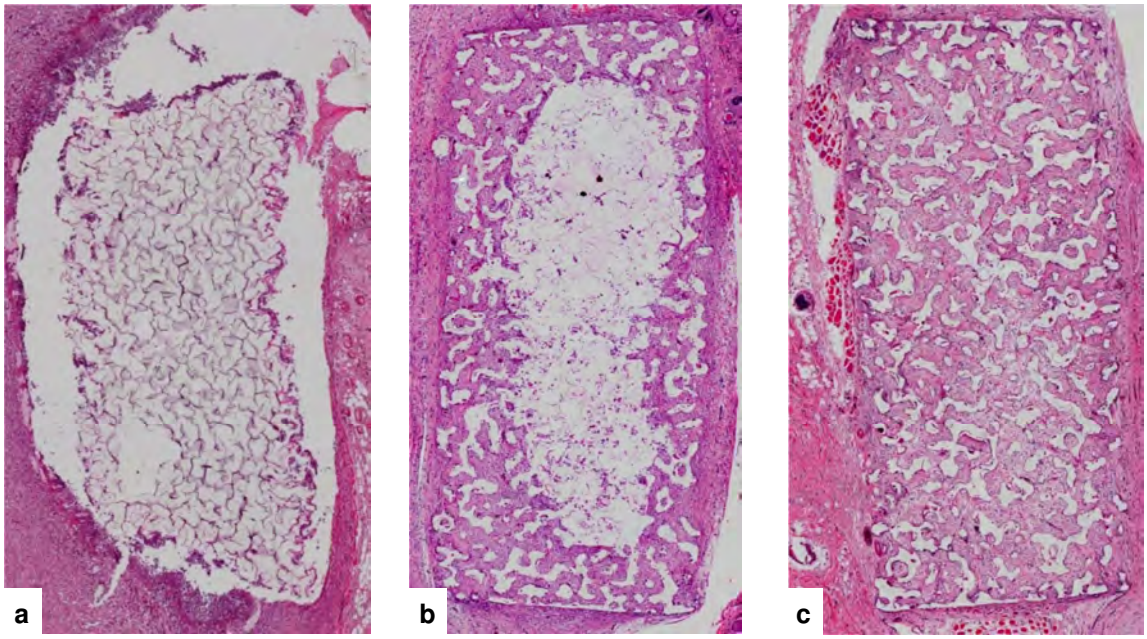

Figure 38: Representative micrographs of H&E stained sections of PU + PEG-Ac/SH/Hep-Ac + GF showing cellular and tissue ingrowth of the porous scaffolds at 7 (a), 14 (b) and 28 (c) days rat subcutaneous implantation

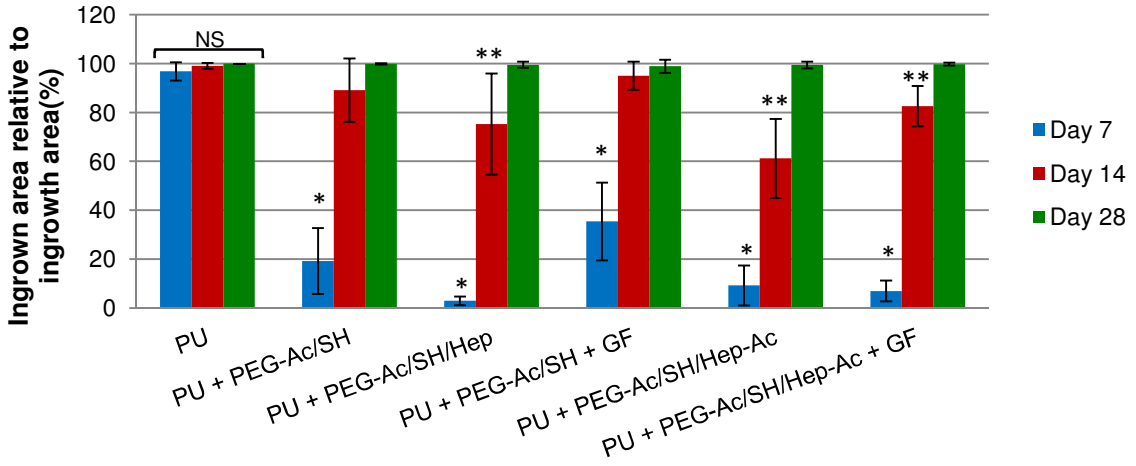

Figure 39: Ingrown area relative to ingrowth area of different explanted samples at different time points. (n = 6; NS shows $p > 0.05$; * shows $p < 0.0001$ against day 14; ** shows $p < 0.05$ against day 28)

Picrosirius red stains (PU + PEG-Ac/SH/Hep-Ac + GF as example) in Fig. 40 suggested an increase in collagen deposition (stained red) over time qualitatively, with or without incorporated gel formulations. Quantitative analysis (Fig. 41) supported this by showing similar trends to those obtained through H&E staining, with the exception of PU disks

without gel containing only 13 ± 3% collagen deposition relative to ingrowth area at 7 days (as opposed to 42 ± 1% at 28 days). Moreover the total collagen deposition areas for all the samples were only 33 ± 3% to 42 ± 1% of the possible ingrowth area at 28 days (as opposed to full ingrowth for H&E stains).

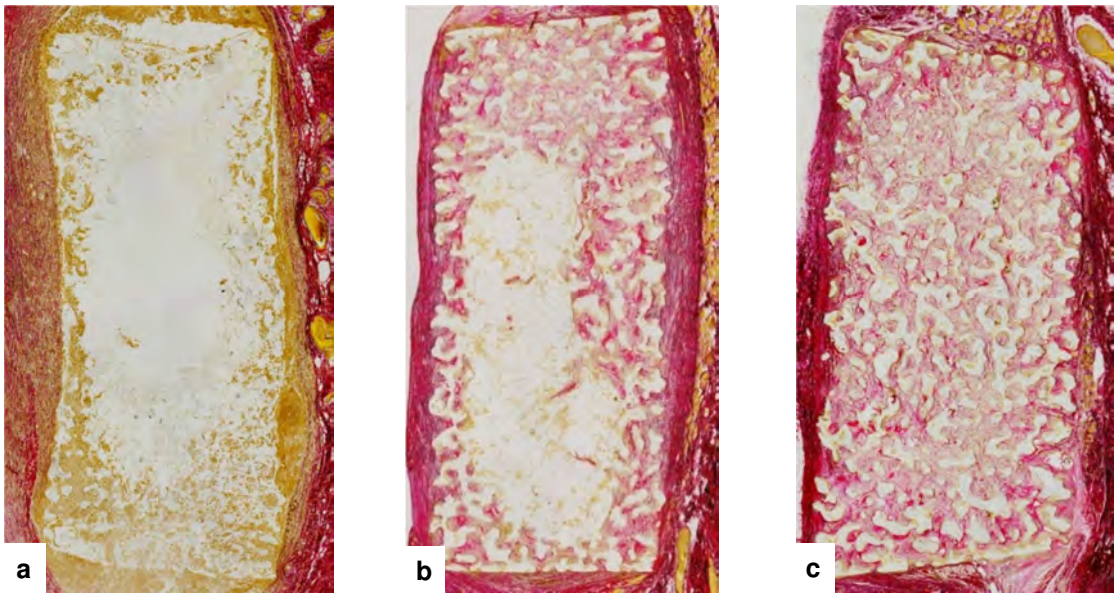

Figure 40: Representative micrographs of picrosirius red stained sections of PU + PEG-Ac/SH/Hep-Ac + GF showing collagen deposition of the porous scaffolds at 7 (a), 14 (b) and 28 (c) days rat subcutaneous implantation

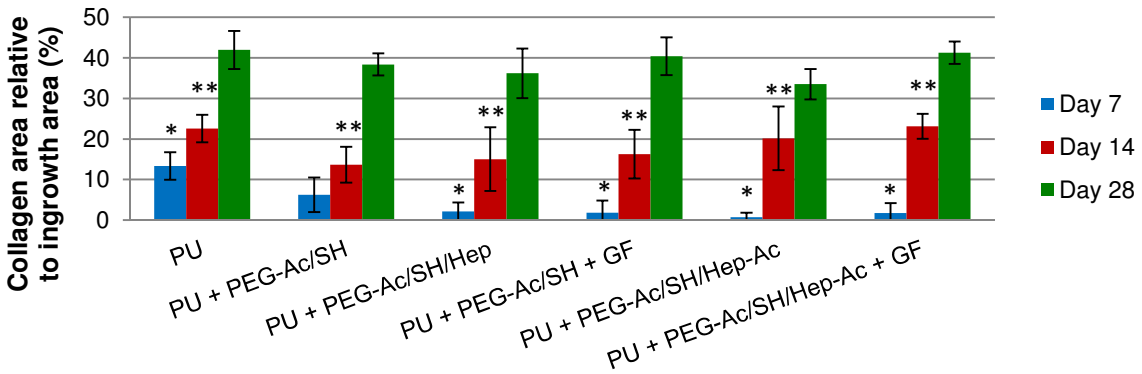

Figure 41: Collagen deposition relative to ingrowth area of different explanted samples at different time points (n = 6; * shows p < 0.005 against day 14; ** shows p < 0.0001 against day 28

Qualitative assessment of vessel ingrowth into PU disks containing gel (Fig. 42) indicated an increase in CD31-positive endothelial cells constituting capillary vessels

when GF (d) or Hep-Ac (e) was added to the gel (PEG-Ac/SH), but the largest increase in capillary vessel ingrowth was observed when Hep-Ac and GF (f) were both added. The first two slides (i and ii) are examples of what were counted as vessels.

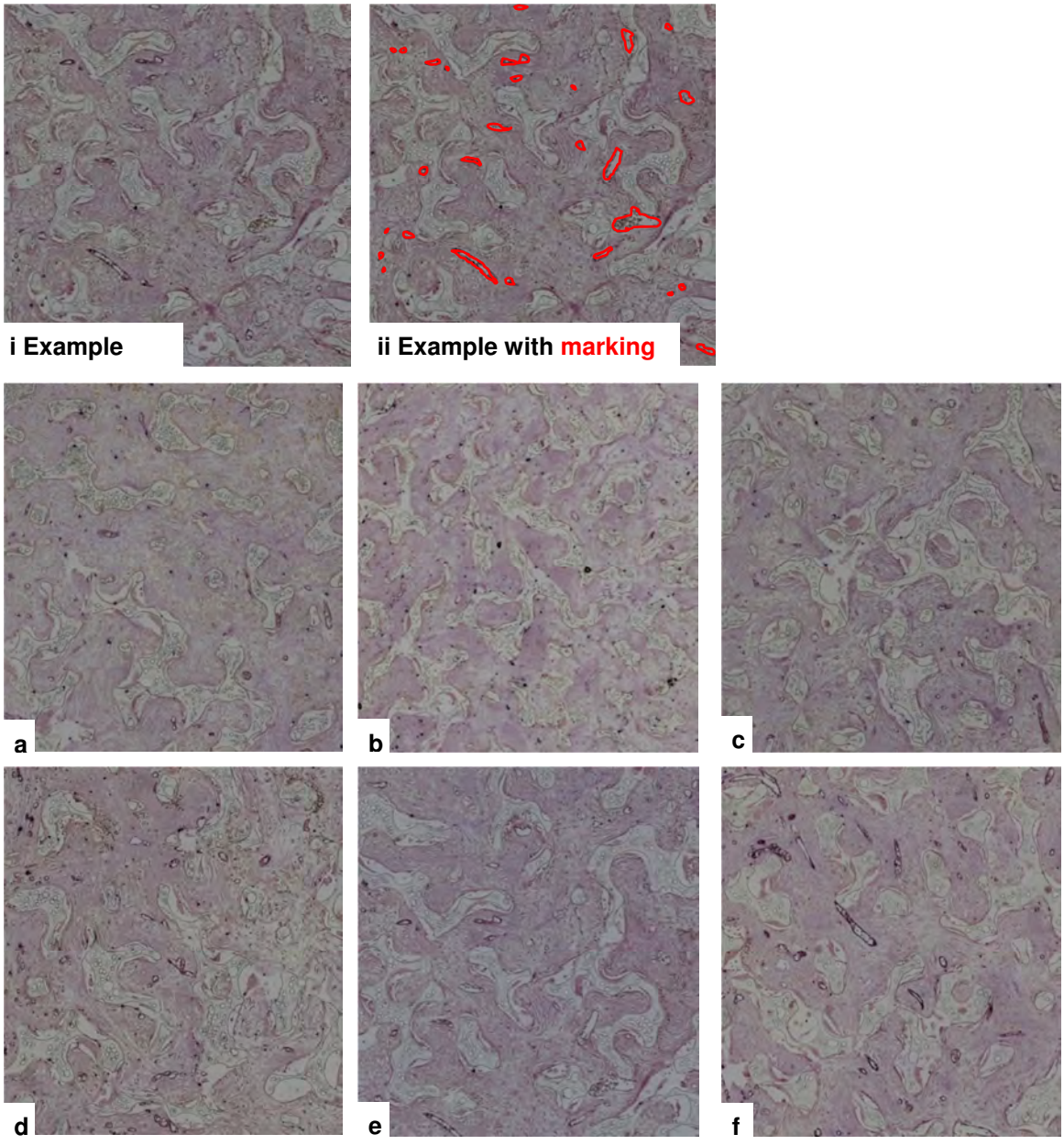

Figure 42: Representative micrographs of CD31 stained sections of PU (a), PU + PEG-Ac/SH (b), PU + PEG-Ac/SH/Hep (c), PU + PEG-Ac/SH + GF (d), PU + PEG-Ac/SH/Hep-Ac (e), and PU + PEG-Ac/SH/Hep-Ac + GF (f) showing vascularization of the porous scaffolds at 28 days rat subcutaneous implantation; (i) and (ii) are examples of vessel count

These findings were corroborated by quantitative data (Fig. 43 a), which showed that the number of capillaries relative to the ingrown area in PU + PEG-Ac/SH/Hep-Ac + GF was between 28 ± 10% ($p = 0.044$) to 694 ± 44% ($p < 0.0001$) higher than in all the other samples. Although the number of capillaries present in PU + PEG-Ac/SH + GF and PU + PEG-Ac/SH/Hep-Ac were significantly lower than in PU + PEG-Ac/SH/Hep-Ac + GF, it was still between 46 ± 11% ($p = 0.030$) to 511 ± 59% ($p < 0.0001$) higher than in the other samples. The capillary area relative to the ingrown area of PU + PEG-Ac/SH/Hep-Ac + GF was between 54 ± 33% ($p = 0.012$) to 349 ± 45% ($p < 0.0001$) higher than in all the other samples (Fig. 43 b). There was no significant difference in the capillary area of PU disks (without gel) and all the other samples, excluding PU + PEG-Ac/SH/Hep-Ac + GF. However PU + PEG-Ac/SH/Hep-Ac was, on average, 123 ± 36% ($p = 0.009$) higher than PU + PEG-Ac/SH and PU + PEG-Ac/SH/Hep.

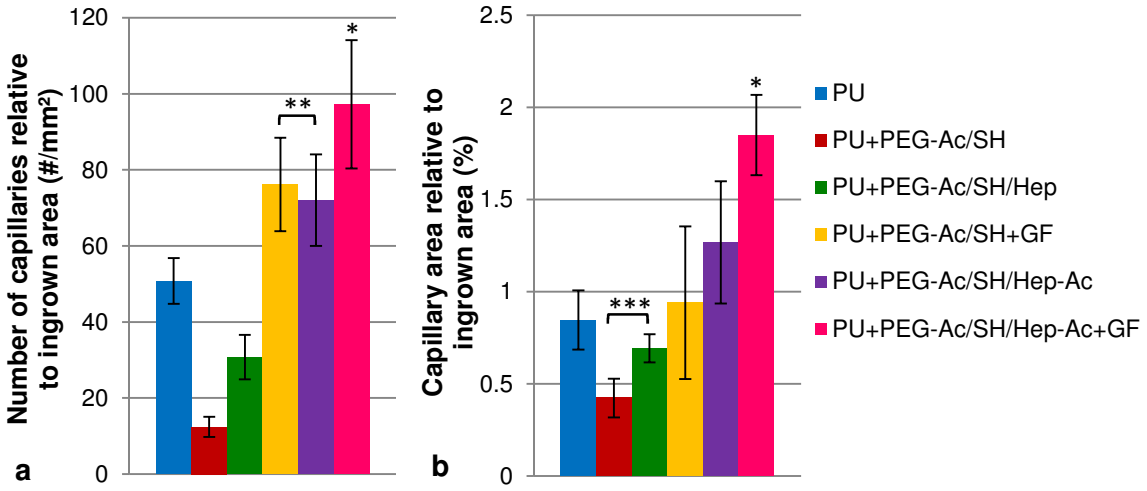

Figure 43: Quantification of blood capillaries in porous PU scaffolds, showing the number of capillaries relative to ingrown area (a) and total capillary area as a percentage of the ingrown area (b) (n = 6; * shows $p < 0.05$ against all other samples; ** shows $p < 0.05$ against PU and $p < 0.0001$ against PU + PEG-Ac/SH and PU + PEG-Ac/SH/Hep; * shows $p < 0.05$ against PU + PEG-Ac/SH/Hep-Ac)**

4 Discussions

This work showed how the controlled release of active heparin or heparan sulfate (Hep/HS) could be achieved by covalent incorporation into spontaneously forming hydrogels, capable of controlled growth factor (GF) delivery to improve angiogenesis *in vivo*. Specifically: (i) 20PEG8Ac and 20PEG8VS copolymers were synthesized by nucleophilic substitution reactions, (ii) Hep and HS were acrylated by Schotten-Baumann reactions using acryloyl chloride (AcCl), (iii) hydrogels were formed by Michael-type addition reactions between acrylated Hep/HS (Hep/HS-Ac) and PEG tetra-thiols (10PEG4SH), to form Type 1 gels, and between the 20PEG8Ac and 20PEG8VS copolymers and 10PEG4SH to form Type 2D and 2N gels, respectively, with or without the covalent incorporation of Hep/HS, (iv) gel properties (gelation time, viscoelasticity, swelling, crosslink density and mesh size) were retained and not significantly influenced by the addition of Hep/HS-Ac, (v) Hep/HS was eluted from the hydrogels in a controlled manner and with retained activity (the anticoagulative properties of eluates from gels and their eluates were controlled as well), (vi) GFs were bound to Hep/HS hydrogels and released in a controlled manner, and (vii) these hydrogels were successful at improving angiogenesis in a rat subcutaneous model.

4.1 Multi-arm PEG copolymers

Polyethylene glycol copolymers were obtained in conversions of 93-94%, which is similar to previously reported for 20PEG8Ac and 20PEG8VS synthesis in literature.[47,80,267] In the current project average yields were obtained and can be ascribed to the extensive purification method used - purification was performed by three subsequent precipitation steps and dialysis, as opposed to only one precipitation step performed in previous studies.[47]

4.2 Modification of Heparin/Heparan Sulfate

Of the different Hep/HS modification methods investigated in this project, the Schotten-Baumann reaction using AcCl was preferred due to high conversions and yields obtained. However, acrylic acid formed due to the high reactivity of AcCl with water

which affected the pH of the solution and, consequently, the degree of acrylation. A syringe pump was therefore used to control AcCl addition and ensure a stable pH between 8 and 9 (favouring the transesterification reaction).[35,130,268] Benefits of this method include its high conversion (up to 80% acrylation), high yields, simplicity and short reaction times (1-2 hours) in comparison to the other methods investigated. Kumar and Gross also obtained as high conversions by using a similar method to acrylate hyaluronic acid (HA).[130] Since the Ac groups were attached directly to the carbohydrate backbone, and not via spacers as previously reported by various researchers,[69,268–271] Hep/HS could be released in its original, unmodified form during hydrolysis. Anhydride and epoxy chemistries were not further used due to the low conversions obtained – low reactivity of methacrylic anhydride with Hep/HS hydroxyls[73,250] resulted in low methacrylation percentages (11-13%), while the competing transesterification and ring opening reactions[69,268] (apparent from NMR analysis of products from reactions with glycidyl methacrylate) resulted in the presence of undesirable spacers.

4.3 Gel Formation

The successful formation of Type 1 gels (Hep-Ac/SH and HS-Ac/SH) and Type 2D and 2N control gels (PEG-Ac/SH and PEG-VS/SH, respectively) through Michael-type addition reactions can be ascribed to the presence of the crosslinker thiols (10PEG4SH, acting as the nucleophile) and α,β-unsaturated end-groups (VS or Ac) of functionalized Hep/HS and/or PEG (rendering the terminal carbon electrophilic).[82,94,96,102,272,273] Hydrogels of these types were previously developed by Hubbell et al.[47,68] and variations by numerous other researchers.[59,81,86,94,97,142,213] The covalent and non-covalent incorporation of Hep/HS into Type 2 gels did not significantly influence the gelation due to the small amount of Hep/HS or Hep/HS-Ac added (1.5m% of 4m% copolymer).

Heparin/HS with 3% (meth)acrylation or lower did not result in gelation upon irradiation since it theoretically represents less than one Ac moiety per Hep/HS chain. It was however expected that Hep/HS-MA and Hep/HS-Ac (with acrylation lower than 20%) would spontaneously form gels through Michael-type addition reactions with 10PEG4SH, since 20% (meth)acrylation theoretically accounts for approximately six functionalized groups.[12,53,69,73,130] Together with NMR results, the gelation of Hep/HS-MA and Hep/HS-

Ac (all acrylation percentages higher than 3%) through photo-polymerization confirms successful Hep/HS modification.

4.4 Rheological Characterization

4.4.1 Gelation time

The slightly faster gelation time of HS-Ac/SH than Hep-Ac/SH might be due to the less ionic nature of HS caused by its less sulfated structure.[36,227] This was however not further investigated since the gelation times of Type 1 gels (5.3 min and 4.0 min for Hep-Ac/SH and HS-Ac/SH, respectively) are both in the range (3 to 10 minutes) obtained for similar gels formed by previous researchers.[35]

Gelation times of Type 2 gels are in expected ranges (7.2 min and 3.1 min for Type 2D and 2N gels, respectively) as obtained in similar studies by Zustiak and Leach.[81] The shorter gelation times of Type 2N gels in comparison to Type 2D gels are due to the higher relative reactivity of VS (in comparison to Ac) towards thiols, since the sulfone groups are more electron deficient and have a higher electron withdrawing capability than the carbonyl groups of Ac.[274–276] In a study by Chatani et al. they found that the reaction rate between VS and thiols was approximately seven times higher than between Ac and thiols.[275] The addition of unmodified or acrylated Hep/HS not significantly affecting the gelation time was expected, since the amount added was very small (1.5m% of 4m% copolymer) and the acrylates present on the Hep/HS-Ac were accounted for by the stoichiometric amount of thiols added.

4.4.2 Viscoelasticity

The existence of complete crosslinked networks in the equilibrium swollen gels are confirmed by the independency of storage and loss moduli (G' and G'') on frequency in the studied range (0.01-100 Hz).[35] These gels perform almost as ideal elastic materials since G' exceeds G",[277] while the slight increase in G' at higher frequencies (above 80 Hz) can be ascribed to gel stiffening.[248] The slightly higher G' value of Hep-Ac/SH, in comparison to HS-Ac/SH (4767 Pa and 4015 Pa for Hep-Ac/SH and HS-Ac/SH, respectively), could be due to the greater ionic nature of Hep which results in greater water uptake and swelling (as also seen by the SR curve in Fig. 25), causing a greater

osmotic pressure and thus stiffer gel at the time of measurement.[278] Storage moduli of Type 1 gels are however in similar ranges as those of gels developed by researchers using similar precursors.[35]

The higher storage moduli of Type 2N gels (9914 Pa) than Type 2D gels (7073 Pa) is ascribed to the greater conversion and better crosslink density achieved at the time of measurement, due to the higher reactivity of VS than Ac towards thiols.[275,276] Although these results are 10-fold lower than the G' found in studies by Lutolf and Hubbel, who crosslinked 20PEG4VS with dithiols[68], Tae et al. showed that an increase in the amount of crosslinking sites (4-arm to 8-arm) increased G' by more than 10-fold.[97] Storage moduli of Type 2 gels evinced again that the presence of unmodified or acrylated Hep/HS did not significantly influence the viscoelastic properties and stiffness of the gels.

4.5 Hydrogel Swelling

Initial swelling (swelling ratio 1 and 2, SR and Q) observed for Type 1 gels was due to equilibrium water uptake, whereafter continued swelling followed due to the steady decrease in crosslink density caused by hydrolysis of the relatively labile β-thio-ether ester linkages. The significantly higher overall swelling of Hep-Ac/SH than that of HS-Ac/SH (by approximately 150%) can again be ascribed to the greater ionic strength of Hep leading to greater water uptake and swelling, as well as a possible difference in acrylation percentage.[278] However, the Q values of both gels at day 3 (24.7 on average) are similar to studies using 40% thiolated Hep and diacrylated PEG for gel synthesis.[97]

Although all Type 2 gels underwent rapid initial swelling due to absorbance of equilibrium amounts of water,[64,252,279] Type 2D gels experiencing a more rapid initial swelling (as opposed to Type 2N gels) can be ascribed to the carbonyl oxygen of the ester, a strong hydrogen bond acceptor, which results in faster water uptake.[81] As with Type 1 gels, the degradable nature of gels consisting of 20PEG8Ac copolymer was due to hydrolysis of the β-thio-ether ester bonds.[102,272] Rapid disintegration after 21 days can be ascribed to the steady decrease in crosslink density caused by hydrolysis as well as bulk degradation – due to the high water content of the gels the probability for each ester bond to be broken via hydrolysis was the same.[81] On the other hand, Type 2N gels

maintaining constant swelling ratios post-equilibrium confirms the stability of these thio-ether sulfone bonds toward hydrolytic degradation *in vitro*.[94,275,276,280] These findings are similar to those obtained in previous work by our group, during which SR values of 3.4-3.6 and 1.7-2.1 were obtained for Type 2D and 2N gels, respectively after 12 days (in the current study the SR is 3.5 and 1.3 after 21 days).[213] The values of Q also correlate well with gels studied by DuBose et al. who thiolated fluoroscopic probes, incorporated them into gels consisting of 20PEG8Ac crosslinked with dithiothreitol (DTT) and recorded Q values in the range of 18-40 between day 8 and 12.[86] It is important to note that since the covalent and non-covalent incorporation of Hep/HS did not significantly influence the SR or Q of Type 2 gels, the presence of Hep/HS did not significantly disrupt the network structure, degree of cross-linking, hydrophilicity or degradation of the gels.[81]

The initial increases in the mesh sizes of Type 2 gels were not necessarily due to bond breaking, but rather as a result of stretching of the polymers in the gel network, while further increases in the mesh sizes of Type 2D gels resulted from bond breaking during hydrolysis.[253] Since the initial mesh size of the gels was 44.6 ± 3.1 Å on average, which is higher than the hydrodynamic diameters of Hep/HS and VEGF (9 ± 1 Å [281] and 38 ± 1 Å [282], respectively), it can be assumed that the diffusion of non-covalently or incompletely incorporated Hep/HS or VEGF caused the initial burst release, whereafter the delivery of covalently incorporated Hep/HS could continue *in vitro*. In a study by Bracher et al., who crosslinked matrix metalloproteinase (MMP) with 20PEG4VS,[244] the gels had higher average mesh sizes after equilibrium swelling due to the lower crosslink density of copolymers used (4-arms as opposed to 8-arms in the current project, for the same molecular weight) as per Flory-Stockmayer's theory.[68,86,217,275]

4.6 Heparin and Heparan Sulfate Elution

Type 1 gels: The initial Hep/HS burst release from Type 1 gels is apparent from swelling kinetics, while the zero order release obtained after covalent incorporation of Hep or HS in hydrogels is usually unattainable by simple incorporation, swelling or diffusion controlled release mechanisms.[86,154,155] The slightly greater initial elution of HS in comparison to Hep was not expected since the levels of acrylation of both were 40%, but can be attributed to incomplete covalent incorporation of HS-Ac during gel formation

(since the G' of equilibrium swollen HS-Ac/SH was also significantly lower than Hep-Ac/SH) or non-idealities, such as multiple arms from the same crosslinker reacting with Ac to form primary cycles and diffuse from the gel upon immersion. This was however not investigated as it was considered outside the scope of this study.

Type 2 gels: Although a small amount of Hep and HS was initially released from CI gels (PEG-Ac/SH/Hep-Ac, PEG-Ac/SH/HS-Ac, PEG-VS/SH/Hep-Ac and PEG-Ac/SH/HS-Ac) probably due to incomplete incorporation and/or rapid equilibrium swelling, the amount was drastically lower than the initial burst from NI gels (PEG-Ac/SH/Hep, PEG-Ac/SH/HS, PEG-VS/SH/Hep and PEG-Ac/SH/HS). This confirms the successful covalent incorporation of the majority of the Hep/HS-Ac. Elution of Hep and HS from NI gels is considered to be of burst release character, since the total amount of non-covalently bound Hep/HS diffused from the gel during the initial two days.

The subsequent near linear, zero order release from Type 2D CI gels (PEG-Ac/SH/Hep-Ac and PEG-Ac/SH/HS-Ac) can be ascribed to the degradation of the two different types of ester bonds, i.e. Hep/HS or 20PEG8Ac attached to 10PEG4SH.[86] Primarily release refers to Hep/HS cleaved from the gel network through hydrolysis (due to β-thio-ether ester bonds) releasing it from the polymer matrix in its unmodified form,[102] while secondary release occurred through cleavage of the β-thio-ether ester bonds linking 20PEG8Ac and 10PEG4SH. As per definition, the release rate is therefore independent of the initial Hep/HS concentration.[153] The rapid release after day 21 can be explained by extensive gel degradation.

The release of Hep and HS from Type 2N CI gels (PEG-VS/SH/Hep-Ac and PEG-VS/SH/HS-Ac) followed first order kinetics, which is expected since only primary cleavage of CI Hep/HS from the gel network through hydrolysis, due to the relatively labile β-thio-ether ester bond of Hep/HS-Ac with 10PEG4SH, was possible. The non-degradable nature of stable thio-ether sulfone linkages between VS and thiols implies the absence of secondary ester bonds and therefore the release rate was dependant on the Hep/HS concentration.[94,153,280] This is consistent with results obtained by Bezuidenhout et al. or DuBose et al. who attached dexamethasone via degradable linkages to degradable and non-degradable PEG gels[213] or incorporated thiolated fluorescent probes into acrylated PEG with DTT, respectively.[86]

4.7 Heparin and Heparan Sulfate Activity

The large effect of Hep and HS addition to INTEM assays was expected since, although Hep is known to affect both the intrinsic and extrinsic coagulation pathways, it has a much greater effect intrinsically due to its function as thrombin amplifier.[283] Heparin and HS do not have a large effect on either fibrinolysis or the contributions of platelets and fibrinogen to final clot strength,[259,284] as indicated by fibrinogen ROTEM (FIBTEM) and aprotinin ROTEM (APTEM) profiles. It is important to note that although clotting times obtained through TEG and ROTEM showed similar trends for both unmodified and acrylated Hep/HS, the clotting times obtained through ROTEM were proportionally shorter due to more diluted samples used in ROTEM.[284] Although native ROTEM (NATEM) is not clinically used (long clot formation times due to the lack of initiators),[260] it was used to evaluate the activity of eluates from Type 2 gels, since the amount of Hep/HS incorporated into and released from the gels was very small.

The addition of unmodified Hep to whole blood (WB) led to an expected large increase in clotting time (5-6 fold longer than PBS control) due to its well documented anticoagulative properties.[285,286] A study by Atha et al., for example, showed that the rate at which Hep bound antithrombin (AT) III inhibited thrombin increased by two to three orders of magnitude.[287] The approximately 4 times shorter clotting time of unmodified HS (in comparison to Hep) was expected since HS is known to be significantly less anti-thrombotic. Even though Hoppensteadt et al. found that a five to ten fold higher dose of HS was required to produce an equal antithrombotic effect as Hep,[14] HS is not completely non-antithrombotic since studies have shown that approximately one to ten percent of the HS molecules have anticoagulant activity.[2,38] The absence in a difference between HS and the control can possibly be due to the small concentration of HS added making it difficult to observe a significant difference (not due to WB dilution, since the control also consisted of WB diluted with PBS).[288] Although the activity of Hep was slightly compromised after acrylation, it retained its activity to a large extent as the clotting time was still significantly longer than that of the PBS control (2-3 fold longer).[289,290] This decrease in activity after modification was also seen in previous studies, where it was shown that the binding affinity of Hep to AT III, after thiolation, decreased with increasing functionalization.[97]

The increased clotting times induced by Hep or HS in the eluates indicate the retained activity of the Hep/HS during incorporation into and release from Type 1 and 2 gels. Eluates from NI gels were active until day 3, while the absence in increased clotting time thereafter supports the result that all of the Hep/HS was released from NI gels by day 3. Importantly, increased clotting times induced by eluates from CI gels show that the released Hep/HS retained activity over the measured elution period. Since the concentrations of the eluates were normalised before performing the TEG and ROTEM, the differences in clotting times are only based on the activities of the Hep/HS in the eluates.

4.8 Growth Factor Binding and Release

Growth factor binding and release experiments were only performed on Type 2D gels. Acrylated Hep bound to the PEG gels retained its ability to bind VEGF, since only 0.8 ± 0.3% of the VEGF initially added was released in the wash-out stage, compared to the 8.6 ± 1.2 % from controls (PEG gel without bound Hep or HS). This high affinity between Hep and VEGF can be ascribed to the presence of Hep binding domains on VEGF.[59] Although HS-Ac was also able to bind VEGF it was to a significantly lesser extent than Hep, since Hep has a greater negative charge than HS and therefore promote stronger bonds with the net positive charge of VEGF.[59,291] Although the Ac groups were in great excess over the amount of VEGF added, control gels were able to bind VEGF possibly due to the presence of unreacted thiols forming disulfide linkages with the cysteine residues of VEGF, as previously reported.[7,16]

Controlled VEGF release from hydrogels containing Hep-Ac was obtained due to the known high affinity of the Hep-VEGF interaction,[53,54] which was expected since computational and experimental results from previous studies showed that a molar ratio of Hep to VEGF of 100:1 was necessary to reduce passive diffusion of GFs from hydrogels[54] (the ratio in the current study is 150:1). Gels with bound HS were also capable of sustained VEGF release, which can be potentially very useful where GF binding without strong anticoagulation is desired. The faster GF release rate from the bound HS gels can once again be ascribed to the higher affinity between Hep and VEGF, in comparison to HS. Both Hep and HS bound PEG gels were able to increase the residence time of VEGF, since only 8 to 13% of the initial amount of VEGF were

released over a period of 12 days *in vitro*, while GFs are known to degrade by proteolysis within 10–20 min after bolus injection.[122,265] Although PEG gels without bound Hep/HS could also retain GFs, as shown in previous research[7] and by the controlled (first order) VEGF release from control gels (PEG-Ac/SH), these gels were not able to eliminate the initial VEGF burst release. A study by Wissink et al. had shown that Hep hydrogels with Hep:GF molar ratios of 13 000:1 was needed to eliminated burst release,[35,52,292] but it was however successfully eliminated at a smaller ratio in the current study due to the covalent incorporation of Hep/HS into PEG gels.

Failure to release the total amount of GF initially incorporated into the gels has also been seen in similar studies by various researchers, but however still led to increased angiogenesis *in vivo*.[7,8,16,35,97] This can possibly be attributed to conformational changes of GF due to surface adsorption, disulfide exchange between the hydrogels and GF, structure loss or the absence of a sequester site during the experimental release period, causing it to not be recorded during the ELISA assay.[7] Incorporation of VEGF into the crosslinked hydrogels could also retard its release leading to a significant fraction of GF not released.[8,122,265]

4.9 *In Vivo* Evaluation in Rat Subcutaneous Model

The near-complete ingrowth of tissue into the polyurethane (PU) scaffolds (without gel) as early as 7 days can be ascribed to the high porosity (82%) and large pores (150 µm with 70 µm interconnectivity) of the disks. Various researchers have reported that scaffolds with pores of these sizes allow for not only cellular ingrowth, but also fibrohistiocytic tissue, capillaries, fibrous tissue and fibro-cartilaginous tissue, ect.[293–296] When the disks are prefilled with any of the hydrogel compositions there is limited ingrowth at the early time point, due to presence of the gel. The increased ingrowth into gel-filled scaffolds at day 14 corresponds to the hydrolytic degradation of the ester bonds seen *in vitro* at approximately this time. No correlation was found between the fluctuation in ingrowth rate and the presence of Hep/HS. This agrees with *in vitro* tests which showed that neither covalent nor non-covalent incorporation of Hep/HS significantly affected the gelation time, viscoelasticity, swelling or degradation of the gels. Full ingrowth achieved for all gel formulations upon gel dissolution agrees with previous work showing that Hep containing PEG acrylate gels were able to be degraded and allow cell

infiltration within two to four weeks *in vivo,* depending on the functionalization and gel formulation.[7–9,203]

Collagen deposition by ingrowing cells followed the same trend for the groups containing hydrogels, however at lower absolute values, as collagen represents only part of the ECM (others include fibrin, laminin and elastin).[277] In the case of the non-gel-filled scaffolds, the stepwise increase in collagen deposition with increased time may be ascribed to a delay between tissue ingrowth and occupation, as well as collagen synthesis and deposition.

Disks containing PEG gels (without Hep or GF) formed fewer blood vessels than disks without gels (control disks) after 28 days, since the presence of the gel caused a delay in tissue ingrowth, while control disks allowed full infiltration (and consequently vessel formation) after the first week of implantation. The slight increase in vascularization of disks containing PEG gels with NI Hep in comparison to the PEG gel alone (no Hep) can be attributed to the released Hep serving as a sequestration site, stabilizer and transporter for GFs present in the local ECM.[24,297] However, since most of the NI Hep was released during the initial burst the effect was not enough to overcome the initial ingrowth inhibition caused by the presence of the gels within a period of 28 days. On the other hand, addition of GFs to PEG gels was capable of overcoming this, since a similar amount of angiogenesis was achieved for PEG gels with GF and control disks and therefore neo-vessels developed during exposure to the active GF. However, due to the short half-life of the GF and the absence of Hep to ensure GF sequestering, the vessel numbers only increased while the GF was released - soon after release GFs become inactive.[9]

The addition of CI Hep to the PEG gels did not only overcome the effect caused by the retarded angiogenic response due to ingrowth inhibition, but also successfully improved angiogenesis relative to control disks and disks containing PEG gels with GFs. Due to controlled release of Hep (sequestration site, stabilizer and transporter for GFs[24,297]) GFs present in the ECM were localized and concentrated in the scaffold during the entire gel degradation and tissue infiltration period, causing an increase in angiogenesis. In a previous project performed by our group porous polyurethane scaffolds were heparinized and a similar increase in vascularization (after 28 days) had been

obtained.[245] Most importantly the addition of CI Hep gels with GFs showed the highest degree of angiogenesis. Since the CI Hep was subjected to controlled release during degradation and VEGF was sequestered by the released Hep, maximum activity of the GF for the longest period of time was ensured, achieving the most profound vascularization. Since the Hep-VEGF complexes are likely to remain in the ECM for some time after complete gel dissolution, continued GF release was possibly allowed and therefore a continuation of vessel growth, leading to even more angiogenesis.[8]

5 Conclusions

In this study injectable degradable and non-degradable Hep and HS containing PEG hydrogels capable of controlled, localized GF delivery were synthesised by utilization of PEG chemistries. These hydrogels showed to be capable of improved angiogenesis *in vivo*. The covalent attachment of α,β-unsaturated groups to Hep and HS were achieved by acrylation through the Schotten-Baumann reaction. Controlled and repeatable degrees of modification were achieved by controlled addition using a syringe pump and product structures were successfully determined by NMR spectroscopy.

Gels formed spontaneously at physiological conditions (37 °C, pH=7.4) by Michael-type (1,4 nucleophilic conjugate) addition chemistry, without the need for initiation by chemical agents or radiation and without producing leaving groups or undesirable by-products. Acrylated Hep or HS crosslinked with PEG tetra-thiols (Type 1 gels) were used to compare the effect of Hep and HS on gel properties and Hep/HS or GF delivery abilities *in vitro*. The acrylated materials were also copolymerized with degradable (acrylate based, 20PEG8Ac) and non-degradable (vinyl sulfone based, 20PEG8VS) 8-arm PEG macro monomers by reaction with 10PEG4SH (Type 2 gels), which allowed for more control over the Hep/HS content and degradation of the gels. Hydrolysis of the thio-ether ester crosslinks between Hep/HS-Ac and 10PEG4SH resulted in the release of Hep/HS in its original, unmodified form.

Gel properties (gelation times and elastic moduli, hydrogel swelling, crosslink densities and mesh sizes) were not significantly influenced by the addition of acrylated Hep/HS. Hydrolytic degradation of the cross-linked network of Type 2D gels resulted in disintegration after 22 days, while Type 2N gels remained stable for more than 6 months. The sustained release of the covalently incorporated Hep/HS from Type 2D and 2N gels followed zero and first order kinetics, respectively (over the 21 and 56 days, respectively), which is usually unattainable by simple incorporation and diffusion control release mechanisms.[86,99,154,155] Type 1 gels also remained stable over the 72 days recording period and followed zero order release during that time. It can therefore be concluded that controlled, extended and localized release of Hep/HS from the hydrogels, copolymerized with 20PEG8Ac or 20PEG8VS (Type 2 gels) or not (Type 1 gels), was achieved.

The anticoagulative properties of the eluates were successfully decreased by using HS instead of Hep. Heparan sulfate is known to be less anti-thrombotic than Hep and this property was retained after chemical modification, as well as after the incorporation and release from the hydrogels, which is potentially very useful where GF binding without strong anticoagulation is desired. Pro-angiogenic GFs were successfully incorporated into Hep/HS containing PEG gels and controlled release of the active GFs was achieved and confirmed *in vitro* by ELISA. Sustained GF release from Hep/HS gels was described by zero order kinetics and showed to be more sustained than from pure PEG gels.

In vivo studies in a rat subcutaneous model demonstrated that the hydrogels degraded sufficiently after 28 days to allow complete displacement of the gel by tissue to populate the PU scaffold interior. The most profound conclusion of this project is that the controlled, low and localized delivery of pro-angiogenic GFs (VEGF) from Hep containing PEG hydrogels successfully led to an increase in angiogenesis *in vivo*. Although these gels were implanted using PU scaffolds, they have the ability to form in situ and spontaneously at physiological pH and temperature by preparing an admixture of two components and injecting it directly into the treatment area, thereby avoiding invasive surgery.

These encouraging results suggest that the injectable hydrogels developed in this project have considerable potential for a spectrum of *in vivo* cardiovascular tissue regeneration applications. In future projects the proven anticoagulative and angiogenic GF binding, stabilization and potentiation ability of Hep hydrogels will be evaluated in vascular grafts to retain patency, prevent early occlusion through its anti-thrombotic properties and to facilitate spontaneous transmural endothelialisation through angiogenesis and healing. For the treatment of myocardial infarction and to prevent heart failures the GF binding and potential anti-inflammatory properties of heparinoids are more important than their anticoagulation properties, and therefore HS containing PEG hydrogels may be preferred. In both cases the sustained release of pro-angiogenic GFs will be implemented as major driving force of angiogenesis and neovascularization, while the covalently attached GAG could further inhibit smooth muscle cell proliferation and moderate inflammation.

6 Recommendations and Future Directions

- In future more *in vivo* experiments should also be performed to compare the effects between Hep and HS containing PEG hydrogels.
- The amount and concentration of Hep/HS added to the gels should be optimized. It should be high enough to ensure the desired antithrombotic (in the case of Hep gels), anti-inflammatory and GF sequestering and activation effects to promote neovascularization, whilst not altering the gel properties, cause excessive bleeding or haemorrhages.
- The amount and concentration of GF incorporated into the gels should be optimized as well. Large amounts can result in dysfunctional and malformed vessels, while too small amounts will not be able to improve healing. The ratio of GF and Hep/HS concentrations should also be investigated to optimize their activities.
- The type of GF optimally delivered through Hep/HS hydrogels should be investigated, such as bFGF, aFGF, KGF and IGF-1, among others. Due to alternative splicing of a single gene, VEGF exists in four isoforms (VEGF121, VEGF165, VEGF189 and VEGF206), showing similar biological activities, but bind with different affinities to the Hep/HS and can therefore result in different secretion patterns.
- Due to the complexity of angiogenesis the delivery of multiple cytokines (delivered simultaneously or in temporally staged sequences) using a single intervention, should be investigated. Delivery of two GFs, one chosen for its ability to initiate an angiogenic response (e.g. VEGF) and the other for promotion of late-stage maturation of newly forming vessels (e.g. KGF), should be investigated in the developed hydrogels, which will potentially stimulate different stages of micro-vessel growth and lead to the formation of neo-vessel beds capable of supporting perfusion.
- Long-term implantation of PU disk containing hydrogels should be performed to follow the healing patterns resulting from continued cellular ingrowth and reorganisation. The formulation of the degradable gels (Type 2D) can also be altered to obtain gels that degrade at different time points, desired for specific applications.

- In future studies planned by our research group the GF eluting Hep/HS hydrogels will be evaluated in the rat looped infra-renal aortic interposition model for thrombogenicity, tissue ingrowth and vascularization, and in the myocardial infarction model for myocardial thickness preservation and functional improvement. Both *in vivo* models are established in our laboratories. Clinical implementation of these gels in vascular grafts, if successful, have the potential to drastically improve the outcome of peripheral small diameter vascular grafts, while in myocardial infarction applications they have the potential to reduce left ventricular remodelling by increased angiogenesis and cease the progression to heart failure. For the latter application the solid content of the gels should be investigated for optimum gel formation time, sufficiently rapid to prevent dilution of the precursor solutions or encapsulation of specific cell types prior to cross-linking,[81] but also not too rapid to prevent homogeneous mixing or cause an increase in the viscosity of the solution, which can jeopardize injection of the gel.[136,298]
- It would be valuable to perform endothelial cell proliferation assays on GF eluates to determine retained activity. In order to avoid GFs becoming inactive in the eluates several additives should be investigated to prevent surface adsorption during the release period and maintain activity in the release buffer. The addition of ethylenediaminetetraacetic acid (EDTA) and sucrose can potentially prevent trace metal-induced disulfide exchange between the gels and GF and maintain the GF structure in solid state, respectively. Even the addition of Hep to the release medium should be investigated, in order to maintain and sequester GF activity after release.

7 Research Outputs

7.1 Conference Presentations

7.1.1 International Conferences

Heparin and Heparan Sulfate Hydrogels for Cardiovascular Tissue Regeneration

A Janse van Rensburg, A Oosthuysen, N Davies, LH Callanan, P Zilla, D Bezuidenhout

POLYCHAR 22 World Forum on Advanced Materials - Poster Presentation

Stellenbosch, April 2014

Award: IUPAC Prize Winner

Heparinized Polyethylene Glycol Hydrogels for Growth Factor Delivery

A Janse van Rensburg, A Oosthuysen, N Davies, C Chokoza, P Zilla, D Bezuidenhout

BIO ENG'14 International Conference - Poster Presentation

Istanbul, November 2014

7.1.2 Local Conferences

Heparinoid Hydrogels for Cardiovascular Applications

A Janse van Rensburg, A Oosthuysen, N Davies, LH Callanan, P Zilla, D Bezuidenhout

University of Cape Town Research Day - Talk

Cape Town, November 2013

Injectable Heparin and Heparan Sulfate Hydrogels for Cardiovascular Tissue Regeneration

A Janse van Rensburg, A Oosthuysen, N Davies, LH Callanan, P Zilla, D Bezuidenhout

2014 UCT Postgraduate Research Week - Poster Presentation

Cape Town, May 2014

Award: McKinsey & Company Prize Winner (Health Sciences and Science)

7.2 Intended Journal Submission

Growth Factor Delivery from Covalently Heparinized Polyethylene Glycol Hydrogels for Improved Tissue Engineering Scaffold Vascularization

A Janse van Rensburg, A Oosthuysen, C Chokoza, N Davies, P Zilla, D Bezuidenhout

Biomacromolecules

8 References

1. McLean, J. The Antithromboplastic Action of Cephalin. *American Journal of Physiology* **41,** 250 (1916).
2. Young, E. The anti-inflammatory effects of heparin and related compounds. *Thrombosis Research* **122,** 743–752 (2008).
3. Ceccarelli, M. *et al.* Anti-inflammatory effects of low molecular weight heparin derivative in a rat model of carrageenan-induced pleurisy. *Journal of Cellular and Molecular Medicine* **13,** 2704–2712 (2009).
4. Virag, J. a I. *et al.* Fibroblast growth factor-2 regulates myocardial infarct repair: effects on cell proliferation, scar contraction, and ventricular function. *The American Journal of Pathology* **171,** 1431–1440 (2007).
5. Lever, R., Hoult, J. R. S. & Page, C. P. The effects of heparin and related molecules upon the adhesion of human polymorphonuclear leucocytes to vascular endothelium in vitro. *British Journal of Pharmacology* **129,** 533–540 (2000).
6. Tae, G., Scatena, M., Stayton, P. S. & Hoffman, A. S. PEG-cross-linked heparin is an affinity hydrogel for sustained release of vascular endothelial growth factor. *Journal of Biomaterials Science, Polymer Edition* **17,** 187–197 (2006).
7. Cai, S., Liu, Y., Zheng Shu, X. & Prestwich, G. D. Injectable glycosaminoglycan hydrogels for controlled release of human basic fibroblast growth factor. *Biomaterials* **26,** 6054–6067 (2005).
8. Pike, D. B. *et al.* Heparin-regulated release of growth factors in vitro and angiogenic response in vivo to implanted hyaluronan hydrogels containing VEGF and bFGF. *Biomaterials* **27,** 5242–5251 (2006).
9. Elia, R. *et al.* Stimulation of in vivo angiogenesis by in situ crosslinked , dual growth factor-loaded , glycosaminoglycan hydrogels. *Biomaterials* **31,** 4630–4638 (2010).
10. Zieris, A. *et al.* FGF-2 and VEGF functionalization of starPEG-heparin hydrogels to modulate biomolecular and physical cues of angiogenesis. *Biomaterials* **31,** 7985–7994 (2010).
11. Zieris, A. *et al.* Dual independent delivery of pro-angiogenic growth factors from starPEG–heparin hydrogels. *Journal of Controlled Release* **156,** 28–36 (2011).
12. Benoit, D. S. W., Durney, A. R. & Anseth, K. S. The effect of heparin-functionalized PEG hydrogels on three-dimensional human mesenchymal stem cell osteogenic differentiation. *Biomaterials* **28,** 66–77 (2007).
13. Mozaffarian, D. *et al.* Heart disease and stroke statistics - 2015 update: a report from the American Heart Association. *Circulation* **131,** 29–322 (2015).

14. Hoppensteadt, D., Walenga, J. M. & Fareed, J. Comparative antithrombotic and hemorrhagig effects of dermatan sulfate, heparan sulfate and heparin. *Thrombosis Research* **60,** 191–200 (1990).
15. Esko, J. D., Kimata, K. & Lindahl, U. in *Essentials of Glycobiology* (2009).
16. Benoit, D. S. W. & Anseth, K. S. Heparin functionalized PEG gels that modulate protein adsorption for hMSC adhesion and differentiation. *Acta Biomaterialia* **1,** 461–470 (2005).
17. Elia, R. *et al.* Stimulation of in vivo angiogenesis by in situ crosslinked, dual growth factor-loaded, glycosaminoglycan hydrogels. *Biomaterials* **31,** 4630–4638 (2010).
18. Trowbridge, J. M. & Gallo, R. L. Dermatan sulfate: new functions from an old glycosaminoglycan. *Glycobiology* **12,** 117R–125R (2002).
19. Padera, R., Venkataraman, G., Berry, D., Godavarti, R. & Sasisekharan, R. FGF-2/fibroblast growth factor receptor/heparin-like glycosaminoglycan interactions: a compensation model for FGF-2 signaling. *Federation of American Societies for Experimental Biology Journal* **13,** 1677–1687 (1933).
20. Imanari, T., Toida, T., Koshiishi, I. & Toyoda, H. High-performance liquid chromatographic analysis of glycosaminoglycan-derived oligosaccharides. *Journal of Chromatography Analysis* **720,** 275–293 (1996).
21. Yates, E. A. *et al.* Effect of substitution pattern on 1H , 13C NMR chemical shifts and 1 J CH coupling constants in heparin derivatives. *Carbohydrate Research* **329,** 239–247 (2000).
22. Yates, E. A. *et al.* 1H and 13C NMR spectral assignments of the major sequences of twelve systematically modified heparin derivatives. *Carbohydrate Research* **294,** 15–27 (1996).
23. Tae, G., Scatena, M., Stayton, P. S. & Hoffman, A. S. PEG-cross-linked heparin is an affinity hydrogel for sustained release of vascular endothelial growth factor. *Journal of Biomaterials Science, Polymer edition* **17,** 187–197 (2006).
24. Folkman, J. & Shing, Y. Control of Angiogenesis by Heparin and other Sulfated Polysaccharides. *Advances in Experimental Medicine and Biology* **313,** 355–364 (1992).
25. Lane, D. A. & Lindahl, U. *Heparin Chemical and biological properties: Clinical Applications*. 25–64 (1989).
26. Gao, A. *et al.* Facile spectrophotometric assay of molar equivalents of N-hydroxysuccinimide esters of monomethoxyl poly-(ethylene glycol) derivatives. *Chemistry Central journal* **6,** 142 (2012).
27. Chuang, W., Christ, M. D. & Rabenstein, D. L. Determination of the Primary Structures of Heparin- and Heparan Sulfate-Derived Oligosaccharides Using Band-Selective Experiments. *Analytical Chemistry* **73,** 2310–2316 (2001).

28. Casu, B., Vlodavsky, I. & Sanderson, R. D. Non-anticoagulant heparins and inhibition of cancer. *Pathophysiology of haemostasis and thrombosis* **36,** 195–203 (2008).
29. Michalopoulos, G. & DeFrances, M. Liver regeneration. *Science* 27660–27666 (1997).
30. Fromm, J. R., Hileman, R. E., Caldwell, E. E. O., Weiler, J. M. & Linhardt, R. J. Pattern and spacing of basic amino acids in heparin binding sites. *Archives of Biochemistry and Biophysics* **343,** 92–100 (1997).
31. Fromm, J. R., Hileman, R. E., Weiler, J. M. & Linhardt, R. J. Interaction of fibroblast growth factor-1 and related peptides with heparan sulfate and its oligosaccharides. *Archives of Biochemistry and Biophysics* **346,** 252–262 (1997).
32. Kamei, K., Wu, X. F., Xu, X. Y., Minami, K. & Huy, N. T. The analysis of heparin–protein interactions using evanescent wave biosensor with regioselectively desulfated heparins as the ligands. *Analytical Biochemistry* **295,** 203–213 (2001).
33. Lianga, O. D., Rosenblattb, S., Chhatwala, G. S. & Preissner, K. T. Identification of novel heparin-binding domains of vitronectin. *Federation of European Biochemical Societies Letters* **407,** 169–172 (1997).
34. Cole, G. J. & Glaser, L. A heparin-binding domain from N-CAM is involved in neural cell-substratum adhesion. *Journal of Cell Biology* **102,** 403–412 (1986).
35. Nie, T., Baldwin, A., Yamaguchi, N. & Kiick, K. L. Production of heparin-functionalized hydrogels for the development of responsive and controlled growth factor delivery systems. *Journal of Controlled Release* **122,** 287–296 (2007).
36. Casu, B. & Lindahl, U. Structure and biological interactions of heparin and heparan sulfate. *Advances in Carbohydrate Chemistry and Biochemistry* **57,** 159–206 (2001).
37. Casu, B. in *Chemistry and Biology of Heparin and Heparan Sulfate* 1–28 (2006).
38. Weitz, J. I. Heparan sulfate: Antithrombotic or not? *Journal of Clinical Investigation* **111,** 952–954 (1996).
39. Petitou, M., Casub, B. & Lindahl, U. 1976–1983, a critical period in the history of heparin: the discovery of the antithrombin binding site. *Biochimie* **85,** 83–89 (2003).
40. Mann, K. G., Butenas, S. & Brummel, K. The dynamics of thrombin formation. *Arteriosclerosis, Thrombosis, and Vascular Biology* **23,** 17–25 (2003).
41. King, M. W. *Integrative Medical Biochemistry: Examination and Board Review*. (2014).
42. Bianchini, P., Osima, B., Parma, B., Nader, H. . & Dietrich, C. P. Lack of correlation between in vitro and in vivo antithrombotic activity of heparin fractions and related compounds. Heparan sulfate as an antithrombotic agent in vivo. *Thrombosis Research* 597–607 (1985).
43. Fernandez, J., Van Ryn, J., Ofosu, F. A., Hirsh, J. & Buchanan, M. R. The haemorrhagic and antithrombotic effects of dermatan sulphate. *British Journal of Haematology* **64,** 309–317 (1986).

44. Casu, B., Guerrini, M. & Torri, G. Structural and Conformational Aspects of the Anticoagulant and Antithrombotic Activity of Heparin and Dermatan Sulfate. *Current Pharmaceutical Design* **10,** 939–949 (2004).
45. Park, T., Murugesan, S. & Robert, J. Cellulose composites prepared using ionic liquids (ILs) - Blood Compatibility to Batteries. *Journal of American Chemical Society* **1017,** 133–152 (2009).
46. Gombotz, W. R. & Pettit, D. K. Biodegradable polymers for protein and peptide drug delivery. *Bioconjugate Chemistry* **6,** 332–351 (1995).
47. Elbert, D. L., Pratt, A. B., Lutolf, M. P., Halstenberg, S. & Hubbell, J. Protein delivery from materials formed by self-selective conjugate addition reactions. *Journal of Controlled Release* **76,** 11–25 (2001).
48. Roberts, M. J., Bentley, M. D. & Harris, J. M. Chemistry for peptide and protein PEGylation. *Advanced Drug Delivery Reviews* **54,** 459–476 (2002).
49. Li, Q., Wang, D. & Elisseeff, J. H. Heterogeneous-Phase Reaction of Glycidyl Methacrylate and Chondroitin Sulfate: Mechanism of Ring-Opening–Transesterification Competition. *Macromolecules* **36,** 2556–2562 (2003).
50. Frokjaer, S. & Otzen, D. E. Protein drug stability: a formulation challenge. *Nature Reviews Drug Discovery* **4,** 298–306 (2005).
51. Veronese, F. M. & Pasut, G. PEGylation, successful approach to drug delivery. *Drug Discovery Today* **10,** 1451–1458 (2005).
52. Yamaguchi, N. & Kiick, K. L. Polysaccharide-poly(ethylene glycol) star copolymer as a scaffold for the production of bioactive hydrogels. *Biomacromolecules* **6,** 1921–1930 (2005).
53. Zisch, A. H., Lutolf, M. P., Bezuidenhout, D., Zilla, P. & Hubbell, J. Cell-demanded release of VEGF from synthetic, biointeractive cell ingrowth matrices for vascularized tissue growth. *Federation of American Societies for Experimental Biology Journal* **17,** 2260–2262 (2003).
54. Sakiyama-Elbert, S. E. & Hubbell, J. A. Development of fibrin derivatives for controlled release of heparin-binding growth factors. *Journal of Controlled Release* **65,** 389–402 (2000).
55. Tessler, S. *et al.* Heparin modulates the interaction of VEGF165 with soluble and cell associated flk-1 receptors. *The Journal of Biological Chemistry* **269,** 12456–12461 (1994).
56. Feyzi, E. *et al.* Characterization of Heparin and Heparan Sulfate Domains Binding to the Long Splice Variant of Platelet-derived Growth Factor A Chain. *The Journal of Biological Chemistry* **272,** 5518–5524 (1997).

57. Lyon, M., Rushton, G. & Gallagher, J. T. The Interaction of the Transforming Growth Factor-βs with Heparin/Heparan Sulfate Is Isoform-specific. *The Journal of Biological Chemistry* **272,** 18000–18006 (1997).
58. Hamilton, J. F. *et al.* Heparin Coinfusion during Convection-Enhanced Delivery (CED) Increases the Distribution of the Glial-Derived Neurotrophic Factor (GDNF) Ligand Family in Rat Striatum and Enhances the Pharmacological Activity of Neurturin. *Experimental Neurology* **168,** 155–161 (2001).
59. Kim, M., Youn, J., Jones, C. N., Revzin, A. & Tae, G. Heparin-based hydrogel as a matrix for encapsulation and cultivation of primary hepatocytes. *Biomaterials* **31,** 3596–3603 (2010).
60. Wu, Z., Zhang, L., Yabe, T. & Kuberan, B. The involvement of heparan sulfate (HS) in FGF1/HS/FGFR1 signaling complex. *Journal of Biological Chemistry* **278,** 17121–17129 (2003).
61. Whitelock, J. & Iozzo, R. Heparan sulfate: a complex polymer charged with biological activity. *Chemical Reviews* **105,** 2745–2764 (2005).
62. Zisch, A. H., Lutolf, M. P. & Hubbell, J. Biopolymeric delivery matrices for angiogenic growth factors. *Cardiovascular Pathology* **12,** 295–310 (2003).
63. Mühlebach, A. *et al.* New water-soluble photo crosslinkable polymers based on modified poly(vinyl alcohol). *Journal of Polymer Science Part A* **35,** 3603–3611 (1997).
64. Martens, P., Holland, T. & Anseth, K. S. Synthesis and characterization of degradable hydrogels formed from acrylate modified poly(vinyl alcohol) macromers. *Polymer* **43,** 6093–6100 (2002).
65. Hoffman, A. S. Hydrogels for biomedical applications. *Advanced Drug Delivery Reviews* **54,** 3–12 (2002).
66. Hubbell, J. A. Synthetic biodegradable polymers for tissue engineering and drug delivery. *Current Opinion in Solid State & Materials Science* **3,** 246–251 (1998).
67. Lin, C. C. & Anseth, K. S. PEG hydrogels for the controlled release of biomolecules in regenerative medicine. *Pharmaceutical Research* **26,** 631–643 (2009).
68. Lutolf, M. P. & Hubbell, J. a. Synthesis and physicochemical characterization of end-linked poly(ethylene glycol)-co-peptide hydrogels formed by Michael-type addition. *Biomacromolecules* **4,** 713–722 (2003).
69. Nilasaroya, A., Poole-Warren, L., Whitelock, J. M. & Jo Martens, P. Structural and functional characterisation of poly(vinyl alcohol) and heparin hydrogels. *Biomaterials* **29,** 4658–4664 (2008).
70. Sun, G. *et al.* Functional neovascularization of biodegradable dextran hydrogels with multiple angiogenic growth factors. *Biomaterials* **32,** 95–106 (2011).

71. Lee, K. & Mooney, D. Hydrogels for tissue engineering. *Chemical Reviews* **101,** 1869–1880 (2001).
72. Zhu, A., Zhang, M., Wu, J. & Shen, J. Covalent immobilization of chitosan/heparin complex with a photosensitive hetero-bifunctional crosslinking reagent on PLA surface. *Biomaterials* **23,** 4657–4665 (2002).
73. Smeds, K. & Grinstaff, M. W. Photocrosslinkable polysaccharides for in situ hydrogel formation. *Journal of Biomedical Materials Research* **54,** 115–121 (2001).
74. Lee, H. J. *et al.* Platelet and bacterial repellence on sulfonated poly(ethylene glycol)-acrylate copolymer surfaces. *Colloids and Surfaces: Biointerfaces* **18,** 355–370 (2000).
75. Miller, D. C., Haberstroh, K. M. & Webster, T. J. Mechanism(s) of increased vascular cell adhesion on nanostructured poly(lactic-co-glycolic acid) films. *Journal of Biomedical Materials Research Part A* **73,** 476–484 (2005).
76. Lutolf, M. & Hubbell, J. Synthetic biomaterials as instructive extracellular microenvironments for morphogenesis in tissue engineering. *Nature Biotechnology* **23,** 47–55 (2005).
77. Peppas, N. A., Hilt, J. Z., Khademhosseini, A. & Langer, R. Hydrogels in Biology and Medicine: From Molecular Principles to Bionanotechnology. *Advanced Materials* **18,** 1345–1360 (2006).
78. Reeve, M. S., McCarthy, S. P., Downey, M. J. & Gross, R. A. Polylactide Stereochemistry: Effect on Enzymatic Degradability. *Macromolecules* **27,** 825–831 (1994).
79. Qiao, M., Chen, D., Ma, X. & Liu, Y. Injectable biodegradable temperature-responsive PLGA-PEG-PLGA copolymers: synthesis and effect of copolymer composition on the drug release from the copolymer-based hydrogels. *International Journal of Pharmaceutics* **294,** 103–112 (2005).
80. Dobner, S., Bezuidenhout, D., Govender, P., Zilla, P. & Davies, N. A synthetic non-degradable polyethylene glycol hydrogel retards adverse post-infarct left ventricular remodeling. *Journal of cardiac failure* **15,** 629–636 (2009).
81. Zustiak, S. P. & Leach, J. B. Hydrolytically degradable poly(ethylene glycol) hydrogel scaffolds with tunable degradation and mechanical properties. *Biomacromolecules* **11,** 1348–1357 (2010).
82. McCarthy, T. J., Hayes, E. P., Schwartz, C. S. & Witz, G. The Reactivity of Selected Acrylate Esters toward Glutathione and Deoxyribonucleosides in Vitro: Structure-Activity Relationships. *Fundamental and Applied Toxicology* **22,** 543–548 (1994).
83. Luo, Y., Kirker, K. R. & Prestwich, G. D. Cross-linked hyaluronic acid hydrogel films: new biomaterials for drug delivery. *Journal of Controlled Release* **69,** 169–184 (2000).
84. Freudenberg, U. *et al.* A star-PEG-heparin hydrogel platform to aid cell replacement therapies for neurodegenerative diseases. *Biomaterials* **30,** 5049–5060 (2009).

85. Van de Wetering, P., Metters, A. T., Schoenmakers, R. G. & Hubbell, J. A. Poly(ethylene glycol) hydrogels formed by conjugate addition with controllable swelling, degradation, and release of pharmaceutically active proteins. *Journal of Controlled Release* **102,** 619–627 (2005).
86. DuBose, J. W., Cutshall, C. & Metters, A. T. Controlled release of tethered molecules via engineered hydrogel degradation: model development and validation. *Journal of biomedical materials research Part A* **74,** 104–116 (2005).
87. Anseth, K. S., Bowman, C. N. & Brannon-Peppas, L. Mechanical properties of hydrogels and their experimental determination. *Biomaterials* **17,** 1647–1657 (1996).
88. Appel, E., del Barrio, J., Loh, X. & Scherman, O. Supramolecular polymeric hydrogels. *Chemical Society Reviews* **41,** 6195–6214 (2012).
89. Haraguchi, K. Nanocomposite hydrogels. *Current Opinion in Solid State and Materials Science* **11,** 47–54 (2007).
90. Guvendiren, M., Lu, H. & Burdick, J. Shear-thinning hydrogels for biomedical applications. *Soft Matter* **8,** 260–272 (2012).
91. Hennink, W. E. & van Nostrum, C. F. Novel crosslinking methods to design hydrogels. *Advanced Drug Delivery Reviews* **54,** 13–36 (2002).
92. Sen, M. & Guven, O. Prediction of the swelling of amphiphilic hydrogels and the determination of average molcular weight between crosslinks. *Computational and Theoretical Polymer Science* **11,** 475–482 (2000).
93. Srinivasan, S., Lee, M. W., Grady, M. C., Soroush, M. & Rappe, A. M. Self-initiation mechanism in spontaneous thermal polymerization of ethyl and n-butyl acrylate: a theoretical study. *Journal of Physical Chemistry* **114,** 7975–7983 (2010).
94. Mather, B. D., Viswanathan, K., Miller, K. M. & Long, T. E. Michael addition reactions in macromolecular design for emerging technologies. *Progress in Polymer Science* **31,** 487–531 (2006).
95. LoPachin, R. M., Barber, D. S. & Gavin, T. Molecular mechanisms of the conjugated alpha,beta-unsaturated carbonyl derivatives: relevance to neurotoxicity and neurodegenerative diseases. *Toxicological Sciences* **104,** 235–249 (2008).
96. Hahn, S. K., Oh, E. J., Miyamoto, H. & Shimobouji, T. Sustained release formulation of erythropoietin using hyaluronic acid hydrogels crosslinked by Michael addition. *International Journal of Pharmaceutics* **322,** 44–51 (2006).
97. Tae, G. *et al.* Formation of a novel heparin-based hydrogel in the presence of heparin-binding biomolecules. *Biomacromolecules* **8,** 1979–1986 (2007).
98. Hahn, S. K., Kim, J. S. & Shimobouji, T. Injectable hyaluronic acid microhydrogels for controlled release formulation of erythropoietin. *Journal of Biomedical Materials Research Part A* **80A,** 916–924 (2006).

99. Bezuidenhout, D., Oosthuysen, A., Davies, N., Ahrenstedt, L. & Zilla, P. Covalent incorporation and controlled release of active dexamethasone from injectable polyethylene glycol hydrogels. *Journal of Biomedical Materials Research Part A* **101,** 1311–1318 (2013).
100. Christman, K. & Lee, R. Biomaterials for the treatment of myocardial infarction. *Journal of the American College of Cardiology* **48,** 907–913 (2006).
101. Lutolf, M. P., Tirelli, N., Cerritelli, S., Cavalli, L. & Hubbell, J. a. Systematic modulation of Michael-type reactivity of thiols through the use of charged amino acids. *Bioconjugate Chemistry* **12,** 1051–1056 (2001).
102. Schoenmakers, R., van de Wetering, P., Elbert, D. & Hubbell, J. The effect of the linker on the hydrolysis rate of drug-linked ester bonds. *Journal of Controlled Release* **95,** 291–300 (2004).
103. Fittkau, M. *et al.* The selective modulation of endothelial cell mobility on RGD peptide containing surfaces by YIGSR peptides. *Biomaterials* **26,** 167–174 (2005).
104. Metters, A. & Hubbell, J. Network formation and degradation behavior of hydrogels formed by Michael-type addition reactions. *Biomacromolecules* **6,** 290–301 (2005).
105. Jo, Y. S., Gantz, J., Hubbell, J. & Lutolf, M. P. Tailoring hydrogel degradation and drug release via neighboring amino acid controlled ester hydrolysis. *Soft Matter* **5,** 440 (2009).
106. Goth, M., Hubina, E., Raptis, S., Nagy, G. & Toth, B. Physiological andpathological angiogenesis in the endocrine system. *Microscopy Research and Technique* **60,** 98–106 (2003).
107. Carmeliot, P. Angiogenesis in Health and Disease. *Nature Medicine* **9,** 653–660 (2003).
108. Williams, D. To engineer is to create: the link between engineering and regeneration. *Trends in Biotechnology* **24,** 4–8 (2006).
109. Laschke, M. *et al.* Angiogenesis in tissue engineering: breathing life into constructed tissue substitutes. *Journal of Tissue Engineering* **12,** 2093–2104 (2006).
110. Schmidt, C. *et al.* Rapid three-dimensional quantification of VEGF-induced scaffold neovascularisation by microcomputed tomography. *Biomaterials* **30,** 5959–5968 (2009).
111. Peattie, R. A. *et al.* Dual growth factor-induced angiogenesis in vivo using hyaluronan hydrogel implants. *Biomaterials* **27,** 1868–1875 (2006).
112. Peattie, R. A. *et al.* Stimulation of in vivo angiogenesis by cytokine-loaded hyaluronic acid hydrogel implants. *Biomaterials* **25,** 2789–2798 (2004).
113. Smith, M., Peters, M., Richardson, T., Garbern, J. & Mooney, D. Locally enhanced angiogenesis promotes transplanted cell survival. *Tissue Engineering* **10,** 63–71 (2004).
114. Isner, J. *et al.* Arterial gene transfer for therapeutic angiogenesis in patients with peripheral artery disease. *Human Gene Therapy* **7,** 959–988 (1996).

115. Schumacher, B., Pecher, P., von Specht, B. & Stegmann, T. Induction of neoangiogenesis in ischemic myocardium by human growth factors: first clinical results of a new treatment of coronary heart disease. *Circulation* **97,** 645–650 (1998).
116. Laham, R. *et al.* Local perivascular delivery of basic fibro- blast growth factor in patients undergoing coronary bypass surgery: results of a phase I randomized, double-blind, placebo-controlled trial. *Circulation* **100,** 1865–1871 (1999).
117. Kipshidze, N. *et al.* Angiogenesis in a pa- tient with ischemic limb induced by intramuscular injection of vascular endothelial growth factor and fibrin platform. Tex Heart Inst J 2000;27: *Texas Heart Institute Journal* **27,** 196–200 (2000).
118. Henry, T. *et al.* Intracoronary administration of recombinant human vascular endothelial growth factor to patients with coronary artery disease. *American Heart Journal* **142,** 872–880 (2001).
119. Hariawala, M. *et al.* VEGF improves myocardial blood flow but produces EDRF-mediated hypotension in porcine hearts. *Journal of Surgical Research* **63,** 77–82 (1996).
120. Horowitz, J. *et al.* Vascular endothelial growth factor/vascular permeability factor produces nitric oxide-dependent hypotension. Evidence for a maintenance role in quiescent adult endothelium. *Arteriosclerosis, Thrombosis, and Vascular Biology* **17,** 2793–2800 (1997).
121. Jain, R. Tumor angiogenesis and accessibility: role of vascular endothelial growth factor. *Seminars in Oncology* **29,** 3–9 (2002).
122. Ferrara, N. Role of vascular endothelial growth factor in physiologic and pathologic angiogenesis: therapeutic implications. *Seminars in Oncology Nursing* **29,** (2002).
123. Lee, R. *et al.* VEGF gene delivery to myocardium: deleterious effects of unregulated expression. *Circulation* **102,** 898–901 (2000).
124. Takeshita, S. *et al.* Therapeutic angiogenesis. A single intraarterial bolus of vascular endothelial growth factor augments revascularization in a rabbit ischemic hind limb model. *Journal of Clinical Investigation* **93,** 662–670 (1994).
125. Benoit, D., Collins, S. & Anseth, K. Multifunctional hydrogels that promote osteogenic human mesenchymal stem cell differentiation through stimulation and sequestering of bone morphogenic protein2. *Advanced Functional Materials* **17,** 2085–2093 (2007).
126. Cushing, M., Liao, J., Jaeggli, M. & Anseth, K. Material-based regulation of the myofibroblast phenotype. *Biomaterials* **28,** 3378–3387 (2007).
127. Yamaguchi, N., Chae, B.-S., Zhang, L., Kiick, K. L. & Furst, E. M. Rheological characterization of polysaccharide-poly(ethylene glycol) star copolymer hydrogels. *Biomacromolecules* **6,** 1931–1940 (2005).
128. Becher, J., Möller, S. & Schnabelrauch, M. Phase transfer-catalyzed synthesis of highly acrylated hyaluronan. *Carbohydrate Polymers* **93,** 438–441 (2013).

129. Liang, Y. & Kiick, K. L. Heparin-functionalized polymeric biomaterials in tissue engineering and drug delivery applications. *Acta Biomaterialia* **10,** 1588–600 (2014).
130. Kumar, V. & Gross, R. A. Acrylated Hyaluronic acid. US20090118423 A1 (2009).
131. Shu, X. Z., Liu, Y., Luo, Y., Roberts, M. C. & Prestwich, G. D. Disulfide cross-linked hyaluronan hydrogels. *Biomacromolecules* **3,** 1304–1311 (2002).
132. Zheng Shu, X., Liu, Y., Palumbo, F. S., Luo, Y. & Prestwich, G. D. In situ crosslinkable hyaluronan hydrogels for tissue engineering. *Biomaterials* **25,** 1339–1348 (2004).
133. Jeon, O., Powell, C., Solorio, L. D., Krebs, M. D. & Alsberg, E. Affinity-based growth factor delivery using biodegradable, photocrosslinked heparin-alginate hydrogels. *Journal of Controlled Release* **154,** 258–266 (2011).
134. Oliviero, O., Ventre, M. & Netti, P. A. Functional porous hydrogels to study angiogenesis under the effect of controlled release of vascular endothelial growth factor. *Acta Biomaterialia* **8,** 3294–3301 (2012).
135. Bulpitt, P. & Aeschlimann, D. New strategy for chemical modification of hyaluronic acid: Preparation of functionalized derivatives and their use in the formation of novel biocompatible hydrogels. *Journal of Biomedical Materials Research* **47,** 152–169 (1999).
136. Baldwin, A. D. *et al.* In situ crosslinkable heparin-containing poly(ethylene glycol) hydrogels for sustained anticoagulant release. *Journal of Biomedical Materials Research Part A* **100,** 2106–2118 (2012).
137. Robinson, K. *et al.* Differential effects of substrate modulus on human vascular endothelial, smooth muscle, and fibroblastic cells. *Journal of Biomedical Materials Research Part A* **100A,** 1356–1367 (2012).
138. Nie, T., Akins, R. & Kiick, K. Production of heparin-containing hydrogels for modulating cell responses. *Acta Biomaterialia* **5,** 865–875 (2009).
139. Kim, M., Kim, S., Kang, S., Kim, Y. & Tae, G. The use of de-differentiated chondrocytes delivered by a heparin-based hydrogel to regenerate cartilage in partial-thickness defects. *Biomaterials* **32,** 7883–7896 (2011).
140. Bhakta, G. *et al.* Hyaluronic acid-based hydrogels functionalized with heparin that support controlled release of bioactive BMP-2. *Biomaterials* **33,** 6113–6122 (2012).
141. Choi, W., Kim, M., Tae, G. & Kim, Y. Sustained release of human growth hormone from heparin-based hydrogel. *Biomacromolecules* **9,** 1698–1704 (2008).
142. Kim, M. *et al.* In Vitro Chondrocyte Culture in a Heparin-Based Hydrogel for Cartilage Regeneration. *Tissue Engineering* **16,** 1–10 (2010).
143. Baumann, L. *et al.* A novel, biased-like SDF-1 derivative acts synergistically with starPEG-based heparin hydrogels and improves eEPC migration in vitro. *Journal of Controlled Release* **162,** 68–75 (2012).

144. Tsurkan, M. V *et al.* Growth factor delivery from hydrogel particle aggregates to promote tubular regeneration after acute kidney injury. *Journal of Controlled Release* **167,** 248–255 (2013).
145. Prokoph, S. *et al.* Sustained delivery of SDF-1α from heparin-based hydrogels to attract circulating pro-angiogenic cells. *Biomaterials* **33,** 4792–4800 (2012).
146. Richardson, T., Peters, M., Ennett, A. & Mooney, D. Polymeric system for dual growth factor delivery. *Nature Biotechnology* **19,** 1029–1034 (2001).
147. Welzel, P. *et al.* Macroporous starPEG–heparin cryogels. *Biomacromolecules* **13,** 2349–2358 (2012).
148. Siepmann, J., Kranz, H., Peppas, N. A. & Bodmeier, R. Calculation of the required size and shape of hydroxypropyl methylcellulose matrices to achieve desired drug release profiles. *International Journal of Pharmaceutics* **201,** 151–164 (2000).
149. Siepmann, J. & Peppas, N. A. Higuchi equation: Derivation, applications, use and misuse. *International journal of pharmaceutics* **148,** 6–12 (2011).
150. Chien, Y., Cabana, B. & Mares, S. *Novel drug delivery systems: fundamentals, developmental concepts, biomedical assessments*. (1982).
151. Harris, M., Hamid, A. & Ismail, R. Evaluation of Drug Release Kinetics from Ibuprofen Matrix Tablets Using HPMC. *Pakistan Journal of Pharmaceutical Sciences* **19,** 119–124 (2006).
152. Kranz, H., Peppas, N. A. & Bodmeier, R. Calculation of the required size and shape of hydroxypropyl methylcellulose matrices to achieve desired drug release profiles. *International Journal of Pharmaceutics* **201,** 151–164 (2000).
153. Shoaib, M. H., Tazeen, J., Merchant, H. A. & Yousuf, R. I. Evaluation of drug release kinetics from ibuprofen matrix tablets using HPMC. *Pakistan Journal of Pharmaceutical* **19,** 119–124 (2006).
154. Siepmann, J. & Peppas, N. A. Modeling of drug release from delivery systems based on hydroxypropyl methylcellulose (HPMC). *Advanced Drug Delivery Reviews* **48,** 139–157 (2001).
155. Lin, C. C. & Metters, A. T. Hydrogels in controlled release formulations: network design and mathematical modeling. *Advanced Drug Delivery Reviews* **58,** 1379–1408 (2006).
156. Wise, D. L. *Handbook of Pharmaceutical Controlled Release Technology*. 902 (2000).
157. Pradhan, S. *et al.* Lumen formation in three-dimensional cultures of salivary acinar cells. *Journal of American Academy of Otolaryngology* **142,** 191–195 (2010).
158. Pradhan-Bhatt, S. *et al.* A novel in vivo model for evaluating functional restoration of a tissue-engineered salivary gland. *The Laryngoscope* 1–6 (2013).

159. Pradhan-bhatt, S. *et al.* Implantable Three-Dimensional Salivary Spheroid Assemblies Demonstrate Fluid and Protein Secretory Responses to Neurotransmitters. *Tissue Engineering* **19,** 1610–1620 (2013).
160. Weitz, J., Young, E., Johnston, M., Stafford, A. & Fredenburgh, J. Vasoflux, a new anticoagulant with a novel mechanism of action. *Circulation* **99,** 682–689 (1999).
161. Xie, W., Chipman, J. & Robertson, D. Expression of a mitogen-responsive gene encoding prostaglandin synthase is regulated by mRNA splicing. *National Academy of Sciences of the United States of America* **88,** 2692–2696 (1991).
162. Sluiter, W., Pietersma, A. & Lamers, J. Leukocyte adhesion molecules on the vascular endothelium: their role in the pathogenesis of cardiovascular disease and the mechanism underlying their expression. *Journal of Cadiovascular Pharmacology* **22,** S37–S44 (1993).
163. Laroux, F., Lefer, D. & Kawachi, S. Role of nitric oxide in the regulation of acute and chronic inflammation. *Antioxidants & Redox Signaling* **2,** 391–396 (2000).
164. Johnson, K., Varani, J. & Smolen, J. Neutrophil activation and function in health and disease. *Immunology Series* **57,** 1–46 (1992).
165. Feuerstein, G. & Hallenbeck, J. Prostaglandins, leukotrienes, and platelet-activating factor in shock. *Annual Review of Pharmacology and Toxicology* **27,** 301–313 (1987).
166. Tomlinson, A., Appleton, I. & Moore, A. Cyclo-oxygenase and nitric oxide synthase isoforms in rat carrageenin induced pleurisy. *British Journal of Pharmacology* **113,** 693–698 (1994).
167. Young, E., Podor, T., Venner, T. & Hirsh, J. Induction of the acute-phase reaction increases heparin-binding proteins in plasma. *Arteriosclerosis, Thrombosis, and Vascular Biology* **17,** 1568–1574 (1997).
168. Weiler, J., Edens, R., Lindhardt, R. & Kapelanski, D. Heparin and modified heparin inhibit complement activation in vivo. *Journal of Immunology* **148,** 3210–3215 (1992).
169. Page, C. Heparin and Related Drugs: Beyond Anticoagulant Activity. *International Scholarly Research Notices: Pharmacology* **2013,** 1–13 (2013).
170. Lever, R. & Page, C. in *Heparin - A Century of Progress* 281–305 (2012).
171. Ahmed, T., Syriste, T. & Mendelssohn, R. Heparin prevents antigen-induced airway hyperresponsiveness: interference with IP3-mediated mast cell degranulation? *Journal of Applied Physiology* **76,** 893–901 (1994).
172. Bazzoni, G. *et al.* Effect of heparin, dermatan sulfate, and related oligo-derivatives on human polymorphonuclear leukocyte functions. *Journal of Laboratory and Clinical Medicine* **101,** 268–275 (1993).
173. Piccardoni, P., Evangelista, V., Piccoli, A., Walz, A. & Cerletti, C. Thrombin-activated human platelets release two NAP-2 variants that stimulate polymorphonuclear leukocytes. *Thrombosis and Haemostasis* **76,** 780–785 (1996).

174. Inase, N., Schreck, R. E. & Lazarus, S. C. Heparin inhibits histamine release from canine mast cells. *American Journal of Physiology* **264,** L387–L390 (1993).
175. Pégorier, S., Wagner, L. A., Gleich, G. J. & Pretolani, M. Eosinophil-derived cationic proteins activate the synthesis of remodeling factors by airway epithelial cells. *The Journal of Immunology* **177,** 4861–4869 (2006).
176. Redini, F. *et al.* Inhibition of leucocyte elastase by heparin and its derivatives. *Biochemical Journal* **252,** 515–519 (1988).
177. Fredens, K., Dahl, R. & Venge, P. In vitro studies of the interaction between heparin and eosinophil cationic protein. *Allergy* **46,** 27–29 (1991).
178. Swaminathan, G. J. *et al.* Eosinophil-granule major basic protein, a C-type lectin, binds heparin. *Biochemistry* **44,** 14152–14158 (2005).
179. Wang, J., Mu, J. & Zhu, H. N-desulfated non-anticoagulant heparin inhibits leukocyte adhesion and transmigration in vitro and attenuates acute peritonitis and ischemia and reperfusion injury in vivo. *Inflammation Research* **51,** 435–443 (2002).
180. Silvestro, L., Viano, I. & Macario, M. Effects of heparin and its desulfated derivatives on leukocyte-endothelial adhesion. *Thrombosis and Hemostasis* **20,** 254–258 (1994).
181. Nelson, R. M. *et al.* Heparin oligosaccharides bind L- and P-selectin and inhibit acute inflammation. *Blood* **82,** 3253–3258 (1993).
182. Salas, A., Sans, M. & Soriano, A. Heparin attenuates TNF-alpha induced inflammatory response through a CD11b dependent mechanism. *Gut* **47,** 88–96 (2000).
183. Dragsted, C. A., Wells, J. A., Rocha, E. & Silva, M. Inhibitory effect of heparin upon histamine release by trypsin, antigen, and protease. *Proceedings of the Society for Experimental Biology and Medicine* **51,** 191–192 (1942).
184. Humphries, D. E., Wong, G. W. & Friend, D. S. Heparin is essential for the storage of specific granule proteases in mast cells. *Nature* **400,** 769–772 (1999).
185. Steyn, K. & Fourie, J. M. The Heart and Stroke Foundation. in *Heart Disease in South Africa* 2–29 (2007).
186. Go, A. S. *et al.* Heart disease and stroke statistics -2013 update: a report from the American Heart Association. *Circulation* **127,** 6–245 (2013).
187. Roger, V. L. *et al.* Executive Summary: Heart Disease and Stroke Statistics - 2011 Update: A Report From the American Heart Association. *Circulation* **123,** 459–463 (2011).
188. Khand, a, Gemmel, I., Clark, a L. & Cleland, J. G. Is the prognosis of heart failure improving? *Journal of the American College of Cardiology* **36,** 2284–2286 (2000).
189. Remme, W. J. & Swedberg, K. Guidelines for the diagnosis and treatment of chronic heart failure. *European Heart Journal* **22,** 1527–1560 (2001).
190. Dickstein, K. *et al.* ESC Guidelines for the diagnosis and treatment of acute and chronic heart failure 2008: the Task Force for the Diagnosis and Treatment of Acute and Chronic

Heart Failure 2008 of the European Society of Cardiology. Developed in collaboration with the Heart. *European heart journal* **29,** 2388–442 (2008).

191. Lloyd-Jones, D. *et al.* Heart disease and stroke statistics - 2010 update: a report from the American Heart Association. *Circulation* **121,** 46–215 (2010).
192. Bezuidenhout, D. & Zilla, P. in *Encyclopedia of Biomaterials and Biomedical Engineering* 1715–1725 (2004).
193. Anderson, J., Gristina, A., Hanson, S. & Harker, L. in *Biomaterials Science: An Introduction to Materials in Medicine* 293–353 (1996).
194. Bezuidenhout, D., Davies, N. & Zilla, P. Effect of Well Defined Dodecahedral Porosity on Inflammation and Angiogenesis. *American Society for Artificial Internal Organs Journal* **48,** 465–471 (2002).
195. Pennel, T., Zilla, P. & Bezuidenhout, D. Differentiating transmural from transanastomotic prosthetic graft endothelialization through an isolation loop-graft model. *Journal of Vascular Surgery* **58,** 1053–1061 (2013).
196. Mikos, A. G. *et al.* Engineering Comple Tissues. *Tissue Engineering* **12,** (2010).
197. Park, K. *et al.* Bacterial adhesion on PEG modified polyurethane surfaces. *Biomaterials* **19,** 851–859. (1998).
198. Borja, J., Arnáiz, E., Izquierdo, I. & Souto, M. Controversies in cardiology. *Lancet* **367,** 1315–1316 (2006).
199. Mann, D. L. Basic mechanisms of left ventricular remodeling: the contribution of wall stress. *Journal of Cardiac Failure* **10,** 202–206 (2004).
200. Aikawa, Y. *et al.* Regional wall stress predicts ventricular remodeling after anteroseptal myocardial infarction in the Healing and Early Afterload Reducing Trial (HEART): An echocardiography-based structural analysis. *American Heart Journal* **141,** 234–242 (2001).
201. Pouleur, H. G., Konstam, M. A., Udelson, J. E. & Rousseau, M. F. Chauges in Ventricular Volume , Wall Thickness and Wall Stress During Progression of Left Ventricular Dysfuncthu. *Journal of the American College of Cardiology* **22,** 43–48 (1993).
202. Konstam, M. Reliability of ventricular remodeling as a surrogate for use in conjunction with clinical outcomes in heart failure. *The American Journal of Cardiology* **96,** 867–871 (2005).
203. Kadner, K. *et al.* The beneficial effects of deferred delivery on the efficiency of hydrogel therapy post myocardial infarction. *Biomaterials* **33,** 2060–2066 (2012).
204. Dai, W., Wold, L. E., Dow, J. S. & Kloner, R. Thickening of the infarcted wall by collagen injection improves left ventricular function in rats: a novel approach to preserve cardiac function after myocardial infarction. *Journal of the American College of Cardiology* **46,** 714–719 (2005).

205. Ifkovits, J. L. *et al.* Injectable hydrogel properties influence infarct expansion and extent of postinfarction left ventricular remodeling in an ovine model. *Proceedings of the National Academy of Sciences of the United States of America* **107,** 11507–11512 (2010).
206. Landa, N. *et al.* Effect of injectable alginate implant on cardiac remodeling and function after recent and old infarcts in rat. *Circulation* **117,** 1388–1396 (2008).
207. Wall, S. T., Walker, J. C., Healy, K. E., Ratcliffe, M. B. & Guccione, J. M. Theoretical impact of the injection of material into the myocardium: a finite element model simulation. *Circulation* **114,** 2627–2635 (2006).
208. Davies, N. *et al.* The dosage dependence of VEGF stimulation on scaffold neovascularisation. *Biomaterials* **29,** 3531–3538 (2008).
209. Deuse, T. *et al.* Hepatocyte growth factor or vascular endothelial growth factor gene transfer maximizes mesenchymal stem cell-based myocardial salvage after acute myocardial infarction. *Circulation* **120,** 247–254 (2009).
210. Ruixing, Y. *et al.* Intramyocardial injection of vascular endothelial growth factor gene improves cardiac performance and inhibits cardiomyocyte apoptosis. *European Journal of Heart Failure* **9,** 343–351 (2007).
211. Yao, Y., Yin, H., Shen, B., Chao, L. & Chao, J. Tissue kallikrein and kinin infusion rescues failing myocardium after myocardial infarction. *Journal of Cardiac Failure* **13,** 588–596 (2007).
212. Zhang, J. *et al.* Collagen-targeting vascular endothelial growth factor improves cardiac performance after myocardial infarction. *Circulation* **119,** 1776–1784 (2009).
213. Bezuidenhout, D., Oosthuysen, A., Davies, N., Ahrenstedt, L. & Zilla, P. Covalent incorporation and controlled release of active dexamethasone from injectable polyethylene glycol hydrogels. *Journal of Biomedical Materials Research Part A* **101 A,** 1311–1318 (2013).
214. Mulloy, B., Heath, A. & Mimms, S. A Collaborative Study to Establish The 2nd International Standard Low Molecular Weight Heparin for Molecular Weight Calibration. in *World Health Organization* 5–8 (2007).
215. Gray, E., Mulloy, B. & Barrowcliffe, T. W. Heparin and low-molecular-weight heparin. *Thrombosis and Haemostasis* **99,** 807–818 (2008).
216. Mulloy, B. *et al.* USP compendial methods for analysis of heparin: chromatographic determination of molecular weight distributions for heparin sodium. *Analytical and Bioanalytical Chemistry* **406,** 4815–4823 (2014).
217. Wyatt, P. J. Light scattering and the absolute characterization of macromolecules. *Analytica Chimica Acta* **272,** 1–40 (1993).
218. Radoff, S. & Danishefskyg, I. Distribution of Glucuronic and Iduronic Acid Units in Heparin Chains. *The Journal of Biological Chemistry* **2238,** 15106–15111 (1985).

219. Lindahl, U., Backstorm, G., Thunderberg, L. & Lender, I. Evidence for 3-O-sulfated D-Glucosamine residue in the antithrombin-binding sequence of heparin. *Proceedings of the National Academy of Science* **77,** 6551 (1980).

220. Casu, B. *et al.* The structure of heparin oligosaccharide fragments with high anti-(factor Xa) activity containing the minimal antithrombin lll-binding sequence. *Biochemical Journal* **197,** 599 (1981).

221. Thunderberg, L., Backstorm, G. & Lindahl, U. Further characterization of the antithrombin-binding sequence in heparin. *Carbohydrate Research* **100,** 393 (1982).

222. Casu, B. & Gennaro, U. A conductimetric method for the determination of sulphate and carboxyl groups in heparin and other mucopolysaccharides. *Carbohydrate Research* **39,** 168–176 (1975).

223. Lam, L., Silbert, J. & Rosenberg, R. The separation of active and inactive forms of heparin. *Biochemical and Biophysical Research Communications* **69,** 570 (1976).

224. Hook, M., Bjork, I., Hopwood, J. & Lindahl, U. Anticoagulant activity of heparin. Separation of high-activity and low-activity heparin species by affinity chromatography on immobilized antithrombin. *Federation of European Biochemical Societies Letters* **66,** 90 (1976).

225. Anderson, L., Barrowcliffe, T., Holmer, E. & Johnson, E. Anticoagulative properties of heparin fractionated by affinity chromatography on matrix bound antithrombin lll and by gel filtration. *Thrombosis Research* **9,** 575 (1976).

226. Choay, G. *et al.* Structure-activity relationship in heparin: A synthetic pentasaccharide with high affinity for antithrombin llland eliciting high anti-factor Xa activity. *Biochemical and Biophysical Research Communications* **116,** 492 (1983).

227. Gallagher, J. T. & Walker, A. Molecular distinctions between heparan sulphate and heparin. *Biochemical Journal* **6,** 665–674 (1985).

228. Fransson, L. A. & Carlstedt, I. Structure of the Heparan Sulfate-Protein Linkage Region. *The Journal of Biological Chemistry* **260,** 14722–14726 (1986).

229. Shaughnessy, B. O. & Vavylonis, D. Interfacial reaction kinetics. *The European Physical Journal* **177,** 159–177 (2000).

230. Hesse, D. & Senz, S. Interfacial reaction mechanisms and the structure of moving heterophase boundaries during pyrochlore- and spinel-forming solid state. *Hanser Publications* **252,** 252–257 (2004).

231. Jha, A. K., Malik, M. S., Farach-carson, M. C., Duncan, L. & Jia, X. Hierarchically structured , hyaluronic acid-based hydrogel matrices via the covalent integration of microgels into macroscopic networks. *Soft Matter* 5045–5055 (2010).

232. Jha, A. K., Xu, X., Duncan, R. L. & Jia, X. Controlling the adhesion and differentiation of mesenchymal stem cells using hyaluronic acid-based, doubly crosslinked networks. *Biomaterials* **32,** 2466–2478 (2011).

233. Jia, X. *et al.* Synthesis and Characterization of in Situ Cross-Linkable Hyaluronic Acid-Based Hydrogels with Potential Application for Vocal Fold Regeneration. *Macromolecules* **37,** 3239–3248 (2004).
234. Leach, J. B. & Schmidt, C. E. Characterization of protein release from photocrosslinkable hyaluronic acid-polyethylene glycol hydrogel tissue engineering scaffolds. *Biomaterials* **26,** 125–135 (2005).
235. Cumpstey, I. Chemical modification of polysaccharides. *International Scholarly Research Notices: Organic Chemistry* **2013,** 417–672 (2013).
236. Fox, S. C., Li, B., Xu, D. & Edgar, K. J. Regioselective esterification and etherification of cellulose: a review. *Biomacromolecules* **12,** 1956–1972 (2011).
237. Toida, T. *et al.* Chemical microdetermination of heparin in plasma. *Analytical Biochemistry* **251,** 219–226 (1997).
238. Nader, H. B. *et al.* Heterogeneity of heparin: characterization of one hundred components with different anticoagulant activities by a combination of electrophoretic and affinity chromatography methods. *International Journal of Biological Macromolecules* **3,** 356–360 (1981).
239. Linhardt, R. J., Cohen, D. M. & Rice, K. G. Nonrandom structural features in the heparin polymer. *Biochemistry* **28,** 2888–2894 (1989).
240. Jansson, E., Kenne, L. & Schweda, E. Nuclear Magnetic Resonance and Conformational Studies on Monoacetylated Methyl D-Gluco- and D-Galacto-pyranosides. *Journal of the Chemical Society* 377–383 (1987).
241. Ravenscroft, N., Walker, S. G., Dutton, G. U. Y. G. S. & Smit, J. Identification , Isolation , and Structural Studies of the Outer Membrane Lipopolysaccharide of Caulobacter crescentus. *Journal of Bacteriology* **174,** 7595–7605 (1992).
242. Klemm, D., Heinze, T., Philipp, B. & Wagenknecht, W. New approaches to advanced polymers by selective cellulose functionalization. *Acta Polymerica* **48,** 277–297 (1997).
243. Koschella, A., Fenn, D., Illy, N. & Heinze, T. Regioselectively Functionalized Cellulose Derivatives: A Mini Review. *Macromolecular Symposia* **244,** 59–73 (2006).
244. Bracher, M. *et al.* Cell specific ingrowth hydrogels. *Biomaterials* **34,** 6797–6803 (2013).
245. Bezuidenhout, D. *et al.* Covalent surface heparinization potentiates porous polyurethane scaffold vascularization. *Journal of Biomaterials Applications* **24,** 401–418 (2010).
246. Chambon, F. & Winter, H. Stopping of crosslinking reaction in a PDMS polymer at the gel point. *Polymer Bulletin* **13,** 499–503 (1985).
247. Winter, H. & Chambon, F. Analysis of Linear Viscoelasticity of a Crosslinking Polymer at the Gel Point. *Journal of Rheology* **30,** 367 (1986).
248. Ghosh, K. *et al.* Rheological characterization of in situ cross-linkable hyaluronan hydrogels. *Biomacromolecules* **6,** 2857–2865 (2005).

249. Kavanagh, G. M. & Ross-Murphy, S. B. Rheological characterisation of polymer gels. *Progress in Polymer Science* **23,** 533–562 (1998).
250. Burdick, J. a, Chung, C., Jia, X., Randolph, M. a & Langer, R. Controlled degradation and mechanical behavior of photopolymerized hyaluronic acid networks. *Biomacromolecules* **6,** 386–391 (2005).
251. Jin, Y. *et al.* Recyclable characteristics of hyaluronate-polyhydroxyethyl acrylate blend hydrogel for controlled releases. *Journal of Controlled Release* **73,** 173–181 (2001).
252. Anseth, K. S. *et al.* In situ forming degradable networks and their application in tissue engineering and drug delivery. *Journal of Controlled Release* **78,** 199–209 (2002).
253. Flory, P. J. & Rehner, R. J. Statistical mechanics of crosslinked polymer networks. II Swelling. *Journal of Chemical Physics* **11,** 512–520 (1943).
254. Andreopoulos, F. M., Beckman, E. J. & Russell, a J. Light-induced tailoring of PEG-hydrogel properties. *Biomaterials* **19,** 1343–1352 (1998).
255. Riesenfeld, J. & Rodén, L. Quantitative analysis of N-sulfated, N-acetylated, and unsubstituted glucosamine amino groups in heparin and related polysaccharides. *Analytical Biochemistry* **188,** 383–389 (1990).
256. Jackson, G. N. B., Ashpole, K. J. & Yentis, S. M. The TEG vs the ROTEM thromboelastography/thromboelastometry systems. *Anaesthesia* **64,** 212–215 (2009).
257. Coakley, M., Reddy, K. & Mackie, I. Transfusion triggers in orthotopic liver transplantation: a comparison of the thromboelastometry analyzer, the thromboelastogram, and conventional coagulation tests. *Journal of Cardiothoracic and Vascular Anesthesia* **20,** 548–553 (2006).
258. Venema, L. F. *et al.* An assessment of clinical interchangeability of TEG and RoTEM thromboelastographic variables in cardiac surgical patients. *Anesthesia and Analgesia* **111,** 339–344 (2010).
259. Sankarankutty, A., Nascimento, B., Teodoro da Luz, L. & Rizoli, S. TEG® and ROTEM® in trauma: similar test but different results? *World Journal of Emergency Surgery* **7,** 2–8 (2012).
260. Whiting, D. & DiNardo, J. TEG and ROTEM: technology and clinical applications. *American Journal of Hematology* **89,** 228–232 (2014).
261. Ingber, D. & Folkmann, J. Mechano-chemical switching between growth and differentiation during growth factor-stimulated angiogenesis in vitro: role of the extracellular matrix. *Journal of Cell Biology* **109,** 317–330 (1989).
262. Suhardja, A. & Hoffman, H. Role of growth factors and their receptors in proliferation of microvascular endothelial cells. *Microscopy Research and Technique* **60,** 70–75 (2003).
263. Carmeliet, P. Mechanisms of angiogenesis and arteriogenesis. *Nature Medicine* **6,** 389–395 (2000).

264. Yancopoulos, G. *et al.* Vascular-specific growth factors and blood vessel formation. *Nature* **407,** 242–248 (2000).
265. Ferrara, N., Gerber, H. & LeCouter, J. The biology of VEGF and its receptors. *Nature Medicine* **9,** 669–676 (2003).
266. Ravanagh, G. & Ross-Murphy, S. B. Rheological Characterization of Polymer Gels. *Progress in Polymer Science* **23,** 533–562 (1998).
267. Lutolf, M. P. *et al.* Synthetic matrix metalloproteinase-sensitive hydrogels for the conduction of tissue regeneration: engineering cell-invasion characteristics. *National Academy of Sciences of the United States of America* **100,** 5413–5418 (2003).
268. Reis, A. V *et al.* Reaction of Glycidyl Methacrylate at the Hydroxyl and Carboxylic Groups of Poly (vinyl alcohol) and Poly (acrylic acid): Is This Reaction Mechanism Still Unclear? *Journal of Organic Chemistry* **74,** 3750–3757 (2009).
269. Khetan, S., Katz, J. S. & Burdick, J. Sequential crosslinking to control cellular spreading in 3-dimensional hydrogels. *Soft Matter* **5,** 1601 (2009).
270. Kim, J. *et al.* Bone regeneration using hyaluronic acid-based hydrogel with bone morphogenic protein-2 and human mesenchymal stem cells. *Biomaterials* **28,** 1830–1837 (2007).
271. Lei, Y., Gojgini, S., Lam, J. & Segura, T. The spreading, migration and proliferation of mouse mesenchymal stem cells cultured inside hyaluronic acid hydrogels. *Biomaterials* **32,** 39–47 (2011).
272. Rydholm, A., Anseth, K. & Bowman, C. Effects of neighboring sulfides and pH on ester hydrolysis in thiol-acrylate photopolymers. *Acta Biomaterialia* **3,** 449–455 (2007).
273. Zacchigna, M. *et al.* Synthesis of a new mPEG-dexamethasone conjugate and preliminary bioavailability studies in rabbits. *Journal of Drug Delivery Science and Technology* **18,** 155–159 (2008).
274. Heyna, J. & Schumacher, W. Dyes containing vinyl sulfone. US2657205 A (1953).
275. Chatani, S., Nair, D. P. & Bowman, C. N. Relative reactivity and selectivity of vinyl sulfones and acrylates towards the thiol–Michael addition reaction and polymerization. *Polymer Chemistry* **4,** 1048 (2013).
276. Nair, D. P. *et al.* The Thiol-Michael Addition Click Reaction: A Powerful and Widely Used Tool in Materials Chemistry. *Chemistry of Materials* **26,** 724–744 (2014).
277. Raeber, G. P., Lutolf, M. P. & Hubbell, J. Molecularly engineered PEG hydrogels: a novel model system for proteolytically mediated cell migration. *Biophysical Journal* **89,** 1374–1388 (2005).
278. Flory, P. Principles of polymer chemistry. *Cornell University Press, Ithaca, New York* 476–482 (1953).

279. Baier Leach, J., Bivens, K. a, Patrick, C. W. & Schmidt, C. E. Photocrosslinked hyaluronic acid hydrogels: natural, biodegradable tissue engineering scaffolds. *Biotechnology and Bioengineering* **82,** 578–589 (2003).

280. Morales-Sanfrutos, J. *et al.* Vinyl sulfone: a versatile function for simple bioconjugation and immobilization. *Organic & Biomolecular Chemistry* **8,** 667–675 (2010).

281. Pavlov, G., Finet, S., Tatarenko, K., Korneeva, E. & Ebel, C. Conformation of heparin studied with macromolecular hydrodynamic methods and X-ray scattering. *European Biophysics Journal* **32,** 437–449 (2003).

282. Sharma, P., Rajalingam, D., Krishnaswamy, T. & Kumar, S. A Light Scattering Study of the Interaction of Fibroblast Growth Factor (FGF) with its Receptor. *Biophysical journal* **94,** 71–73 (2008).

283. Béguin, S., Lindhout, T. & Hemk, C. The Mode of Action of Heparin in Plasma. *Thrombosis and Haemostasis* **60,** 457–462 (1988).

284. Nielsen, V. A comparison of the Thrombelastograph and the ROTEM. *Blood Coagullation Fibrinolysis* **18,** 247–252 (2007).

285. Hirsh, J., Anand, S., Halperin, J. & Fuster, V. Guide to anticoagulant therapy: heparin. *Circulation* **103,** 2994–3018 (2001).

286. Casu, B. & Lindahl, U. Structure and biological interactions of heparin and heparan sulfate. *Advances in carbohydrate chemistry and biochemistry* **57,** 159–206 (2001).

287. Atha, D. H., Lormeau, J. C., Petitou, M., Rosenberg, R. D. & Choay, J. Contribution of 3-O- and 6-O-sulfated glucosamine residues in the heparin-induced conformational change in antithrombin III. *Biochemistry* **26,** 6454–6461 (1987).

288. Ruttmann, T., Lemmens, H., Malott, K. & Brock-Utne, J. The haemodilution enhanced onset of coagulation as measured by the thrombelastogram is transient. *European Journal of Anaesthesiology* **23,** 574–579 (2006).

289. Macafee, B. *et al.* Reference ranges for thromboelastography (TEG) and traditional coagulation tests in term parturients undergoing caesarean section under spinal anaesthesia. *Anaesthesia* **67,** 741–747 (2012).

290. Lang, T. *et al.* Multi-centre investigation on reference ranges for ROTEM thromboelastometry. *Blood Coagulation Fibrinolysis* **16,** 301–310 (2005).

291. Shah, S. S., Kim, M., Cahill-Thompson, K., Tae, G. & Revzin, A. Micropatterning of bioactive heparin-based hydrogels. *Soft Matter* **7,** 3133 (2011).

292. Wissink, M. J. . *et al.* Improved endothelialization of vascular grafts by local release of growth factor from heparinized collagen matrices. *Journal of Controlled Release* **64,** 103–114 (2000).

293. Hiratzka, L., Goeken, J., White, R. & Wright, C. In vivo comparison of replamineform, Silastic, and bioelectric polyurethane arterial grafts. *Archives of Surgery* **114,** 698–702 (1979).

294. Beahan, P. & Hull, D. A study of the interface between a fibrous polyurethane arterial prosthesis and natural tissue. *Journal of Biomedical Materials Research* **16,** 827–838 (1983).

295. White, R., Hirose, F., Sprout, R., Lawrence, R. & Nelson, R. Histopathologic observations after short-term implantation of two porous elastomers in dogs. *Biomaterials* **2,** 171–176 (1981).

296. Leidner, J. & Wong, E. A novel process for the manufacturing of porous grafts: Process description and product evaluation. *Journal of Biomedical Materials Research* **17,** 229–247 (1983).

297. Folkman, J. & Ingbar, D. *Angiogenesis: Regulatory Role of Heparin and Related Molecules*. 316–333 (1989).

298. Yu, L. & Ding, J. Injectable hydrogels as unique biomedical materials. *Chemical Society Reviews* **37,** 1473–1481 (2008).

9 Appendices

9.1 Appendix A - Standard solutions

9.1.1 Phosphate Buffered Saline

In this project two different forms of phosphate buffered saline (PBS) were used. Phosphate buffered saline formula 1 (PBS_1) was used as supernatant during the swelling, drug elution and in vitro drug activity experiments, while phosphate buffered saline formula 2 (PBS_2) was used as solvent during gelling through conjugate addition since it has a higher buffering capacity than PBS_1.

PBS_1 (sterilized, pH = 7.4) was prepared by dissolving disodium hydrogen phosphate ($Na_2HPO_4 \cdot 12H_2O$, 2.89 g, 8.1 mmole), potassium dihydrogen phosphate (KH_2PO_4, 0.2 g, 1.5 mmole), potassium chloride (KCl, 0.2 g, 2.7 mmole) and sodium chloride (NaCl, 8 g, 136.9 mmole) in 1 L deionised water (DI)

PBS_2 (sterilized, pH = 7.4) was prepared by mixing solution A (65 mL), solution B (435 mL) and solution C (500 mL). Solution A: sodium dihydrogen phosphate ($NaH_2PO_4 \cdot H_2O$, 0.15M, 5.175 g, 15.0 mmole, 250 mL DI); Solution B: disodium hydrogen phosphate ($Na_2HPO_4 \cdot 12H_2O$, 0.15M, 13.425 g, 75.0 mmole, 250 mL DI); Solution C: sodium chloride (NaCl, 0.15M, 4.383 g, 77.0 mmole, 500 mL DI).

9.1.2 Fixatives

In this project two different fixatives were used, 10% Formalin and Zinc fixative. Formalin fixative (10%) was prepared by dissolving sodium chloride (42.5 g), disodium hydrogen phosphate (6.4 g) and sodium dihydrogen orthophosphate anhydrous (0.7 g) in 5 L DI. The pH was adjusted to 7.6, formaldehyde (500 mL, 40%) was added and the fixative was stored at 4 °C. The Zinc fixative was prepared by dissolving calcium acetate (0.5 g), zinc acetate (5 g) and zinc chloride (5 g) in Tris buffer (0.1M, 1000 mL, pH = 7.4) and stored the fixative at RT.

9.2 Appendix B – Nuclear Magnetic Resonance Spectra

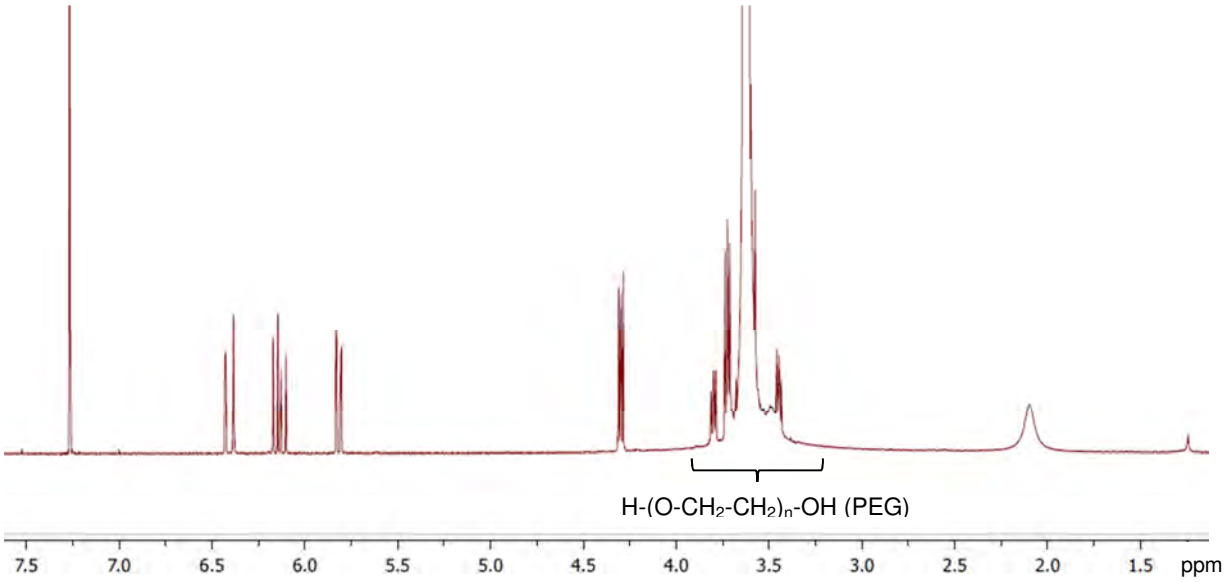

Figure 44: ^{1}H NMR spectrum of 20PEG8Ac

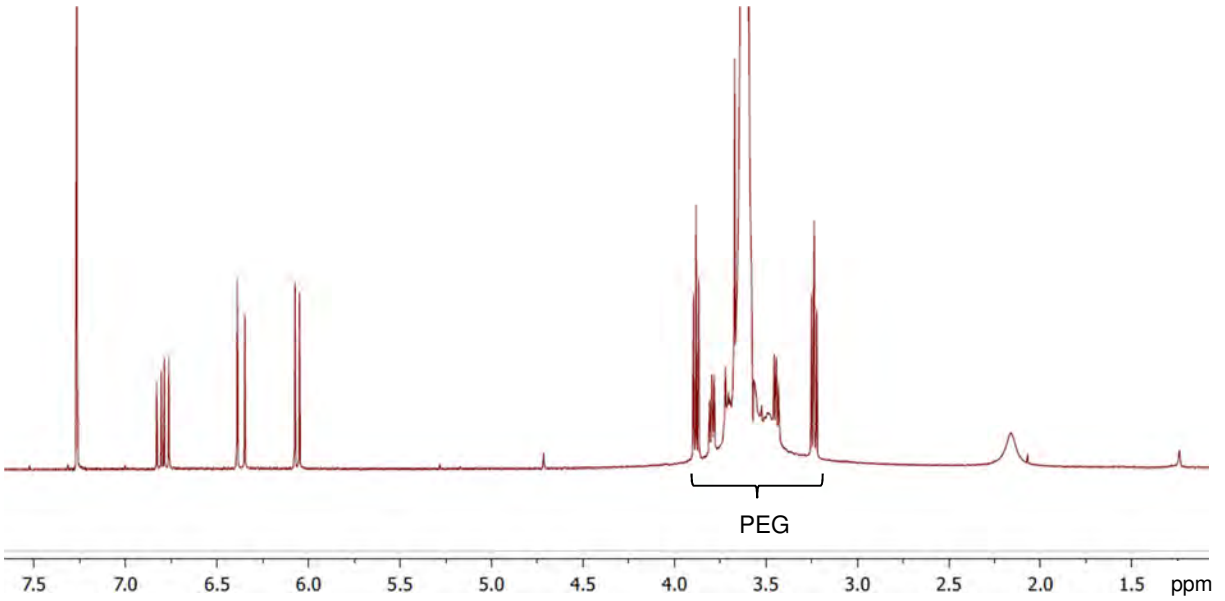

Figure 45: ^{1}H NMR spectrum of 20PEG8VS

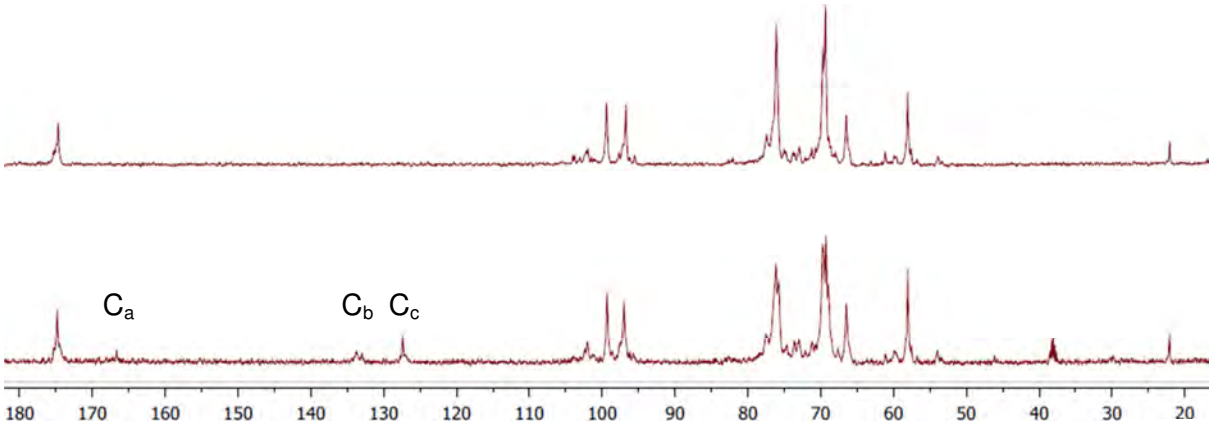

Figure 46: ^{13}C NMR spectra of Hep (above) and Hep-Ac (below)

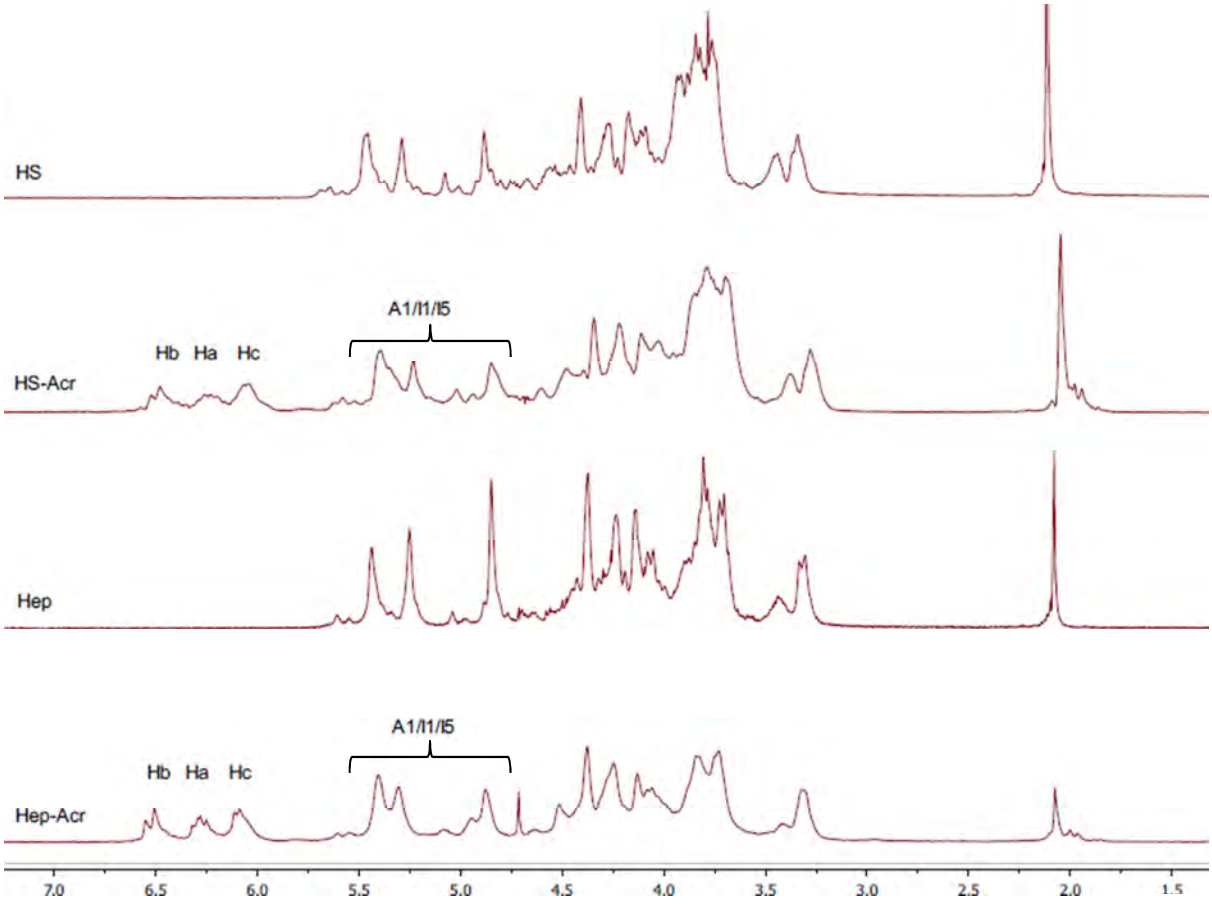

Figure 47: ^{13}H NMR spectra of HS, HS-Ac, Hep and Hep-Ac

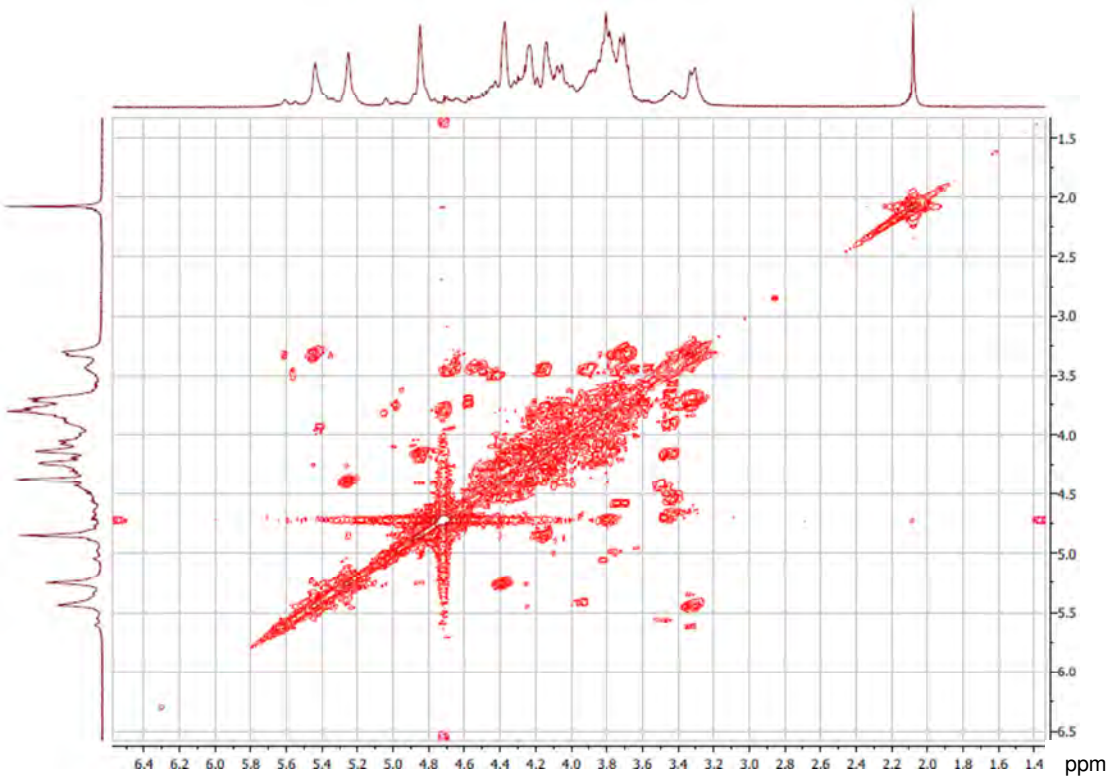

Figure 48: COSY NMR spectrum of Hep

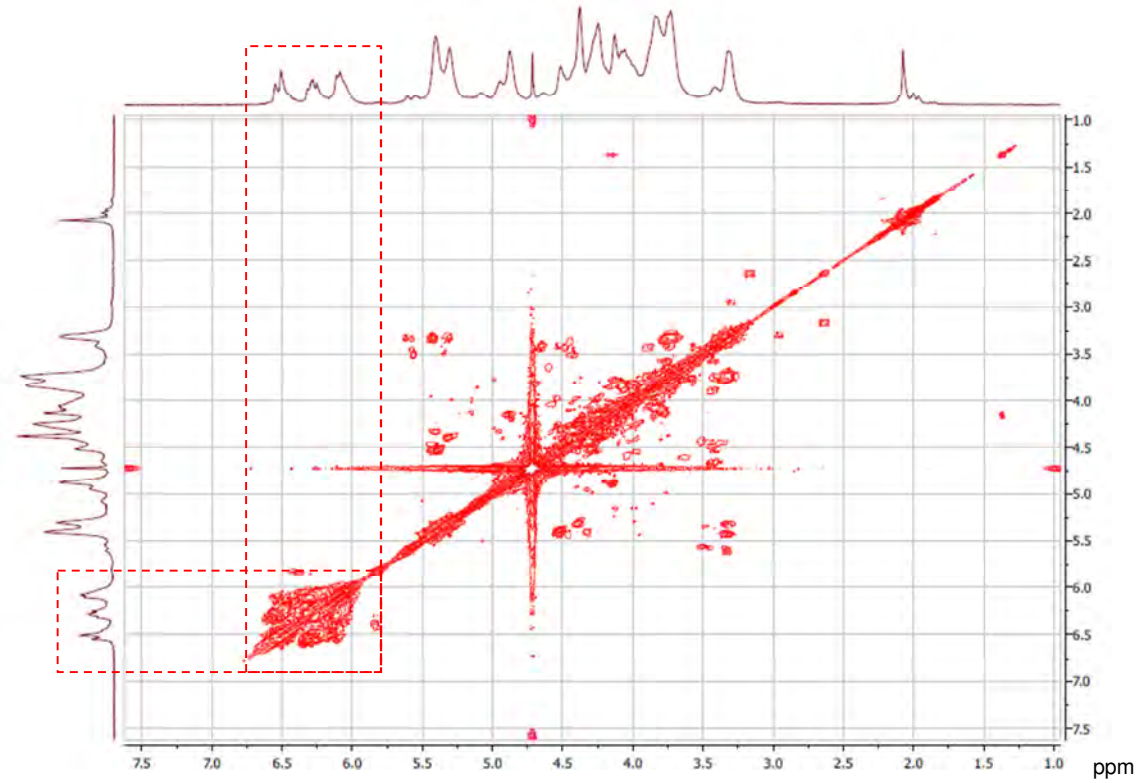

Figure 49: COSY NMR spectrum of Hep-Ac

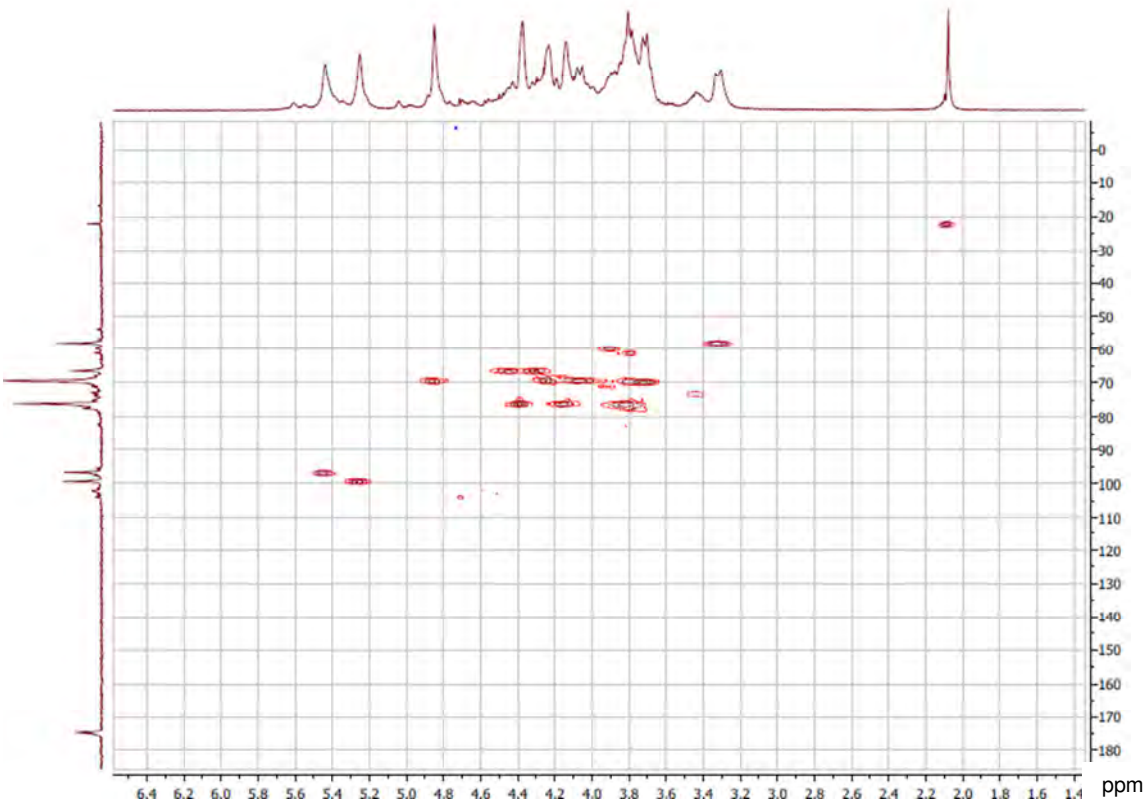

Figure 50: HSQC NMR spectrum of Hep

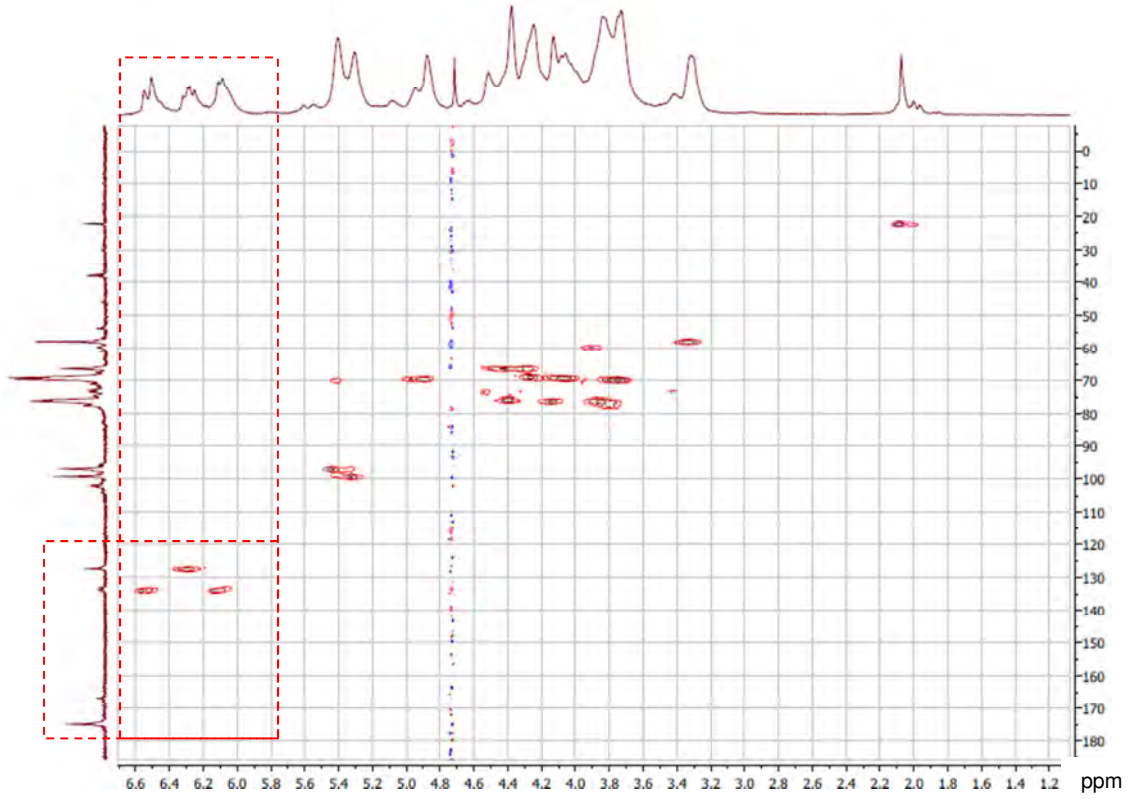

Figure 51: HSQC NMR spectrum of Hep-Ac

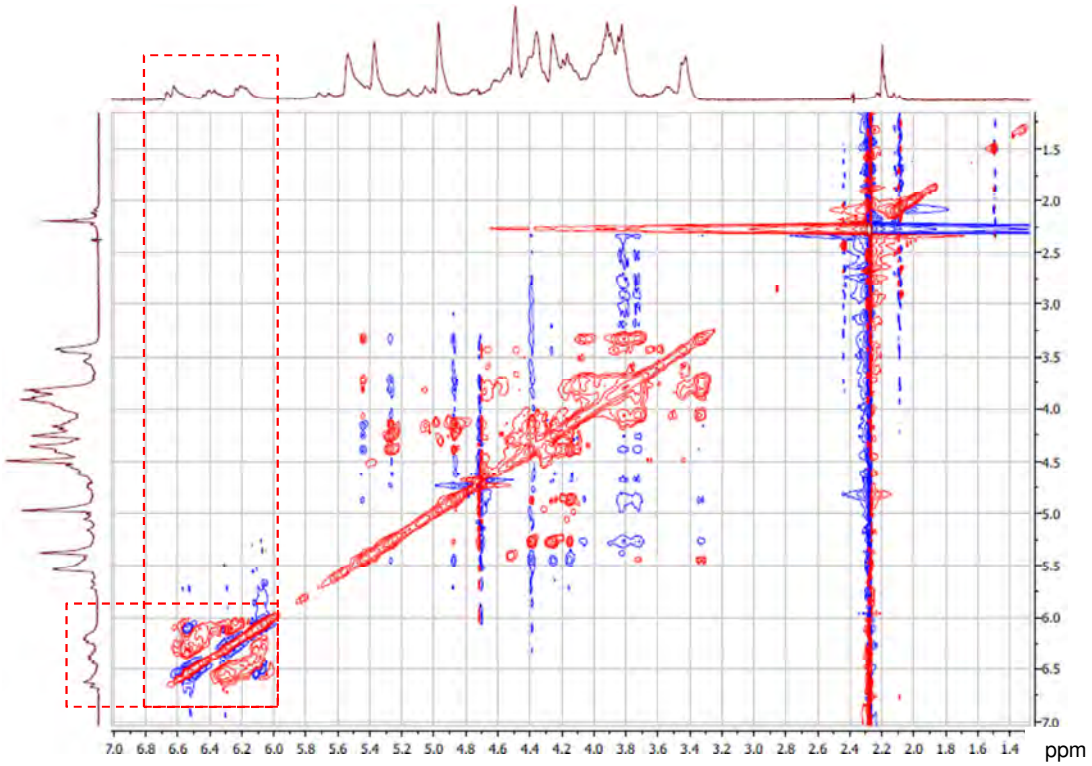

Figure 52: TOCSY NMR spectrum of Hep-Ac

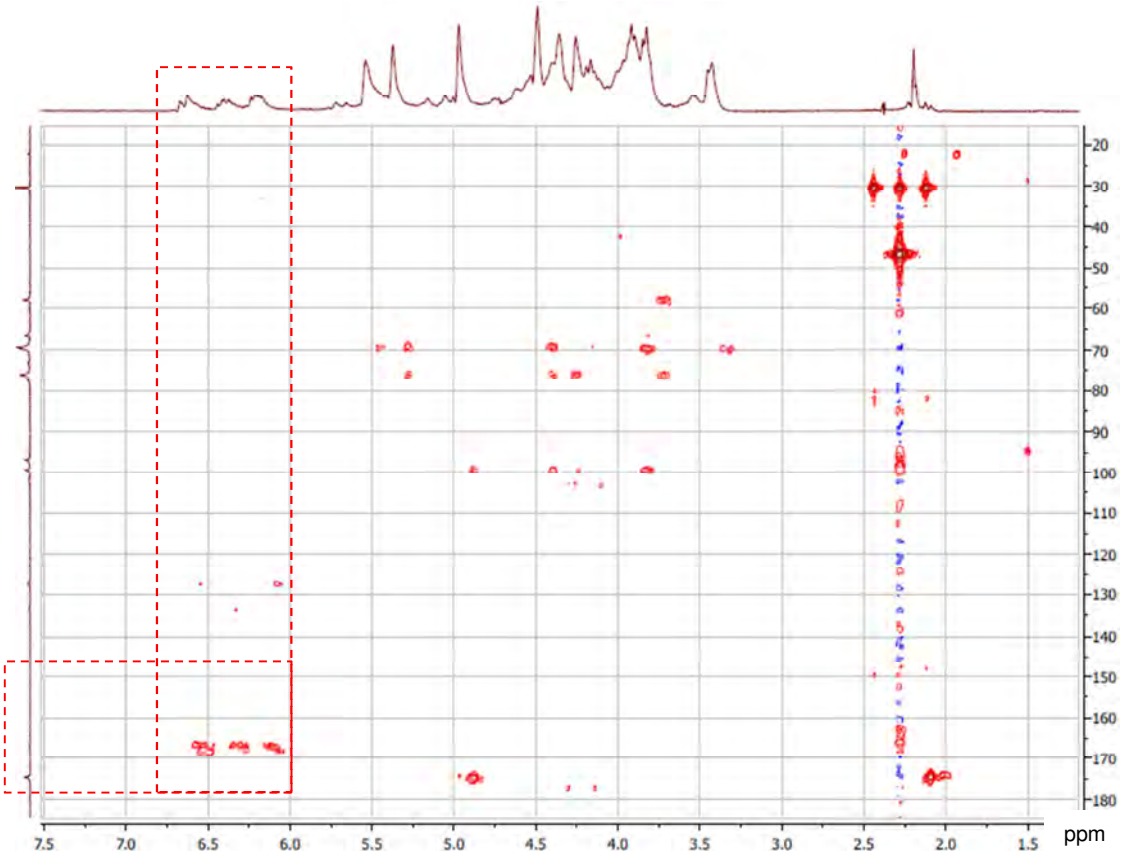

Figure 53: HMBC NMR spectrum of Hep-Ac